Thesis
S692

Library
U. S. Naval Postgraduate School
Monterey, California

DUDLEY KNOX LIBRARY
NAVAL POSTGRADUATE SCHOOL
MONTEREY, CALIFORNIA 93943-5002

A STUDY OF THE EFFECT OF VERTICAL LOADS ON THE DYNAMIC RESPONSE OF STRUCTURES

BY

HENRY EDWARD STEPHENS

B.S., U. S. Naval Academy, 1944
M.S., Rensselaer Polytechnic Institute, 1948

THESIS

SUBMITTED IN PARTIAL FULFILLMENT OF THE REQUIREMENTS
FOR THE DEGREE OF DOCTOR OF PHILOSOPHY IN ENGINEERING
IN THE GRADUATE COLLEGE OF THE
UNIVERSITY OF ILLINOIS, 1954

URBANA, ILLINOIS

Thesis
S692

DUDLEY KNOX LIBRARY
NAVAL POSTGRADUATE SCHOOL
MONTEREY, CALIFORNIA 93943

A STUDY OF THE EFFECT OF VERTICAL LOADS ON THE DYNAMIC RESPONSE OF STRUCTURES

TABLE OF CONTENTS

		Page
	ACKNOWLEDGEMENT	iii
	LIST OF FIGURES	iv
I.	INTRODUCTION	
	1.1 Summary	1
	1.2 Nomenclature	3
II.	HORIZONTAL RESISTANCE FOR STRUCTURE WHOSE SPRING CONSTANT AFTER YIELD IS 0	
	2.1 Object of Section	6
	2.2 Material and Moment Relation	6
	2.3 Resistance of Pinned-Base Frame	6
	2.4 Resistance of Fixed-Base Frame	9
	2.5 Use of the Resistance Curves	10
	2.6 Comparison of Effect of Vertical Load with Approximate Method	12
III.	EFFECT OF VERTICAL LOAD ON NATURAL FREQUENCY OF VIBRATION	
	3.1 Frequency and Period	13
IV.	HORIZONTAL RESISTANCE OF STRUCTURE WHEN α OF THE SECTION M VS. θ RELATION IS GREATER THAN 0	
	4.1 Form of Resistance	14
	4.2 Slope of Resistance Curves	15
V.	HORIZONTAL RESISTANCE OF STRUCTURE WHEN α OF THE STRUCTURE RESISTANCE, NOT M/M_e VS. θ/θ_e, IS NOT 0	
	5.1 Form of Resistance	18
VI.	COMPUTATION OF RESPONSE OF STRUCTURES	
	6.1 Discussion of Methods	19

22999

A STUDY OF THE EFFECT OF VERTICAL LOADS ON THE DYNAMIC
RESPONSE OF STRUCTURES

TABLE OF CONTENTS

Page

ACKNOWLEDGEMENT iii

LIST OF FIGURES iv

I. INTRODUCTION

1.1 Summary 1

1.2 Nomenclature 3

II. HORIZONTAL RESISTANCE FOR STRUCTURES WHOSE STRING COEFFICIENT AFTER YIELD IS 0

2.1 Object of Section 6

2.2 Material and Moment Relation 8

2.3 Resistance of Fixed-Base Frame 8

2.4 Resistance of Fixed-Base Frame 9

2.5 Use of the Resistance Curves 10

2.6 Comparison of Effect of Vertical Load with Approximate Method 12

III. EFFECT OF VERTICAL LOAD ON NATURAL FREQUENCY OF VIBRATION

3.1 Frequency and Period 13

IV. HORIZONTAL RESISTANCE OF STRUCTURE WHEN α OF THE SECTION M VS. θ RELATION IS GREATER THAN 0

4.1 Form of Resistance 14

4.2 Slope of Resistance Curves 15

V. HORIZONTAL RESISTANCE OF STRUCTURE WHEN α OF THE STRUCTURE RESISTANCE, NOT M/M_0 VS. θ/θ_0, IS NOT 0

5.1 Form of Resistance 18

VI. COMPUTATION OF RESPONSE OF STRUCTURES

6.1 Discussion of Methods 19

eeess

TABLE OF CONTENTS (Concluded)

Page

VII. APPROXIMATE EQUIVALENT UNIFORM RESISTANCE TO PRODUCE A GIVEN MAXIMUM DEFLECTION WHEN THE VERTICAL LOAD IS CONSTANT

7.1 Summary of Section 21

7.2 Maximum Deflection Equal to the Collapse Deflection 21

7.3 Maximum Deflection Less Than the Collapse Deflection 22

7.4 Correction to the Aproximate Equivalent Uniform Resistance Method 25

VIII. STUDY OF EFFECT OF PULSE SHAPE WHEN α OF RESISTANCE EQUALS 0 AND y_m EQUALS y_f

8.1 Scope of Section 26

8.2 Analytical Computation for Step Pulse 26

8.3 Numerical Computation for Initial and Terminal Peak Pulses 28

8.4 Summary of Frames A and B 30

CONCLUSIONS 32

BIBLIOGRAPHY 33

APPENDIX I. INITIALLY CROOKED ELASTIC COLUMN

I.1 Scope and Computations 34

I.2 Discussion 35

APPENDIX II. INITIALLY STRAIGHT ELASTIC COLUMN GIVEN INITIAL DISPLACEMENT

II.1 Scope and Computations 37

II.2 Discussion 38

APPENDIX III. FIGURES 40

VITA 73

7.1 Summary of evaluation 23

7.2 Overview of the evaluation 23

7.3 [illegible] 25

7.4 Comments on the recommended evaluation criteria 28

VIII. [illegible] 29

8.1 Scope of [illegible] 29

8.2 [illegible] 29

8.3 Structural [illegible] 30

8.4 Summary of [illegible] 30

[illegible] 32

[illegible] 32

I. [illegible] 34

1.1 [illegible] 34

1.2 Introduction 34

11.1 Scope and Constraints 37

11.2 [illegible] 38

Appendix III. [illegible] 42

[illegible] 43

ACKNOWLEDGEMENT

The writer wishes to express his sincere gratitude to his advisor, Dr. N.M. Newmark, Research Professor of Structural Engineering, University of Illinois, for his valuable advice and encouragement during the course of investigation.

LIST OF FIGURES

Figure		Page
1	Stress-Strain Curve for Ideal Plastic Material	40
2	M vs. θ Curve for Ideal Plastic Material and H Type Section	40
3	M/M_e vs. y/y_e for P and α Equal to 0	40
4	Pinned-Base Frame	41
5	Fixed-Base Frame	41
6	Plastic Resistance Paths and Yield Loci for α of Structure Resistance Equal to 0	42
7	Resistance Paths for $\tau = 2\gamma$	43
8	Resistance Paths for $\tau = 1/2\gamma$	44
9	Variation of M with Changes in P in Plastic Range	45
10	Step Function Variation of Vertical Load	45
11	Transition Between Resistance Paths for Step Function	46
12	Comparison of Interaction Method with Approximate Method for $P_e = P_{cr}$	47
13	Comparison of Interaction Method with Approximate Method for $P_e = 1/2\ P_{cr}$	48
14	Idealized M/M_e vs. θ/θ_e Diagram for Work Hardening Material	49
15	Stress-Strain Curve for Work Hardening Material	49
16	M/M_e vs. θ/θ_e Relation for $\alpha = 0.2$: Showing Effect of Axial Load on Section	50
17	M/M_e vs. y/y_e for Idealized H Section and α of M/M_e vs. θ/θ_e Equal to 0.8, τ/γ = 1.0 and 2.0	51
18	α Designation	52
19	Form of Structure Resistance When $\alpha \neq 0$	52
20	Equivalent Uniform Resistance for $y_m = y_f$	52
21	Equivalent Uniform Resistance for $y_m < y_f$	52
22	Error in Δ_1/y_e From Approximate Equivalent Uniform Resistance Method for $y_m = y_f$	53
23	Load Pulse Shapes	54

List of Figures

Figure	
1	[illegible]
2	ψ_0 vs. θ for Ideal Plastic material and β Type Material
3	ψ/ψ_0 vs. x/y_0 for β and α Equal to 0
4	Plotted-Area Curve
5	[illegible]
6	Simple Beam Subjected to Pure Bending by Moments
7	[illegible]
8	Derivation Factor for $\tau = \tau/\sigma_y$
9	Variation of β with Poisson Ratio ν in Elastic Range
10	[illegible]
11	Theoretical Relations [illegible]
12	[illegible]
13	[illegible]
14	Combined ψ/ψ_0 vs. θ/θ_0 Curves for Beam Combining Symmetry
15	[illegible]
16	ψ/ψ_0 vs. θ/θ_0 Values for $\alpha = 0.05$ Showing Effect of [illegible]
17	ψ/ψ_0 vs. x/y_0 for Location θ Position and α of ψ/ψ_0 vs. θ/θ_0 Equal to C.S. $\tau/\tau = 1.0$ at 1.0
18	[illegible]
19	[illegible]
20	[illegible]
21	[illegible]
22	[illegible]
23	[illegible]

LIST OF FIGURES (Concluded)

Figure		Page
24	Velocity, $\frac{(\dot{y}/y_e)}{\omega_o}$, Required at t_1 and $y\|_{t_1}$ for $y_m = y_f$	54
25	Structure Response Curves for Frame A for Step Pulse	55
26	Structure Response Curves for Frame A for Step Pulse	56
27	Structure Response Curves for Frame A for Initial Peak Pulse . .	57
28	Structure Response Curves for Frame A for Terminal Peak Pulse .	58
29	Structure Response Curves for Frame B for Step Pulse	59
30	Structure Response Curves for Frame B for Initial Peak Pulse . .	60
31	Composite Structure Response Curves for Frame A for Step, Initial and Terminal Peak Pulses	61
32	Composite Structure Response Curves for Frame B for Step, Initial and Terminal Peak Pulses	62
33	Proportionality Between Pulse Types for $\gamma_1 = 0$ and $y_m = y_f$ . . .	63
34	Equivalence Between Initial Peak and Step Pulse for $y_m = y_f$ . .	63
35	Δ_1/H_e for Initial and Terminal Peak Pulses Expressed as % of Δ_1/H_e for Step Pulse	64
36	Approximate % Conversion Factor to Construct Δ_1/H_e vs. t_1/T_o Curves for Initial and Terminal Peak Pulses for $y_m = y_f$ Using Δ_1/H_e vs. t_1/T_o for Step Pulse	65
37	Column Model for Appendixes I and II	66
38	u_{neut} vs. u_o for $p/q = 1.02$, 1.00 and 0.98	67
39	Phase Plane Diagrams for Initial Crookedness. $p/q = 1.00$ and 1.02	68
40	Time to Deflect, u_{max} and u_{neut} vs. Initial Crookedness	69
41	Phase Plane Diagrams for Initially Straight Elastic Column Given Disturbance u_1	70
42	u_{max} vs. u_1 for Initially Straight Elastic Column Given Initial Displacement u_1	71
43	Time to Displace vs. Initial Displacement for Initially Straight Column	72

Index

A STUDY OF THE EFFECT OF VERTICAL LOADS ON THE DYNAMIC RESPONSE OF STRUCTURES

I. INTRODUCTION

1.1 Summary

In the main text a study is made of the effect of vertical time dependent and dead loads on the horizontal response of single degree of freedom frames. In appendixes I and II a pinned-end column is simulated by a single degree of freedom model and a study is made of the effect of initial crookedness and initial displacement on the maximum displacement and time required to deflect.

In solving for the response of the single degree of freedom frame, using the acceleration numerical method, the horizontal acceleration of the floor mass is taken as the difference between the horizontal load and the horizontal resistance divided by the mass of the system. For simplification the system is taken with the mass concentrated at the floor level and the horizontal external force taken to act at the floor level. To determine the response it is then necessary to know the horizontal resistance when vertical loads are included.

Addition of the vertical loads will change the structure horizontal resistance because of both an increase in the column moments due to the eccentricity of the vertical loads and by the axial load on the column section causing inelastic action to begin with less section moment. In an existing approximate method for allowing for the vertical load the effect of the additional moment is allowed for, but not the effect of the axial load on the section inelastic action. Further, the vertical loads, whether live or dead load, will cause a change in the natural frequency in the elastic range. The mass is dependent only on the dead load; but the effective spring constant is dependent on the total vertical load, including live load.

The form of the horizontal resistance is shown for:

1. The case where α of the structure resistance, R vs. y, is zero.

1.3 Summary

2. The case where α of the structure resistance, V vs. y, is not zero.

3. The case where α of the column section moment-curvature relation is greater than zero.

For case (1) above it is possible to determine the collapse deflection (the deflection at which any increase in the dead load with only dead load acting will cause the structure to continue to deflect to failure) and the horizontal resistance. And for case (2) it is easy to determine if the structure has a collapse deflection as defined above, and if so its value. It is also easy to determine the form of the resistance for this case. But for case (3) the relation is shown not to be so simple. For case (3) some criteria must be established for a relation between vertical load and α to determine when the structure will have a collapse deflection. A relation is found in that if $r \leq \alpha$, for case (3), no failure deflection exists. If no collapse deflection, as defined, exists some other failure criteria must be established.

Prof. N.M. Newmark, University of Illinois, has developed an approximate equivalent uniform resistance method for determining the load-time relation which will produce a maximum deflection equal to some predetermined value when α of the structure resistance is not zero, but k_E constant. If the yield and maximum deflections, when put in the proper terms, are used in this expression it can be used to compute the response including the effect of the vertical load. A comparison of the results of this approximate relation has been made with more exact values found for the maximum deflection equal to the collapse deflection. A statistical correction factor for use with the approximate equivalent uniform resistance is recommended for the range of t_1/T_0 between 0.1 and 1.0.

When time dependent loads are applied to a structure the shape of the pulse will influence the response. In the range of t_1/T_0 less than 0.1 the vertical time dependent load has little effect on the horizontal response. For pulses of equal amount of impulse the initial peak pulse will produce a greater amount of

response than the step pulse. For low values of t_1/T_o the terminal peak response approaches that of the initial peak and for larger values of t_1/T_o the terminal peak response approaches that of the step pulse. A general trend, independent of the amount of vertical load, can be found for the response of the terminal and initial peaks in terms of the response for the step pulse. For the initial peak pulse it is possible to find an equivalent step pulse for the case of $y_m = y_f$.

If an axial load step pulse, equal to or greater than the critical buckling load, is applied to a pinned-end column which has initial crookedness the amount of the initial crookedness will influence the response. The greater the initial crookedness the greater will be the maximum deflection and the less time required to reach maximum deflection. This is investigated in appendix I.

In appendix II an investigation is made of the effect of the magnitude of an initial displacement given to an initially straight column when a step pulse, equal or greater in magnitude than the critical buckling load, is applied. These phase diagrams, plots of time to reach maximum deflection vs. initial displacement and magnitude of maximum deflection vs. initial displacement are used to show the effect of the initial displacement on the response of the column.

1.2 Nomenclature

H	Horizontal force per column.
H_e	Static horizontal force, per column, that produces yielding with no vertical load acting.
H_{er}	Reduced horizontal force, per column, that produces yielding when vertical load is included.
H_{eq}	Static horizontal force, per column, at yield of the equivalent uniform resistance.
k_1	Spring force, per column, up to yield, no vertical load.
k_2	Spring force, per column, after yield, no vertical load.
k_{1r}	Spring force up to yield, vertical load acting.
k_{2r}	Spring force after yield, vertical load acting.
L	Length of column.

M_o Moment at top of pinned-end column, and at top and bottom of fixed-base column.

M_e Section moment at yielding, no axial load.

P_e Elastic limit axial load, per column.

P Vertical or axial load acting, per column.
$P = \tau P_e = \gamma P_{cr}$

P_{cr} Critical buckling load, per column.

t_1 Duration of load pulse.

T Natural period with vertical load.

T_o Natural period without vertical load.

u $y/L/2$, appendixes I and II.

$\dot{u}$ du/dt, appendixes I and II.

$\ddot{u}$ d^2u/dt^2, appendixes I and II.

u_o y_o/e, appendixes I and II (initial crookedness).

y Lateral displacement.

y_o Differential displacement between top and bottom of frame columns and initial center deflection for pinned-end model of appendixes I and II.

y_e Yield deflection, no vertical load.

y_{er} Yield deflection, with vertical load.

y_m Maximum deflection.

y_f Collapse deflection; that deflection at which the vertical load will cause the structure to continue to deflect without horizontal load.

y_{eq} Yield deflection of approximate equivalent uniform resistance.

$\dot{y}|_{t_e}$ Velocity of top of column at time of yielding.

$\dot{y}|_{t_1}$ Velocity of top of column at end of load pulse.

α The ratio between the slope after yielding to the slope before yielding of structural resistance, R vs. y, and R vs. $\frac{}{}$ curves when the curves have constant slope before and after yielding.

γ $P = \gamma P_{cr}$: γ is the fraction of P_{cr} that the vertical load is equal to.

γ_{wt} The fraction of P_{cr} that the dead load is equal to.

γ_t The fraction of P_{cr} that the time dependent vertical load is equal to.

$\gamma_{total} = \gamma_{st} + \gamma_t$.

γ_1 The fraction of P_{cr} that the average of the time dependent vertical load is equal to.

θ Section rotation.

θ_e Section rotation at yield, no axial load.

σ_e Yield stress, uni-axial state of stress.

Δ_1 The average horizontal time dependent load.

ω_o Natural frequency, no vertical load.

ω_i Natural frequency, with vertical load.

τ The designation of τ is the same as γ except that it refers to P_e instead of P_{cr}.

II. ESSENTIAL RESISTANCE FOR STRUCTURES KNOWN DURING COLLAPSE TO HAVE SLOPE AFTER YIELD IS 0

2.1 Object of Section

In this section the relation of horizontal load, vertical load and displacement is studied to show the interaction between these for the case where α of the structural resistance is zero. This is done for both fixed and pinned-base single story frames. The girder moment of inertia is taken to be very large in comparison to the moment of inertia of the columns. The axial load will increase the end moments by an amount equal to Py_o. This increase in moment must be allowed for, as well as the reduction in magnitude of M_o at yielding due to the axial load. Throughout this report values will be worked out in terms of individual column loads and properties.

2.2 Material and Moment Relation

The column material is taken to be an ideal plastic one (stress-strain curve shown figure 1). As the column section an H type section is assumed and the bending axis is taken perpendicular to the web. For this type section and ideal plastic material the M vs. θ relation for the section will be of the type shown in figure 2 as M/M_e vs. θ/θ_e. This curve can be idealized to two straight lines as also shown figure 2. With the value of M_e chosen, the curve can be converted to dimensionless form. If any allowance is to be made for the effect of increase in yield point because of speed of loading, or strain rate, it would be reflected in value of σ_e, thus producing a change in the actual M vs. θ relation. Any allowance for non-perfect section would be made in choice of M_e. A practical choice of M_e is to take it as the moment when inelastic action just penetrates through the flanges. The structure horizontal resistance, no vertical load, for this idealized H/H_e vs. θ/θ_e curve is shown in figure 3.

2.3 Resistance of Pinned-base Frame

For the pinned-base frame, shown figure 4, and for the elastic condition the moment, M, at any section will be:

II. [illegible]

2.1 [illegible]

In this section the solution of [illegible], applied load and displacement is studied by [illegible] method. Since the beam theory of [illegible] structural resistance is zero. This is true for both fixed and planned-base single story frames. The plastic moment of inertia is taken to be very large in comparison to the moment of inertia of the columns. The axial load will increase the end moments by an amount equal to Ty_o. This increase in moment must be allowed for, as well as the reduction in magnitude of M_p at yielding for the different column loads and properties.

2.2 Material and support relation

The column material is taken to be an ideal elastic [illegible] [illegible] plastic [illegible]. In the column section is neglected and the bending axis is taken perpendicular to the web. The ideal type bending and ideal elastic [illegible] is as a relation for the web will be of the type shown in figure 2 as $c/\rho = \sigma/\sigma_o$. This curve can be simplified to two straight lines as also shown figure 2. Into the value of σ_o chosen, the curve may be extended to dimensionless form. If any allowance is to be made for the effect of increase in yield point because of speed of loading, or strain rate, it would be reflected in value of σ_o. Some variation [illegible] relation, [illegible] allowance for [illegible] would be made in choice of σ_o. [illegible] limits of σ_o is to say it is the moment when [illegible] through the flanges. The [illegible] [illegible], or material [illegible] for this idealized M/M_p vs. θ/θ_p curve is shown in figure 3.

2.3 [illegible] of [illegible]

For the planned-base frame, shown figure 4, and for the elastic evaluation the moment, M, at any section will be:

$$M = -M_o + Py + Hx = -EI\, d^2y/dx^2 \qquad (2.3.1)$$

This leads to an expression for the deflection at any point as follows:

$$y = H/P \left\{ \sqrt{\frac{EI}{P}} \left[\sin \sqrt{\frac{P}{EI}}\, x - \tan \sqrt{\frac{P}{EI}}\, L \cos \sqrt{\frac{P}{EI}}\, x + \tan \sqrt{\frac{P}{EI}}\, L \right] - x \right\} \qquad (2.3.2)$$

Let P per column be defined as $P = \tau P_{cr} = \tau P_e$, where $P_{cR} = \pi^2 EI/4L^2$ (per column) for the pinned-base frame. Then the deflection y_o at x=L is:

$$y_o = \frac{H}{P} L \left[\frac{2}{\sqrt{\tau}\pi} \tan \frac{\sqrt{\tau}\pi}{2} - 1 \right] \qquad (2.3.3)$$

It can be seen from (2.3.3) that for a constant P the deflection is a linear function of H.

With the idealized moment-curvature curve, figure 2, the relation $M/M_e + P/P_e = 1$ defines the yield conditions and also must be satisfied after yielding has occurred and the deflection increased beyond the yield deflection. An elasto-plastic analysis, with a hinge forming at the top of the column, is used. A decrease in deflection after yielding has occurred will be elastic.

Then at yield:

$$\frac{P y_e + HL}{M_e} + P/P_e = 1 \qquad y_e = \frac{(1-\tau)M_e - HL}{P} \qquad (2.3.4)$$

Then:

$$H_{eR} = \frac{(1-\tau)}{\frac{2}{\sqrt{\tau}\pi} \tan \frac{\sqrt{\tau}\pi}{2}} \left(M_e/L \right) \qquad (2.3.5)$$

For the elastic range $H = k_{lr} y$, where k_{lr} is the reduced spring constant because of the axial load. As previously noted, for a constant P, the H vs. y relation is linear. Hence k_{lr} is constant for the constant P.

Then: $$K_{lR} = H/y = \frac{P}{L\left(\frac{2}{\sqrt{\tau}\pi} \tan \frac{\sqrt{\tau}\pi}{2} - 1\right)} = \frac{\tau \pi^2 EI/4L^3}{\left(\frac{2}{\sqrt{\tau}\pi} \tan \frac{\sqrt{\tau}\pi}{2} - 1\right)} \qquad (2.3.6)$$

By a graphical comparison this can be shown to reduce to:

$$W = -W^o + p\lambda + Hx = -EI\,c_5\lambda^3 \qquad (8.3.1)$$

$$K_{IR} = \frac{3EI}{L^3}(1-\tau) \qquad (2.3.7)$$

Thus:

$$y_{eR} = \frac{H_{eR}}{K_{IR}} = \left(\frac{1-\tau}{(1-\gamma)\frac{2}{\sqrt{\tau\pi}} + \tan\frac{\sqrt{\tau\pi}}{2}}\right)\left(M_e/3EI/L^2\right) \qquad (2.3.8)$$

Equations (2.3.5) and (2.3.8) for H_{er} and y_{er} will then define the yield conditions when axial load is included. For this information to be readily useable it must be possible to make a plot from which the yield deflection and resistance for any column and axial load can be taken. The relation of these depend on the relative values of P_e and P_{cr}. Thus a variation in the ratio of $\tau/\gamma = P_{cr}/P_e$ will cause a change in the yield deflection and yield resistance magnitudes. To represent this variation the yield loci for different values of the τ/γ ratio are plotted in dimensionless form in figure 6. The resistance path from the origin will be along a straight line, the slope of which is dependent only on the magnitude of γ. The intersection of this resistance path with the different yield loci will define the yield point for each τ/γ ratio. After yielding the slope will become negative. For the pinned-base column $y_e = M_e/3EI/L^2$ and $H_e = M_e/L$. In addition to yield loci for several ratios of τ/γ, resistance paths for several values of γ are also shown in figure 6.

The expression for y_{er} becomes indeterminate as $\gamma \to 1$. To determine y_{er} for $\gamma = 1$ and $\tau/\gamma \leq 1$ use the following expression:

$$y_{eR} = \frac{12(1-\tau)}{\gamma\pi^2}\left(M_e/3EI/L^2\right) \qquad (2.3.9)$$

For $\tau/\gamma \leq 1$ and $\gamma = 1$ y_{er} is also y_r.

To define the elastic portion of the resistance curve all that it is necessary to do is to choose the τ/γ locus corresponding to the column properties, and then follow the γ resistance path, corresponding to the load, out to the yield locus. The portion of the γ path between the origin and yield locus will be the elastic resistance path.

For values of $\tau/\gamma \geq 1$ the yield loci at the origin will be parallel to the γ resistance path corresponding to $\tau = 1$. Then $\tau = 1$, $(\gamma \leq 1)$, is the limiting

$$K_{IR} = \frac{3EI}{L^3}(1-\nu) \tag{8.3.4}$$

Then:

$$\gamma_{cr} = H_{cr}^{*} \cdot \left(\frac{(1-\nu)\frac{\pi^2}{5}\tan\left(\frac{\pi}{2}\right)}{1-\nu}\right)\left(\frac{M_c}{3EI/L^2}\right) \tag{8.3.5}$$

Simplifying and solving for the unit load during the yield sensitivity when axial load is included. For this information to be readily usable it must be possible to make a plot which delineates yield boundaries and determines the new values and which load can be taken. The definition of these depends on the stability values of λ^{*} and γ_{cr}. Then a variation in the ratio of λ^{*} will cause a change in the plastic buckling and plastic instance magnitudes. To investigate this variation the yield load may be plotted against the ratio of λ^{*} to γ_{cr} as in Figure 8. The resulting plot from the origin will be almost a straight line. The slope of which is dependent upon the variation of ν. The intersection of this curve with the ordinate will yield the plastic collapse load $\gamma_p = M_p/3EI/L^2$ and $\lambda^{*} = \gamma_{cr}$. In addition to yield load the general values of λ^{*} and γ_{cr} for various values of ν are also given in Figure 8.

The restraints for γ_{cr} become indeterminate as $\nu \to 1$. To investigate the case $\nu = 1$ and $\lambda^{*} \neq 1$ use the following expressions:

$$\gamma_{cr} = \frac{\pi^2 EI}{12(1-\nu)}\left(M_c/3EI/L^2\right) \tag{8.3.6}$$

For $\lambda^{*} \neq 1$ and $\nu = 1$ γ_{cr} is also γ_p.

To define the stability region of the derivations shown all that is necessary is to plot points for λ^{*} lines corresponding to the ultimate instability, and then for a particular ν value, corresponding to the 'line' with the yield locus. The portion of the λ^{*} path between the origin and yield locus will be the elastic resistance path.

If $\lambda^{*} = 1$ then yield and the stable will be unstable in the restraint $\nu = 1$. Then $\lambda^{*} \neq 1$ is an instability when axial load is included. For this information to be readily usable it must be possible to make a plot which delineates yield boundaries and determines the new values and which load can be taken. The definition of these depends on the stability values of λ^{*} and γ_{cr}. Then a variation in the ratio of λ^{*} will cause a change in the plastic buckling and plastic instance magnitudes. To investigate this variation the yield load may be plotted against the ratio of λ^{*} to γ_{cr} as in Figure 8. The resulting plot from the origin will be almost a straight line. The slope of which is dependent upon the variation of ν. The intersection of this curve with the ordinate will yield the plastic collapse load $\gamma_p = M_p/3EI/L^2$ and $\lambda^{*} = \gamma_{cr}$. In addition to yield load the general values of λ^{*} and γ_{cr} for various values of ν are also given in Figure 8.

The restraints for γ_{cr} become indeterminate as $\nu \to 1$. To investigate the case $\nu = 1$ and $\lambda^{*} \neq 1$ use the following expressions:

$$\gamma_{cr} = \frac{\pi^2 EI}{12(1-\nu)}\left(M_c/3EI/L^2\right) \tag{8.3.6}$$

For $\lambda^{*} \neq 1$ and $\nu = 1$ γ_{cr} is also γ_p.

To define the stability region of the derivations shown all that is necessary is to plot points for λ^{*} lines corresponding to the ultimate instability, and then for a particular ν value, corresponding to the 'line' with the yield locus. The portion of the λ^{*} path between the origin and yield locus will be the elastic resistance path.

vertical load for no positive horizontal resistance. Inelastic action will then begin at $y = 0$ and $y_f = 0$. For this case for $\tau = 1$, $y_{er} = y_f$. The slope of the negative resistance path for this case after yielding is the same as k_{2r} found for the same γ for any other value of τ/γ . This case is illustrated in figure 7.

When $\tau/\gamma < 1$ the yield loci do not start from the origin as shown in figure 6 and expressed by equation (2.3.9). The limiting load for no positive horizontal resistance is $\gamma = 1$. For $\gamma = 1$ the horizontal resistance is 0 until $y_{eR}/y_e = \frac{12(1-\tau)}{\gamma \pi^2}$ is reached; where the horizontal resistance then becomes negative. This case is illustrated in figure 8.

At the collapse deflection $M/M_e + P/P_e = 1$.

and: $$P y_f/M_e + P/P_e = 1 \qquad y_f = \frac{12(1-\tau)}{\gamma \pi^2}\left(M_e/3EI/L^2\right) \quad (\tau \text{ and } \gamma \text{ not to exceed } 1) \qquad (2.3.10)$$

The resistance path between the yield point and the collapse deflection will also be a straight line; the slope being determined by γ .

The spring constant, k_{1r}, up to the yield point is $K_{1R} = 3EI/L^3 (1-\gamma)$. The spring constant k_{2r} between the yield point and the collapse deflection is

$$K_{2R} = \frac{-K_{1R}}{(y_f/y_{eR} - 1)} \quad .$$

The value of y_{er}, H_{er} and y_f when put into dimensionless form are:

$$y_{eR}/y_e = \frac{(1-\tau)}{(1-\gamma)\frac{2}{\sqrt{\gamma}\pi} + AN\frac{\sqrt{\gamma}\pi}{2}} \qquad y_f/y_e = \frac{(1-\tau)12}{\gamma \pi^2} \qquad (2.3.11)$$

$$H_{eR}/H_e = \frac{(1-\tau)}{\frac{2}{\sqrt{\gamma}\pi} + AN\frac{\sqrt{\gamma}\pi}{2}}$$

2.4 Resistance of Fixed-Base Frame

For the fixed-base frame, shown figure 5, the moment, M, at any section is:

$$M = -M_o + Hx + Py = -EI\, d^2y/dx^2$$

The solution of this equation and the substitution of $\tau = \gamma_{er}$ and

$$\frac{M^o}{M_{fe}^o} = \frac{\frac{4\pi}{3}\tan\frac{\pi}{12}}{(1-\alpha)} \qquad \frac{\lambda^o}{\lambda_{fe}^o} = \frac{(1-\alpha)\frac{\pi}{12}\tan\frac{\pi}{12}}{(1-\alpha)} \qquad \frac{\lambda^o}{\lambda_{fe}^o} = \frac{4\pi^2}{(1-\alpha)12}$$

[12.12]

3.4 Buckling of Fixed-Base Pylon

For the fixed-base pylon, given figure 3, the moment M^o at any section is:

$$M = -W^o + Hx + P\lambda = -EI\, q_2\lambda/q x_2$$

The solution of this equation and the substitution of $P = \lambda L^2/4\pi^2$ and

$$\frac{M^o}{M_{fe}^o} = \frac{\frac{4\pi}{3}\tan\frac{\pi}{12}}{(1-\alpha)} \qquad \frac{\lambda^o}{\lambda_{fe}^o} = \frac{(1-\alpha)\frac{\pi}{12}\tan\frac{\pi}{12}}{(1-\alpha)} \qquad \frac{\lambda^o}{\lambda_{fe}^o} = \frac{4\pi^2}{(1-\alpha)12}$$

[12.12]

$$\frac{M^o}{M_{fe}^o} = \frac{\frac{4\pi}{3}\tan\frac{\pi}{12}}{(1-\alpha)} \qquad \frac{\lambda^o}{\lambda_{fe}^o} = \frac{(1-\alpha)\frac{\pi}{12}\tan\frac{\pi}{12}}{(1-\alpha)} \qquad \frac{\lambda^o}{\lambda_{fe}^o} = \frac{4\pi^2}{(1-\alpha)12}$$

[12.12]

$P_{CR} = \pi^2 EI/L^2$ will lead to the following expression for the value of the deflection y_o at x = L:

$$y_o = HL/P\left[\frac{2}{\sqrt{\tau}\pi} \tan\frac{\sqrt{\tau}\pi}{2} - 1\right] \quad , \qquad (2.4.1)$$

which is the same as for the pinned-base frame. However, it is noted that for the same column section and length the value of P_{cr} for the fixed-base frame is four times that for the pinned-base. An elasto-plastic analysis is used with plastic hinges assumed to form simultaneously at the top and bottom of column. Following the same reasoning as for the pinned-base frame the following equations for the fixed-base frame are arrived at:

$$H_{eR} = \frac{(1-\tau)}{\frac{2}{\sqrt{\tau}\pi}\tan\frac{\sqrt{\tau}\pi}{2}}\left(2M_e/L\right) \qquad y_{eR} = \frac{(1-\tau)}{(1-\gamma)\frac{2}{\sqrt{\tau}\pi}\tan\frac{\sqrt{\tau}\pi}{2}}\left(M_e/6EI/L^2\right) \qquad (2.4.2)$$

$$K_{1R} = 12EI/L^3\,(1-\gamma) \qquad y_f = \frac{12(1-\tau)}{\gamma\pi^2}\left(M_e/6EI/L^2\right)$$

$$K_{2R} = \frac{-K_{1R}}{(y_f/y_{eR} - 1)}$$

When put into dimensionless form these are:

$$H_{eR}/H_e = \frac{(1-\tau)}{\frac{2}{\sqrt{\tau}\pi}\tan\frac{\sqrt{\tau}\pi}{2}} \qquad y_{eR}/y_e = \frac{(1-\tau)}{(1-\gamma)\frac{2}{\sqrt{\tau}\pi}\tan\frac{\sqrt{\tau}\pi}{2}} \qquad (2.4.3)$$

$$K_{2R}/K_1 = \frac{(1-\gamma)}{(y_f/y_{eR}-1)} \qquad K_{1R}/K_1 = (1-\gamma) \qquad y_f/y_e = \frac{12(1-\tau)}{\gamma\pi^2}$$

Equations (2.4.3) are of the same form as the corresponding ones for the pinned-base frame. Therefore the resistance curves for both the fixed and pinned-ended frames, when in the dimensionless form, are the same and figure 6 may also be used for the fixed-base frame.

2.5 Use of Resistance Curves for Determining Resistance for Use in Step by Step Numerical Solution

Typical families of resistance curves for τ/γ = 1 and 1/2 are illustrated in figures 7 and 8.

When the load P, including dead load, remains constant the resistance will follow along the appropriate γ resistance path. However, if P is a varying quantity the resistance will undergo a transition between the different paths, but not always in a direct manner. The possible methods of change are covered in the following cases.

Case I - Structure not yielded.

P can vary in any manner, increase or decrease, and at a given y the resistance for use in the numerical procedure will be that corresponding to the value of γ at the given y. This is illustrated in figure 9.

Case II - Structure yielded and there is a decrease in P occurring as a step function.

Let P vary as shown in figure 10. In the dynamic analysis the change in P takes place at displacement y_1 at a given instant of time. In the numerical solution of the dynamic problem when P changes, changes in curvature and deflection do not take place until some later time. Therefore because of the time element there will be no instantaneous change in moment and the moment at the column end will be maintained at $M = (1 - \tau_1) M_e$ until after t_1. To maintain the moment at this value, M will have to instantaneously increase to some value M_2 at t_1.

Thus: $$M_2/M_e = \left[(1-\tau_1) - \frac{\gamma_2 \pi^2 y_1}{12 y_e}\right] \qquad (7.5.1)$$

τ_1 for load before t_1
γ_2 for load after t_1
y_1 = y at t_1

This value of M_2 will be less than the M of the γ_2 path for the deflection y_1 at the load step. From this value of M_2 at y_1 the structure will act elastically until the γ_2 path is intersected, and at the elastic slope of γ_2, and will again go plastic when the γ_2 curve is intersected. A graphical method for obtaining the value of M_2 is shown in figure 11. However, in the numerical solution, if the deflection at the end of the first time interval after the load change is much larger than the deflection at the load change, the small amount of elastic action may be neglected as it would then introduce little error. If the elastic action is to be neglected, at t_1 go vertically from the γ_1 to the γ_2

curve.

Case III - Structure yielded and P increasing.

In this case $M/M_o + P/P_o = 1$ will be maintained during the change. As P increases P/P_o increases and therefore M/M_o must decrease. To accomplish the decrease, M must decrease to the value corresponding to the new value of γ at the particular deflection. Therefore, as P increases, whether as step function or by constantly varying, go downward directly to the appropriate γ curve at the particular deflection (figure 11). When the γ resistance path passes its failure deflection the horizontal resistance will no longer be positive, but negative.

Case IV - Structure yielded and P decreasing by continuous variation.

As was shown in figure 11 for the step function, it takes very little additional deflection after a large decrease in P to fully develop the additional elastic resistance and have the structure again go plastic. Consequently for the numerical procedure where P is continuously decreasing go directly to the resistance path at the particular deflection in a manner similar to figure 9 to determine the horizontal resistance.

2.6 Comparison of Effect of Vertical Load with Approximate Method

In reference 1 an approximate method was given for allowing for the vertical load on a frame. This method consists of reducing the moment carrying capacity of the unloaded frame (no vertical load) by the amount of the moment created by the vertical load and deflection. The preceding method, developed for allowing for the vertical load, differs from the approximate method in that it allows also for a decrease in yield moment due to the axial load on the column section. The slope of the elastic portion of the resistance was found to be less than that of the approximate method for the same axial load.

A comparison of the two methods is shown in figures 15 and 16. The difference between the two methods is also dependent on the value of the τ/γ ratio.

III. EFFECT OF VERTICAL LOAD ON NATURAL FREQUENCY OF VIBRATION

3.1 Frequency and Period

If the mass of the girder and floor load is taken to be large in comparison to the column weight, and/or a portion of the column weight included in the girder weight, the natural frequency of vibration will be: $\omega = \sqrt{K/m}$.

As previously noted $k_{1r} = 3\pi I/L^3 (1 - \gamma)$ for pinned-end frame and $12\pi I/L^3 (1 - \gamma)$ for fixed-end frame. The mass will be $\gamma_{w+}\pi^2 EI/4g L^2$ for pinned-base and $\gamma_{w+}\pi^2 EI/g L^2$ for fixed-base. Then the natural frequency for both pinned and fixed-bases will be:

$$\omega = \sqrt{\frac{12\, g\, (1-\gamma_{w+})}{\pi^2 L\, \gamma_{w+}}} \qquad (3.1.1)$$

In the elastic range, when live vertical load is added, the frequency of vibration will be:

$$\omega_1 = \sqrt{\frac{12\, g (1-\gamma_{tot\,AL})}{\pi^2 L\, \gamma_{w+}}} \qquad (3.1.2)$$

The frequency not allowing for reduction in I (this later being used as a multiplier) is:

$$\omega_o = \sqrt{\frac{12g}{\pi^2 L \gamma_{w+}}} \qquad \omega_1 = \omega_o \sqrt{(1-\gamma_{tot\,AL})} \qquad (3.1.3)$$

If t_1 is expressed in terms of T ($1/\omega_o$), then:

$$T = \frac{2\pi}{\omega_o \sqrt{(1-\gamma_{tot\,AL})}} \qquad t_1/T = \frac{N\sqrt{(1-\gamma_{tot\,AL})}}{2\pi} \qquad (3.1.4)$$

and $t_1/T_o = N/2\pi$;

where T_o is period of structure not including effect of any vertical load.

$$t_1/T_o = \frac{t_1}{T\sqrt{(1-\gamma_{tot\,AL})}} \qquad (3.1.5)$$

$$f_1\sqrt{T_0} = \frac{1}{t}\sqrt{\frac{(1-r^{2n+2})}{(1-r^{2n+1})}} \qquad (5.1.6)$$

and $f_1\sqrt{T_0} = N\sqrt{\pi S}$;

$$T = \frac{\pi S}{N^2(1-r^{2n+1})} \qquad f_1\sqrt{T_0} = \frac{\pi S}{N\sqrt{(1-r^{2n+1})}} \qquad (5.1.7)$$

Si f_1 è espressa in unità di $\sqrt{\omega_0}$, allora:

$$\omega_0 = \sqrt{\frac{\pi^2 L^{2n+1}}{\rho S^2}} \qquad \omega_1 = \omega_0\sqrt{(1-r^{2n+1})} \qquad (5.1.8)$$

Infine:

$$\omega_1 = \sqrt{\frac{\pi^2 L^{2n+1}}{\rho S^2 (1-r^{2n+1})}} \qquad (5.1.9)$$

Nel caso di filtro misto si ha:

$$\omega = \sqrt{\frac{\pi^2 L^{2n+1}}{\rho S^2 (1-r^{2n})}} \qquad (5.1.10)$$

Nel caso di filtro passa-basso si ha:

$$\omega = \sqrt{\frac{\pi^2 L^{2n}}{\rho S^2 (1-r^{2n})}} \qquad (5.1.11)$$

Nel caso di filtro passa-banda si ha: $\omega = \sqrt{K/m}$.

Nel caso di filtro passa-banda misto si ha:

$$\omega = \sqrt{\frac{\pi^2 L^{2n+1}}{\rho S^2 (1-r^{2n+2})}} \qquad (5.1.12)$$

Nel caso di filtro passa-banda passa-basso si ha:

$$\omega = \sqrt{\frac{\pi^2 L^{2n}}{\rho S^2 (1-r^{2n+1})}} \qquad (5.1.13)$$

IV. [illegible] α OF TYPE SECTION M VS. θ RELATION IS GREATER THAN 0

4.1 Form of Resistance

Instead of a flat top M/M_e vs. θ/θ_e diagram as represented by figure 7, let the section M vs. θ relation be such that it is better given by a M/M_e vs. θ/θ_e relation shown by figure 14. This type M/M_e vs. θ/θ_e diagram might represent:

(1) an idealization of the actual M vs. θ diagram.

(2) The M vs. θ curve for an idealized H section of a material with a stress-strain curve such as figure 15.

Up to and including the yield point, the form of the resistance will be the same as before.

$$y_{eR}/y_e = \frac{(1-\tau)}{(1-\tau)\frac{2}{\sqrt{\tau}\pi} + \tan\frac{\sqrt{\tau}\pi}{2}} \qquad H_{eR}/H_e = \frac{(1-\tau)}{\frac{2}{\sqrt{\tau}\pi} + \tan\frac{\sqrt{\tau}\pi}{2}}$$

Beyond the yield point the resistance will be of a different form. The case of the idealized H section is chosen to illustrate the general form of the horizontal resistance curves after yielding. The M/M_e vs. θ/θ_e diagram for such an idealized section, with a value of $\alpha = 0.2$, is shown in figure 16. It is noted that for large values of θ/θ_e the axial load on the idealized section does not affect the M/M_e vs. θ/θ_e relation. However, for an actual section there would be a small difference, and the curve for the actual section would lie below and to the right of this idealized curve. But as θ/θ_e increases, the two approach each other.

To show the effect of the vertical load, and also the effect of the ratio between P_e and P_{cr}, the case of the fixed-base idealized H section has been worked out for $\alpha = 0.2$. γ has been taken as 0, 0.1, 0.2 and 0.3. For each of these γ values, τ/γ was taken as 1 and 2. To obtain the relation between M/M_e and y/y_e a numerical procedure, as outlined in reference 7, was used. The column was divided into eight segments and because of the assumed symmetry for this case only four segments, or one half of the column, were worked with. To work the

$$\frac{\sum \frac{M_u}{\phi} \tan \frac{\pi}{n}}{\frac{\pi}{n}} = \frac{(1-\alpha)}{(1-\frac{1}{n})} \left(\tan \frac{\pi}{n}\right) \qquad M_{cr} = \frac{\sum \frac{M_u}{\phi} \tan \frac{\pi}{n}}{(1-\alpha)}$$

same as before.

Up to and including the yield point, the form of the resistance will be the

struts onto each as figure 12.

(2) The n arcs a' cause the n radial cracks to open, thereby splitting the column

(1) The tangential portion of the column n arcs a displace

numerical procedure a deflected shape and end moment were chosen. For the chosen moment and estimated deflection a new deflection shape was worked out. If the derived deflection shape did not agree with the assumed deflection shape the values were iterated, maintaining the end moment fixed at the chosen value. Usually, if the value of the assumed deflection y_o was even close to the correct value for the chosen end moment, the derived value of the deflection y_o and M from only one iteration would lie on or very close to the resistance curve.

It can be seen from figure 17 that for large values of y/y_e the value of M/M_e is relatively independent of the value of τ/γ, but highly dependent on γ; as the curves for $\tau = \gamma$ and $\tau = 2\gamma$ approach each other as y/y_e becomes large. This can also be seen by looking at the M/M_e vs. θ/θ_e diagram, figure 16. For the larger values of M/M_e the value of θ/θ_e is independent of the value of τ; but for a lower range, just above the yield point, the value of θ/θ_e depends on the value of τ. For the larger deflections the inelastic action will approach the center of the columns and much of the column M/M_e will be above the range of dependence on τ. Consequently, for larger deflections the M/M_e vs. y/y_e will primarily depend on γ, not τ/γ. However, for smaller values of y/y_e the value of τ will exercise a great influence on the shape of the M/M_e vs. y/y_e curves as also shown by figure 17.

4.2 Slope of Resistance Curves

It is noted in figure 17 that for the value of $\gamma = \alpha$ the M/M_e vs. y/y_e curve approaches a horizontal asymptote for the large values of y/y_e. This can also be shown by the following: To find the (γ, α) relation for the resistance curve to approach a horizontal asymptote consider yielding progressed up to center. This is only approximate, as at center $\theta = \theta_e$; but yielding does approach very close to center for this work hardening material as was found in working out numerical examples. Then:

$$\delta M_o = 1/2\, P(\delta y_o) \qquad (4.2.1)$$

$$\Omega M^0 = \lambda^2 \, b(\Omega \lambda^0) \qquad (4.7)$$

and δM at any point is: $\delta M = -\delta M_o + P(\delta y)$

and $d^2(\delta y)/dx^2 = -\delta M/EI\alpha$,

from which:

$$\delta y = -\delta M_o/P \cos\sqrt{\frac{P}{EI\alpha}}x + B\sin\sqrt{\frac{P}{EI\alpha}}x + \delta M_o/P \quad . \qquad (4.2.2)$$

at $x=L$
and $x=0$ $\quad d(\delta y)/dx = 0 = \delta M_o/P \sin\sqrt{\frac{P}{EI\alpha}}x + B\cos\sqrt{\frac{P}{EI\alpha}}x$;

from which B = 0. Therefore to satisfy the slope at x = L, $\sin\sqrt{P/EI\alpha}\,L$ must then also be equal to 0, and for compatibility of deflection; $\cos\sqrt{P/EI\alpha}\,L/2 = 0$ and $\cos\sqrt{P/EI\alpha}\,L = -1$.

Then $\sqrt{P/EI\alpha}\,L$ must equal π , and $\sqrt{\frac{\gamma\pi^2}{\alpha}} = \pi$. To fulfill this requirement γ must equal α.

As inelastic action was assumed to penetrate to the center the value of $\gamma = \alpha$ will be slightly in error. However, the value $\gamma = \alpha$ is sufficiently close for use as a collapse criteria. Then for $\gamma \leq \alpha$ the M/M_e vs. y/y_e curve will everywhere have a slope ≥ 0. For $\gamma \leq \alpha$, some failure criteria other than the point at which the dead load will cause the structure to continue to deflect, will have to be established.

For relatively large deflections, assuming inelastic action approaches the center, the slope of the M/M_e vs. y/y_e curve, for γ other than $\gamma = \alpha$ may be found in a similar manner.

$$\delta M = -\delta M_o + \delta H\, x + (\delta y)\, P \quad , \qquad (4.2.3)$$

from which:

$$\delta y = -\left(\delta M_o/P - \delta H\, x/P\right)\cos\sqrt{\frac{P}{EI\alpha}}x + \frac{\delta H}{P\sqrt{\frac{P}{EI\alpha}}}\sin\sqrt{\frac{P}{EI\alpha}}x + \frac{(\delta M_o - \delta H\, x)}{P}$$

and $d(\delta y)/dx = 0$ At $x = 0$ & L .

Taking the value of $d(\delta y)/dx\big|_{x=L}$, and eliminating δM_o by use of the relation $\delta M_o = \delta H L/2 + P(\delta y_o)/2$ and substitution of $\sqrt{P/EI\alpha} = \sqrt{\gamma/\alpha}\,\pi/L$, gives an expression for the slope for relatively large values of y/y_e of:

$$\delta W = -\delta W^0 + P(\delta\eta)$$

and $\delta\eta$ at one point has

$$q_{\frac{1}{2}}(\delta\eta)\Big/_{\delta x_2} = -\delta W \Big/ EI\alpha \quad ,$$

from which we:

$$\delta\eta = -\delta W^0 \frac{1}{P}\cos\sqrt{\frac{EI\alpha}{E}}x + B\sin\sqrt{\frac{EI\alpha}{E}}x + \delta W^0 \frac{1}{P} \qquad (4-1a)$$

and $x=0 \quad q(\delta\eta)\Big/_{\delta x} = 0 = \delta W^0 \frac{1}{P}\sin\sqrt{\frac{EI\alpha}{E}}x + B\cos\sqrt{\frac{EI\alpha}{E}}x$)

or $x=\ell$

then also be zero, or α must be such that $\cos\sqrt{\frac{EI\alpha}{E}}\ell = 0$

and $\cos\sqrt{\frac{EI\alpha}{E}}\ell = -1$.

Then $\sqrt{\frac{EI\alpha}{E}}\ell$ must equal π, and $\alpha = \frac{\pi}{\lambda\ell}$, the Euler rule

constant λ must equal α.

$\lambda = \alpha$ will be slightly in error. However, the value $\lambda = \alpha$ is sufficiently close

for use as a working estimate. Since for $\lambda \neq \alpha$ the δW^0 curve will

approximate $\lambda = \alpha$ for $\lambda \neq \alpha$, more bulging deflection occurs than the

natural α which the same load will cause the structure to assume in buckling.

will have to be determined.

- for relatively large deflections, requiring involute relations

is a similar manner.

$$\delta W = -\delta W^0 + \delta H x + (\delta\eta)\, P \qquad (4-3a)$$

Then we have:

$$\delta\eta = -\left(\delta W^0 - \delta H\frac{1}{P}\right)\cos\sqrt{\frac{EI\alpha}{E}}x + \delta H\frac{1}{P}\sin\sqrt{\frac{EI\alpha}{E}}x + \frac{1}{P}\left(\delta W^0 - \delta H x\right)$$

and $q_{\frac{1}{2}}(\delta\eta)\Big/_{\delta x} = 0 \quad \delta H + x = 0 \text{ at } \Gamma$.

Factor the sums of $q(\delta\eta)\Big/_{\delta x}\Big|_{x=\Gamma}$, and eliminate δW^0 as one of the relation

expression for the given for relatively large values of λ/α as:

$$\delta W^0 = \delta H\Gamma + P(\delta\eta^0)\Big/_{\delta x}$$

$$\frac{d\left(\frac{H}{H_e}\right)}{d\left(\frac{y}{y_e}\right)} = \frac{\frac{\gamma\pi^3}{24}\left[1-\cos\sqrt{\frac{\gamma}{\alpha}}\pi\right]\left[\sqrt{\frac{\gamma}{\alpha}}\right]\left[\sin\sqrt{\frac{\gamma}{\alpha}}\pi\right]}{\left[-1-\frac{1}{2}\left(1-\cos\sqrt{\frac{\gamma}{\alpha}}\pi\right)+\frac{\sin\sqrt{\frac{\gamma}{\alpha}}\pi}{\sqrt{\frac{\gamma}{\alpha}}\pi}\right]\left[\sqrt{\frac{\gamma}{\alpha}}\sin\sqrt{\frac{\gamma}{\alpha}}\pi\right]-2\left[\cos\sqrt{\frac{\gamma}{\alpha}}\pi-1\right]} \quad (4.7.4)$$

The comparison of this equation with figure 17 is good.

TABLE I

	Slope from equation	Slope from figure 17 for $y/y_e = 9$
0.1	-0.063	-0.07
0.2	0	0.01
0.3	0.105	0.10

Figure 17 in the dimensionless form will also hold for pinned-base frame.

$$\frac{q(\lambda^m)}{q(\lambda^{m+1})} = \frac{\left[\frac{\lambda^m}{\pi}\right]\left[\sin\frac{\lambda^m}{\pi}\right]\left[\frac{\lambda^m}{\pi}\right]\left[1-\cos\frac{\lambda^m}{\pi}\right]}{\left[-1-\frac{\lambda^m}{\pi}\left(1-\cos\frac{\lambda^m}{\pi}\right)+\sin\frac{\lambda^m}{\pi}\right]\left[\frac{\lambda^m}{\pi}\sin\frac{\lambda^m}{\pi}\right]-\left[\cos\frac{\lambda^m}{\pi}-1\right]}$$

V. HORIZONTAL RESISTANCE OF STRUCTURE WHEN α OF THE STRUCTURE RESISTANCE, NOT M/M_e VS. θ/θ_e, IS NOT 0

5.1 Form of Resistance

The case of structure resistance of the form shown by figure 18 is treated in this section. As before, the yield point is defined by:

$$y_{eR}/y_e = \frac{(1-\gamma)}{(1-\gamma)\left(\frac{2}{\sqrt{\gamma}\pi} + AN\frac{\sqrt{\gamma}\pi}{2}\right)} \qquad H_{eR}/H_e = \frac{(1-\gamma)}{\frac{2}{\sqrt{\gamma}\pi} + AN\frac{\sqrt{\gamma}\pi}{2}}$$

The second spring force, k_{gr}, is taken to become effective at y_{er}. After yield the moment of P multiplied by additional deflection must be subtracted from the $\gamma = 0$ resistance curve. For vertical load, $\delta M_o = \gamma\pi^2 EI(\delta y)/2L^2$; which must be subtracted from $\delta M_o = \alpha K_1 L(\delta y)/2$ to determine the change in M.

Net
$$\begin{aligned} \delta M_o &= \left[\alpha - \gamma\pi^2/12\right] K_1 L(\delta y)/2 \qquad \text{(fixed-base)} \\ &= \left[\alpha - \gamma\pi^2/12\right] K_1 L(\delta y) \qquad \text{(pinned-base)} \end{aligned} \tag{5.1.1}$$

Thus the effective spring constant after yield for both fixed and pinned-base end frames will be: $\left[\alpha - \gamma\pi^2/12\right] K_1$. α is (x) and (y) .

The collapse deflection will then be defined by:

$$y_f/y_e = \frac{(1-\gamma)}{\frac{2}{\sqrt{\gamma}\pi} + AN\frac{\sqrt{\gamma}\pi}{2}} \left[\frac{1}{(1-\gamma)} + \frac{1}{(-\alpha + \gamma\pi^2/12)}\right] \tag{5.1.2}$$

The range of validity of this expression is for values of α less than $\gamma\pi^2/12$. For values of $\alpha \geq \gamma\pi^2/12$, a failure deflection as defined in the introduction will not be reached.

The form of the reduced resistance curves is the same as in section II. The only difference from section II is the slope after yield and collapse deflection. A typical curve is shown in figure 19.

VI. COMPUTATION OF RESPONSE OF STRUCTURE

6.1 Discussion of Methods

For known values of $(\gamma_1, \gamma_{wt}, \Delta_1 \& t_1)$ applied to a structure the numerical method described in reference 3 may be used to compute the response. Reference 4 contains comparative information on other numerical methods. When the vertical time dependent load occurs as a step function, analytical equations may be used to compute the response. However, if the vertical load is continuously varying, or if it is desired to completely trace out the motion the numerical method is much more advantageous. The refinement here to the numerical method of reference 3 is in the method of obtaining the horizontal resistance curves. Units used in the numerical method are:

Quantity	Terms of	Quantity	Terms of
$\ddot{y}/y_e$	ω_o^2	t	$1/\omega_o$
y/y_e, Δ_t/R_e & R/R_e	Dimensionless	m	k_1/ω_o^2
$\dot{y}/y_e$	ω_o		

The first step towards solving the problem is to establish a series of γ resistance curves, such as figures 7 and 8, covering the range of vertical loads to be encountered. For the flat top section moment-curvature relation of section II and for the case where the structure resistance after yield is a straight line, section V, but not horizontal, the construction of these curves is very easy. But for the inclined moment-curvature relation after yield, section IV, the construction of a set of resistance curves is not so easy. A typical set of these was shown in figure 17. The method of obtaining these was outlined in section 4.1. After the resistance curves are constructed the numerical step by step process can be started. At each time interval the values of y and γ_{total} at that instant determine R. The method of transition between the various resistance curves was shown in section 4.3 and figure 11. This step by step procedure traces out the deflection, velocity and acceleration at each time interval. The

5.1 Discussion of results

(T, ρ_{mix}, ψ)

accuracy depends on the chosen time interval and beta value used (reference 3). For rapid approximations beta equal to 0 may be used. Also this numerical method will give the maximum deflection and motion thereafter and will detect if structure is unstable.

When the vertical time dependent load occurs as step function the analytical equations can be used to give the response. For more than an isolated point of the response the numerical method still has advantages; especially if the deflection at the end of the load pulse is greater than the yield deflection. The analytical equations are used in section 8.5 where the same equation constants can be used several times. The procedure used in section 8.2 is slightly modified in that at the end of the load pulse the kinetic energy of the system is used to match with the resistance work of the structure to determine what the additional deflection will be after the end of the load pulse and to determine if the structure is stable under the applied loads. Using the energy in this manner does not determine the time to reach the maximum deflection.

VII. [illegible] CONSTANT VERTICAL LOAD TO PRODUCE A GIVEN [illegible] DEFLECTION

7.1 Summary of Section

Prof. N.M. Newmark, University of Illinois, has devised a method for determining an approximate equivalent uniform resistance to produce a maximum deflection equal to some predetermined value for the case where k_g of the structure $\neq 0$ but of constant value. In this section Prof. Newmark's method is taken and adapted to the case of the frame with constant vertical loads; i.e., set up in terms of the structural properties when the effect of the vertical load on the spring constants and yield point is considered. After computation of certain quantities pertaining to the structure, reference 5 can be used to find the load-time relation for the structure for horizontal loads occurring as step function, initial peak, terminal peak and intermediate peak. Also the error if this approximate uniform equivalent method, for the case of maximum deflection equal to collapse deflection, is shown and a recommendation for a statistical correction factor is given. The correction factor covers the range of t_1/T_0 between 0.1 and 1.0. This method is for a rapid approximation of the responses when dead load is to be taken into account and vertical time dependent load not included.

7.2 Case I - Maximum Deflection Equal to Collapse Deflection (Fixed and Pinned-Bases)

The meaning of an equivalent uniform resistance and relation of the quantities involved is illustrated in figure 20. As before:

$$y_{eR}/y_e = \frac{(1-\tau)}{(1-\gamma)\left(\frac{2}{\sqrt{\tau}\pi} + AN\frac{\sqrt{\tau}\pi}{2}\right)} \qquad H_{eR}/H_e = \frac{(1-\tau)}{\frac{2}{\sqrt{\tau}\pi} + AN\frac{\sqrt{\tau}\pi}{2}}$$

$$y_f/y_e = \frac{12(1-\tau)}{\gamma\pi^2} \quad (\text{FOR } \alpha = 0)$$

$$\text{or } y_f/y_e = \frac{(1-\tau)}{\frac{2}{\sqrt{\tau}\pi} + AN\frac{\sqrt{\tau}\pi}{2}}\left[\frac{1}{(1-\tau)} + \frac{1}{(-\alpha + \gamma\pi^2/12)}\right] \quad \text{(as appropriate for } \alpha \neq 0\text{)}$$

k designation is (+) (-).

$$\frac{\lambda_{max}}{\lambda_0} = \frac{(1-\alpha)}{\left(\frac{\pi}{2}+\tan\frac{\pi}{2}\right)} \qquad \frac{M_{max}}{M_0} = \frac{\frac{\pi}{2}+\tan\frac{\pi}{2}}{(1-\alpha)}$$

$$\frac{\lambda_t}{\lambda_0} = \frac{\pi}{2(1-\alpha)} \quad (\text{for } \alpha = 0)$$

$$\frac{\lambda_{max}}{\lambda_0} = \frac{\frac{\pi}{2}}{\frac{\pi}{2}+\tan\frac{\pi}{2}} \left[(1-\alpha) + \frac{(-\alpha+\frac{\pi}{2})^2}{1} \right] \qquad \text{for } \alpha < 1$$

λ denotation is $\frac{(x)}{(-)}$.

$$x = \frac{K_{2R}}{K_{1R}} = -\frac{1}{\left(y_f/y_{eR} - 1\right)} \qquad H_{eq}/H_e = (1-a)H_e = \frac{(1-a)(1-\tau)}{\frac{2}{\sqrt{\tau}\pi}\tan\frac{\sqrt{\tau}\pi}{2}} \qquad (7.2.1)$$

$$y_{eq}/y_e = (1-a)y_{eR} = \frac{(1-a)(1-\tau)}{\frac{2}{\sqrt{\tau}\pi}\tan\frac{\sqrt{\tau}\pi}{2}} \qquad a = \frac{1-\sqrt[3]{1-x}}{x} \qquad (7.2.2)$$

$$y_f/y_{eq} = X_m/X_y \quad \text{(Reference) (5 Designation)}$$

The ratio t_1/T is used as a parameter in reference 5. t_1 is the duration of the load pulse in seconds. T in this case is: $2\pi/\omega_1 = 2\pi/\omega_0\sqrt{1-\gamma_{total}}$

The procedure for use of reference 5 is to compute the ratio X_m/X_y. Then if the time t_1 is known the ratio t_1/T can be computed. From the appropriate chart of reference 5 for the type load pulse the value of β that will just cause the maximum deflection to be equal to the collapse deflection can be taken.

The factor β is equal to F_{eq}/Δ_1. If the magnitude of the average of the load instead of t_1 is known the value of t_1/T that will just cause collapse can be found.

7.3 Case II - Where the Desired Maximum Deflection is Less Than the Collapse Deflection (Fixed and Pinned-Base)

The quantities involved are illustrated in figure 21.

As before: $y_{eR}/y_e = \text{SAME}$ $\quad H_{eR}/H_e = \text{SAME}$ $\quad x = K_{2R}/K_{1R} = -\dfrac{1}{\left(y_f/y_{eR} - 1\right)}$

$$a = \frac{1-\sqrt[3]{1-x}}{x}$$

$$y_f/y_e = \frac{12(1-\tau)}{\gamma\pi^2} \quad (\alpha = 0) \quad \underline{\text{OR}} \quad y_f/y_e = \frac{(1-\tau)}{\frac{2}{\sqrt{\tau}\pi}\tan\frac{\sqrt{\tau}\pi}{2}}\left[\frac{1}{(1-\tau)} + \frac{1}{(-\alpha+\gamma\pi^2/12}\right] \quad (\text{for } \alpha \neq 0)$$

Then:

$$H_{eq}/H_e = \frac{(1-\tau)}{\frac{2}{\sqrt{\tau}\pi}\tan\frac{\sqrt{\tau}\pi}{2}}\left[1 - a\,\frac{\left(y_f/y_{eR} - 1\right)}{\left(y_f/y_{eR} - 1\right)}\right] \qquad A = \frac{\left(y_m/y_{eR} - 1\right)}{\left(y_f/y_{eR} - 1\right)} H_{eR}$$

$$y_{eq}/y_e = y_{eR}/y_e\left[1 - \frac{aA}{H_{eR}}\right] = \frac{(1-\tau)}{(1-\tau)\frac{2}{\sqrt{\tau}\pi}\tan\frac{\sqrt{\tau}\pi}{2}}\left[1 - \frac{aA}{H_{eR}}\right] \qquad t_1/T = \frac{t_1/2\pi}{\sqrt{\frac{12g(1-\gamma_{total})}{\pi^2 L\,\gamma_{wt}}}}$$

$$y_m/y_{eq} = X_m/X_y \quad \text{(reference) (5 Designation)}$$

Here again the ratio of X_m/X_y will be computed. Then the appropriate charts in reference 5 can be entered to find the t_1/T ratio for a specified β ; or if

The question involved are illustrated in Figure 21.

the t_1/T ratio is known the value of β determined that will cause the maximum deflection to be equal to y_m. $\beta = M_{eq}/\Delta_1$.

7.4 Correction Factor

In section VIII plots are made of the average horizontal and vertical load vs. the t_1/T_o ratio that will produce the maximum deflection equal to the collapse deflection. Two different structures are analyzed. One is with $\tau = 1/2\gamma$, or P_e twice P_{cr}, and with dead load of 0.1 P_{cr} and 0.05 P_e. The other one is with $\tau = 2\gamma$, or P_e one half of P_{cr}, and with a dead load of 0.2 P_{cr} and 0.4 P_e. These two cases cover a wide range of an elastic column with a very light dead load to an inelastic column with a much heavier dead load. These structures are subjected to load functions in the form of step, initial and terminal peak pulses.

Values of Δ_1/M_e for different values of t_1/T_o have been computed using the approximate equivalent uniform resistance and compared with the values from section VIII for γ_1 equal to 0. The ratio t_1/T_o is used as a base of comparison in section VIII and thus the ratio t_1/T used in the approximate method has to be converted to t_1/T_o. A plot of the % error found for the range of t_1/T_o between 0.1 and 1.0 is shown in figure 22. It is shown that the error for all cases at a given t_1/T_o ratio is not a constant amount, but that a general trend is followed without a large spread. The spread in the % of error could possibly be from both error in reading the charts of reference 5 and in the structure response itself. The error is given in percentage of correct Δ_1/M_e at a particular t_1/T_o ratio.

A value of the error in the range of t_1/T_o between 0.1 and 1.0 that fits the average of the cases worked out is: % error = 12 $(1 - (t_1/T_o)^{.5})$ - 4 (parabolic). Although this error is based on the correct value of Δ_1/M_e, to construct a Δ_1/M_e vs. t_1/T_o curve for the maximum deflection equal to the collapse deflection, using the equivalent uniform resistance, the resistance may be figured for the equivalent uniform resistance and then the error for that t_1/T_o subtracted. Re-

cause of the small amount of the percentage of the error the corrections may be based on the % error multiplied by the computed Δ_1/F_e.

VIII. STUDY OF EFFECT OF PULSE SHAPE, WHEN α OF STRUCTURE RESISTANCE EQUALS 0 AND $y_m = y_f$

8.1 Scope of Section

In this section a study is made of the effect of the dead load and time dependent vertical loads on the horizontal response of a simple frame when also subjected to a horizontal time dependent load. Then in the dimensionless form the response of the fixed and pinned-base frames is the same. Points to be investigated are: (a) can the vertical dead load under any circumstances be neglected; (b) what effect does the dead load have on the response; (c) what effect does the shape of the forcing function have on the response; (d) when may the vertical time dependent load be neglected and (e) can a relation be found to relate the response of the structure when subjected to the different type forcing functions.

As a first step towards studying this problem two different fixed-base structures were taken. The two were chosen to be very different in characteristics to determine if both followed the same general trend in response. The first, frame A, was with elastic columns with a very light dead load. For this frame $\tau = \frac{1}{2}\gamma$ and γ and τ were assigned the values of 0.1 and 1.05 respectively. The other frame, frame B, was with inelastic columns, with $\tau = 2\gamma$ and γ and τ chosen as 0.2 and 0.4 respectively to represent a column with a much higher amount of dead load.

Then to obtain a picture of the response of these two frames they were each first subjected to horizontal time dependent load functions in the form of step pulse, initial and terminal peak pulses. With these type load functions it was then found for different magnitudes of the average horizontal load, Δ_1, what duration of time in terms of t_1/T_0 the load could be applied and have the maximum deflection equal the collapse deflection. Then Δ_1 is plotted vs. t_1/T_0 for the two frames. The collapse deflection for frame A is $y_f/y_e = 11.35$ and for frame B $y_f/y_e = 3.65$. These plots are shown in figures 53 to 58.

8.1 Scope of Section

Next, vertical loads in addition to the horizontal were applied to each of the frames. The vertical loads were of the same type function as the horizontal load and of the same time duration (figure 23). It was then found what combination of Δ_1, γ_1 (average time dependent vertical load) and duration, t_1/T_0, would produce the maximum deflection equal to the collapse deflection. The values of Δ_1 vs. t_1/T_0 were then plotted, for curves of constant amount of γ_1, for each structure, for each type of load function. These curves are shown in figures 24 to 28.

8.2 Analytical Computation for Step Pulse

The vertical load, other than the dead load, occurs as a step function (figure 23a). The solution of the equation of motion, $m\ddot{y} = \Delta_1 - F$, in the elastic range while Δ_1 acts will be of the form:

$$\frac{y}{y_e} = \left[\frac{\Delta_1/H_e}{(1-\gamma_{total})}\right]\left[1 - \cos\sqrt{(1-\gamma_{total})}\,\omega_0 t\right] \quad ; \tag{8.2.1}$$

where $\gamma_{total} = (\gamma_{wt} + \gamma_1)$.

While Δ_1 and γ_1 are still acting and frame elastic:

$$\frac{\dot{y}}{y_e} = \left[\frac{\Delta_1/H_e}{(1-\gamma_{total})}\right]\left[\omega_0\sqrt{(1-\gamma_{total})}\,\sin\omega_0\sqrt{(1-\gamma_{total})}\,t\right] \tag{8.2.2}$$

If Δ_1 is still acting when y_{er} (y_{er} based on γ_{total}) is reached, t_e, the time to reach y_{er}, will be:

$$t_e = \frac{\cos^{-1}\left[1 - \dfrac{(1-\pi)}{\dfrac{\Delta_1}{H_e}\dfrac{2}{\sqrt{\pi}\pi}\,tAN\dfrac{\sqrt{\pi}\pi}{2}}\right]}{\omega_0\sqrt{(1-\gamma_{total})}} \tag{8.2.3}$$

Velocity at yield, Δ_1 still acting, will be:

$$\frac{\dot{y}|_{t_e}}{y_e} = \left[\frac{\Delta_1/H_e}{(1-\gamma_{total})}\right]\left[\omega_0\sqrt{(1-\gamma_{total})}\,\sin\sqrt{(1-\gamma_{total})}\,\omega_0 t_e\right] \tag{8.2.4}$$

If Δ_1 still acts after y_{er} the equation of motion will be:

$$\frac{y}{y_e} = A_2\frac{e^{\psi t}}{y_e} + B_2\frac{e^{-\psi t}}{y_e} + \frac{\xi}{y_e} \qquad \text{(for which } t = 0 \text{ at } t_e\text{)}$$

and where:

$$\frac{\dot{\lambda}_{n+1}}{\dot{\lambda}_n} = \frac{\Delta^1}{\lambda_n^{tot}} \left[\frac{1}{\pi} \frac{\sin \frac{n\pi}{2}}{\frac{n}{2}} \right] \Big/ \cos^2 \lambda_n^{tot}$$

(8.8.3)

Velocity at field Δ^1 still active, will be:

$$\frac{\dot{\lambda}_{n+1}}{\dot{\lambda}_n} = \left[\frac{\Delta^1 \dot{H}_e}{(1 - \lambda_{n+1}^{tot})} \right] \left[\cos \phi_n - \lambda_{n+1}^{tot} \right] \cos \phi_n$$

(8.8.4)

If Δ^1 is still active when λ_n^{tot} found on λ_{n+1} is reached, ϕ_n the slope to reach λ_{n+1} will be:

$$\phi_n = \cos^{-1} \left[1 - \frac{\Delta^1}{\dot{H}_e} \sin \phi_n \sqrt{(1 - \lambda_{n+1}^{tot})} \right]$$

(8.8.5)

Δ^1 still acts after λ_n the completion of motion will be:

$$\frac{\dot{\lambda}_{n+1}}{\dot{\lambda}_n} = \left[\frac{\Delta^1 \dot{H}_e}{(1 - \lambda_{n+1}^{tot})} \right] \left[\cos \phi_n - \lambda_{n+1}^{tot} \right] \sin \phi_n \sqrt{(1 - \lambda_{n+1}^{tot})} \cos \phi_n$$

(8.8.6)

Δ^1 still acts after λ_n the completion of motion will be:

$$\frac{\dot{\lambda}_{n+1}}{\dot{\lambda}_n} = \left[\frac{\Delta^1 \dot{H}_e}{(1 - \lambda_{n+1}^{tot})} \right] \left[\cos \phi_n - \lambda_{n+1}^{tot} \right] \sin \phi_n \sqrt{(1 - \lambda_{n+1}^{tot})} + \frac{\dot{\lambda}_{n+1}}{\dot{\lambda}_n}$$

Time when $\lambda = 1$ or ϕ_n

8.8 Impulsional Consumption for Open Jaws

The "Impulsional Load" value when the load impacts on a step function [Figure 8.8]. The solution of the equation of motion, $\frac{d^2\lambda}{dt^2} = \Delta^1 - E$, in the elastic range while Δ^1 acts will be of the form:

$$\frac{\dot{\lambda}}{\dot{H}_e} = \left[\frac{\Delta^1 \dot{H}_e}{(1 - \lambda_{n+1})} \right] \left[1 - \cos \sqrt{(1 - \lambda_{n+1})} \cos t \right]$$

(8.8.1)

where $\lambda_{total} = (\lambda_n + \lambda^1)$.

While Δ^1 and λ^1 are still acting one finds similarly:

$$\frac{\dot{\lambda}}{\dot{H}_e} = \left[\frac{\Delta^1 \dot{H}_e}{(1 - \lambda_{n+1})} \right] \left[\cos \sqrt{(1 - \lambda_{n+1})} \sin \cos \sqrt{(1 - \lambda_{n+1})} + \right]$$

(8.8.2)

Δ^1 still acts after λ_n the completion of motion will be:

$$\frac{\dot{\lambda}_{n+1}}{\dot{\lambda}_n} = \left[\frac{\Delta^1 \dot{H}_e}{(1 - \lambda_{n+1}^{tot})} \right] \left[\cos \phi_n - \lambda_{n+1}^{tot} \right] \sin \sqrt{(1 - \lambda_{n+1}^{tot})} \cos \lambda_n$$

(8.8.6)

Time when $\lambda = 1$ or ϕ_n

$$\frac{\dot{\lambda}_{n+1}}{\dot{\lambda}_n} = \Delta^1 e^{\frac{\lambda}{\dot{\lambda}_n}} + B^1 e^{-\frac{\lambda}{\dot{\lambda}_n}} + \frac{\dot{\lambda}}{\dot{\lambda}_n}$$

$$A_2/y_e = \frac{1}{2} y_e \left[\dot{y}|_{t_e} - \frac{\dot{y}|_{t_e}}{\psi} - \xi \right] \qquad B_2/y_e = A_2/y_e + \dot{y}|_{t_e}/\psi y_e$$

$$\psi = \frac{\omega_0 \sqrt{(1-\gamma)}}{\sqrt{y_f/y_e - 1}} \qquad \xi/y_e = \frac{\frac{-\Delta_1}{K_1 y_e}\left[y_f/y_{eR} - 1 \right]}{(1-\gamma)} + y_f/y_e \qquad (A.1.2)$$

[Equation 6.3.5 based on γ_{total}].

When Δ_1 becomes 0 at t_1, for the maximum deflection to equal the ultimate deflection, its kinetic energy at the instance of t_1 must then be equal in value to the energy under the resistance curve between $y|_{t_1}$ and y_f [y_f based on γ_{wf}]. So the following must hold:

$$\frac{\frac{1}{2} m \left(\dot{y}|_{t_1} \right)^2}{y_e^2} = \frac{\left[y_f - y|_{t_1} \right]^2 \left[-K_{2R} \right]}{2 y_e^2} \qquad (A.1.3)$$

or $$\dot{y}|_{t_1}/y_e = \left[\frac{y_f - y|_{t_1}}{y_e \sqrt{y_f/y_{eR} - 1}} \right] \left[\omega_0 \sqrt{(1-\gamma_{wf})} \right]$$

[The small amount of elastic recovery may be neglected, see section 6.3]

The values of Δ_1 and t_1 cannot be chosen directly to fulfill the last expression. Therefore a successive approximation process must be resorted to. To find the combinations of γ_1, Δ_1 and t_1 to fulfill these requirements the following sequence was used.

1. For a value of Δ_1 and γ_1, γ_{wf} given.

2. For curve-jump onto a plot of $\frac{\dot{y}/y_e}{\omega_0}$ against for $\gamma_{max} = \gamma_2$ vs. t_2. It is other words at any deflection what $\frac{\dot{y}/y_e}{\omega_0}$ is required to stop structure just as y_f with only γ_{wf} acted. This will be in the form of tables.

3. Compute t_e and $\dot{y}|_{t_e}/y_e \omega_0$. Enter with resultant value in chart 2. Obtain t_e in terms of $(1/\omega_0)$.

4. If $\dot{y}|_{t_e}/y_e \omega_0$ of step 3 is greater than value from step 2, t_1 must be less than t_e. Then by successive approximation plot values of t_1 until the computed value of $\dot{y}|_{t_e}/y_e \omega_0$ coincides with the value from step 2. Computed value of $\dot{y}|_{t_1}/y_e$, $\dot{y}|_{t_e}/y_e \omega_0$ and t_1/t_e are obtained by equations (A.1.2) and (A.1.3).

$$\psi = \frac{\lambda_{2t}/\lambda_e - 1}{\omega_o a(1-a)} \qquad \lambda_e = \frac{K_{2e}\left[\lambda_{2e}^{\omega_o} - 1\right]}{(1-a)} + \lambda_{2t}/\lambda_e$$

$$A_{2e}/\lambda_e = \lambda_{2e}\left[\lambda_e^{\omega_o} - \frac{\psi}{\lambda_{2e}^{\omega_o}} - 1\right] \qquad B_{2e}^{\omega_o} = A_{2e}^{\omega_o}/\psi + \lambda_{2e}^{\omega_o}/\psi$$

$$\frac{\lambda_{2e}^{\omega_o}}{\lambda_{2e}^{\omega_o}} = \left[\frac{\lambda_{2e}^{\omega_o}/\lambda_{2t}^{\omega_o} - 1}{\lambda_t - \lambda_{2t}^{\omega_o}}\right]\left[\omega_o a(1-\omega_t)\right]$$

$$\frac{\frac{\lambda_2}{\lambda_e}}{\frac{1}{\omega}\left(\lambda_e^{\omega}\right)_2} = \frac{\left[\lambda_t - \lambda_e^{\omega}\right]_2}{\left[-K_{2t}\right]}$$

5. If $\dot{y}|_{t_e}/y_e\omega_o$ from step 4 is less than value at y_e from step 1 equation 5.1.5 is used for the motion after yield.

6. Constants A_2, B_2, ξ and ψ are computed.

7. Pick a trial value of t (in terms of $1/\omega_o$) for use in equation 5.1.5. This will be time after yield ($t_1 = t + t_e$). Compute $y|_{t_1}/y_e$ and $\dot{y}|_{t_1}/y_e\omega_o$ and compare with value from step 2.

8. Repeat step 7 until values obtained agree with those from step 2. The value of t_1 then obtained will be in terms of $1/\omega_o$. The ratio t_1/T_o or t_1/T as desired may be computed.

Caution must be exercised as in some places y_f and y_{er} depend on γ_{wt} and others γ_{total}.

Results of this are plotted in figures 28, 29, 30, 31 and 32 for frames A and B. Results are plotted in terms of Δ_1 vs. t_1/T_o for lines of constant amount of γ_{total}. t_1/T_o was chosen in lieu of t_1/T, because plots taken from reference 5 for comparison use the time ratio t_1/T_o.

5.3 Numerical Computation for Initial and Terminal Peak Pulses

The determination of the proper combination of Δ_1, t_1 and γ_1, (in form of figures 23 b and c) does not readily lend itself to mathematical equations. For these the numerical step by step procedure is used. The determination of the proper combination of (Δ_1 t_1 & γ_1) is more tedious than the procedure for the step function.

Here values of Δ_1, t_1 and γ_1 are chosen (γ_{wt} being given). Response is then worked out by a step by step numerical procedure.

The values of $\dot{y}|_{t_1}/y_e\omega_o$ and $y|_{t_1}/y_e$ are checked for agreement with available energy as in step 2 of 5.2 for the step function. If agreement is not obtained, t_1 is changed and a new solution obtained. This process is continued until agreement is obtained.

Results for this procedure are shown in figures 27, 28, 29, 31 and 32. Here again results are plotted as Δ_1/y_e vs. t_1/T_o for lines of constant γ_{total}.

The response curve for low-level or initial peak pulses is fairly like -- except the dead load, that $\gamma_i = 0$, may be very well approximated, that the curve for the step function is known, by using the relation $\delta = \alpha \cdot (g/b)$. The equation of this expression are shown in figure 35.

Another relation between the step and initial peak pulses that holds very close is: The response of a structure when subjected to a vertical time dependent load in the form of an initial peak pulse with ordinate of $2\gamma_i$ and isosceles of γ_i, is equivalent to the response of the structure when subjected to a step pulse of magnitude of $1.93\gamma_i = .3E$; the maximum deflection being equal to the ordinate deflection for the dead load of the structure. This is shown graphically in figure 34.

For the exact curves, the magnitude of Δ_i for the initial and terminal peak pulses has been expressed in terms of the magnitude of the allowable Δ_i for the step pulse and shown in figure 35. The general trend of these is shown in figure 36.

Using the percentage relation of figure 35 it is possible to construct approximate response lines for the initial and terminal peak cases when the response for the step pulse is known. For the case of $\gamma_i = 2$ it is possible to construct a response line for the step function using the procedure outlined in section 5.2. To construct a curve of Δ_i vs. t_i/T_s for $\gamma_i > 2$ for the step pulse the graphical method of section 5.2 is best used. To approximate from the step function curve to the initial and terminal peak case using the correlation relation of figure 35, it is first necessary to construct the step function response curve for the case γ_i and γ_{it} as the case desired for the initial -or terminal peak cases. For the initial peak case the relation between it and the step function of the earlier in this section can also be used.

If it is desired to determine what minimum Δ_i in the form of a time pulse, $\gamma_i = 2$, can cause collapse with E_i as large as necessary for failure, correspon-

may be used:

$$\Delta_{min}/H_e = H_{eR}/H_e \left[1 + \frac{1}{y_f/y_{eR} - 1}\right] \sqrt{\left[1 + \frac{1}{y_f/y_{eR} - 1}\right]\left[\frac{1}{y_f/y_{eR} - 1}\right]} \qquad (8.3.1)$$

where H_{eR}, y_f and y_{eR} are based on γ_{wt}.

8.4 Summary of Frames A and B for $y_m = y_f$

It is seen that the effect of the dead load [illegible] be neglected for any value of t_1/T_o. As γ_{wt} and γ_1 are increased the [illegible] reduction in Δ_1, from the value obtained for the case of $\gamma_{wt} = \gamma_1 = 0$, is increased. [illegible] for the % decrease are given in table II.

TABLE II

			Frame A			Frame B		
			Step Pulse	Initial Peak	Terminal Peak	Step Pulse	Initial Peak	Terminal Peak
t_1/T_o	γ_{wt}	γ_1	% reduction of Δ_1 from Δ_1 for $\gamma_{total} = 0 (y_m = y_f)$					
0.15	0.1	0	31.2	29.4	29.4			
0.5	0.1	0	31.5	28.5	31.5			
1.0	0.1	0	27.0	25.3	27.6			
0.15	0.2	0				45.5	43.3	45.3
0.5	0.2	0				48.2	46.3	49.0
1.0	0.2	0				52.4	49.5	52.5
0.2	0.1	0.2	37.5	36.3	36.3			
0.2	0.1	0.4	37.3					
0.2	0.1	0.6	40.9					
0.5	0.1	0.2	30.5	29.2	31.2			
0.5	0.1	0.4	36.3					
0.5	0.1	0.6	44.7					
1.0	0.1	0.2	50.5	46.6	50.3			
1.0	0.1	0.4	58.6					
1.0	0.1	0.6	81.7					
0.2	0.2	0.15				49.3	44.3	
0.5	0.2	0.15				65.7	58.5	
1.0	0.2	0.15				77.0	70.3	

For t_1/T_o less than [illegible] the effect of the [illegible] may be neglected. In this range the loading is mostly impulsive; as the deflection at the end of the pulse is not great enough to cause a serious reduction in the resistance work up to the failure deflection.

$$\Delta_{min}/H_0 = H_{ss}/H_0 \left[1 + \frac{1}{e^{2\pi H_{ss}/H_0} - 1} \right] \left[1 + \frac{1}{e^{2\pi H_{ss}/H_0} - 1} \right] \left[\frac{1}{e^{2\pi H_{ss}/H_0} - 1} \right]$$

For the case of γ_{Δ} = 0 a similarity, or proportionality, is noted between the curves for all three type values and the curve for γ_{total} = 0 known from reference 5. The relation is shown in figure 33.

Figures 35 and 36 show the general trend among the responses for the three type pulses.

An equivalence is noted between the response of step and initial peak pulse vertical loads when subjected to the same horizontal load. The relation is shown in figure 34 and explained in section 8.3.

It was found that vertical loads, to any appreciable quality, seriously reduces the horizontal yield resistance of a structure. The yield deflection and resistance, when vertical load is included, is a function of both γ and the ratio π/γ. Even the F vs. ρ curve, without vertical load, consists of straight lines before and after yield, the resistance, when vertical load is included, also consists of straight lines. The ductility deflection, designated as π, γ and α, is easily computed. In figure 6 a plot was made from which the elastic portion of the resistance curve can be taken for different values of γ and π/γ.

When the α of the F vs. ρ relation is > 0 the resistance beyond the yield point is a curved path. It was found for γ equal to or less than α of the F vs. ρ relation the structure did not have a ductile deflection as previously defined. Also an asymptotic value of the slope of F/F_0 vs. ρ/ρ_0 for small values of γ is defined for large deflections.

In comparing the average horizontal time dependent load of the approximate equivalent uniform resistance to have equal values for the widely different structures and dead loads, a general trend of error was found in the ratio of t_1/T_0 between 0.2 and 1.2 and ρ_1 equal to ρ_2. This F error is at $(1 - (t_1/T_0)^2) = 4$.

In arriving at the responses of the two widely different forms, for $\rho_1 = \rho_2$, it was found that the Δ_1/ρ_0 of the initial rectangular pulse also followed a general trend in % of the value of Δ_1/ρ_0 for the step pulse. From this, when $\gamma_1 > 3$, approximate resistance curves for the initial rectangular pulse can be established from the more easily obtainable resistance curve of the step pulse. When $\gamma_1 = 3$, use the approximate equivalent uniform resistance.

It was found that an initial peak pulse of maximum magnitude of $2\gamma_1$ was equivalent to a rectangular pulse of magnitude γ_1 [illegible]. Resistance curves for the three type pulses and the two forces are shown in figures 31 and 32. These curves show the relation of the response for the three type pulses.

BIBLIOGRAPHY

1. Newmark, N.M.: "An Engineering Approach To Blast Resistant Design", ASCE Proceedings, Vol. 79, Separate No. 306.

2. Newmark, N.M.: "Numerical Procedure for Computing Deflections, Moments and Buckling Loads", ASCE Transaction, Vol. 108, 1943, p 1161.

3. Newmark, N.M.: "Method of Analysis for Structures Subjected to Dynamic Loading", Directorate of Intelligence, USAF, 1950.

4. Newmark, N.M. and Chan, S.P.: "A Comparison of Numerical Methods for Analyzing the Dynamic Response of Structures", Structural Research Series No. 36, University of Illinois.

5. Newmark, N.M. and Brooks, Nancy R.: "The Response of Simple Structures to Dynamic Loads", Structural Research Series No. 51, University of Illinois.

APPENDIX I. INITIALLY CROOKED ELASTIC COLUMN

I.1 Scope and Computation

A study is made here of the effect of initial crookedness on the response of an elastic column when subjected to an axial load, equal or greater in magnitude than the critical buckling load, and which load reduces to 0 for $t < 0$. The large deflection theory is used.

The column will be simulated by the model illustrated in figure 37.

Disturbing Moment = Py

Restoring Moment: $K(\phi - \phi_0) = K\left(\sin^{-1} y/a - \sin^{-1} y_0/a\right)$; (I.1.1)

where $a = L/2$.

Then: $\frac{M \ddot{y} L/2}{2} = Py - K\left(\sin^{-1} y/a - \sin^{-1} y_0/a\right)$ (I.1.2)

Let: $u = y/a$ $u_0 = y_0/a$ Then: $\ddot{u} = \frac{P}{aM} 2u - \frac{K}{Ma^2} 2\left(\sin^{-1} u - \sin^{-1} u_0\right)$

and let: $p = \frac{2P}{Ma}$; $q = \frac{2K}{Ma^2}$. $P = K/a = K/L/2$ for critical load.

Then: $\ddot{u} = q\left[p/q\, u - (\sin^{-1} u - \sin^{-1} u_0)\right]$ $p = q$ for critical load.

At $t = 0$, $u = u_0$ & $\dot{u} = 0$

For each combination of u_0 and P, P being within dynamic capacity of the column, there exists a unique point, u_{neut}, of static equilibrium at which the acceleration will be zero.

Thus: $p/q\, u_{neut} = \sin^{-1} u_{neut} - \sin^{-1} u_0$ (I.1.3)

A plot of u_{neut} vs. u_0 for three cases, p/q = 0.98, 1.00 and 1.02, is shown in figure 38. It is noted that for the case of p/q = 1.00 the plot of u_{neut} vs. u_0, when plotted on log-log paper, is a straight line. Then a load of the step pulse form, for which P = 0 for $t < 0$, is applied to the model with initial crookedness the column will displace to some maximum deflection and then return to u_0 and repeat the cycle over and over as long as P acts and there is no damping.

Phase plane diagrams of $\dot{u}$ vs. u for u_0 = 0.0001, 0.001 and 0.01 and p/q = 1.00 and 1.02 are shown in figure 39. These diagrams were obtained using step by

1.3 Jumps and Compatibility

A study is made here of the effects of initial perturbations in the neighbourhood of an elastic driven plane wave propagated by an axial load, which is liable to undergo deflection theory is used.

The motions will be examined by the model illustrated in figure 17.

Governing moment = M

Restoring moment = $k(\theta - \psi)$: [1.3.1]

where $\theta = \frac{dy}{dx}$.

Then: $\frac{M}{EI} = \frac{d\psi}{ds} = k\left(\sin^{-1}\frac{y}{a} - \sin^{-1}\frac{y}{a}\right)$ [1.3.2]

And: $M = M_0$ $\psi = \psi_0$ Then $M = \frac{EM}{a} - \frac{Ks}{M}\left(\sin^{-1}\frac{y}{a} - \sin^{-1}\frac{y}{a}\right)$

and $\frac{M}{EI} = \frac{M_0}{EI}$; $\beta = \frac{Ma^2}{EK}$ $\qquad \beta = k/\psi_0 = k/\psi_0$

Then: $\ddot{\psi} = \beta\left[\psi/\psi_0 - (\sin\psi - \sin\psi_0)\right]$ $\qquad \psi = \psi_0$ for equilibrium

At $t = 0$, $u = u_0$ & $\dot{u} = 0$

The wave velocities of c_0 and V_0 behind elastic dynamic boundary at the column. There exists a motion $\psi_{(x,t)}$ of simple equilibrium to which the motion will be zero.

Then: $\psi_0 = \psi_{(x,t)} = \psi_0 e^{-\alpha x} - \psi_0 e^{-\alpha x}$ [1.3.3]

ψ plot of $\psi_{(x,t)}$ are of the given curve: $\psi_0 = \psi_0 e^{-\alpha x}$, $\psi_0 = \psi_0 e^{-\alpha x}$ as shown in figure 18. It is noted that for this case of $\psi_0 = \psi_0 e^{-\alpha x}$ the plot of $\psi_{(x,t)}$ are ψ_0 then elastic or inelastic column, for a unstable flow. Then a limit of the wave below there for which $\psi = \psi_0$ is applied to the model with initial

In ψ_0 all members the static case may occur as long as ψ value not above in the deflection theory the column will display in more realistic deformations and show reduced

step numerical integration. Also the time required to reach u_{max} and u_{neut} for p/q = 1.00 and 1.02 is plotted vs. u_o in figure 40.

To determine the velocity at any isolated point on the phase plane diagram without working the complete numerical solution up to that point the energy of the system may be used to determine this velocity. The force at u:

$$\text{Force} = Maq\left[p/q\, u - (\sin^{-1}u - \sin^{-1}u_o)\right] \qquad (I.1.4)$$

The work performed up to some u_2 is:

$$\text{Work} = Ma^2q\left[p u^2/2q - u\sin^{-1}u - \sqrt{1-u^2} + (\sin^{-1}u_o)u\right]_{u_o}^{u_2} \qquad (I.1.5)$$

This work goes into change of kinetic energy. With $\dot{u} = 0$ at $t = 0$ this yields:

$$\dot{u}_2 = \sqrt{q}\sqrt{\left[p u^2/q - 2u\sin^{-1}u - 2\sqrt{1-u^2} + 2u(\sin^{-1}u_o)\right]_{u_o}^{u_2}} \qquad (I.1.6)$$

If u_2 is chosen greater than u_{max} for the particular u_o this expression for $\dot{u}_2$ will be imaginary.

I.2 Discussion

The primary object here is to discuss the effect initial crookedness has on the maximum response and the time required to reach this maximum response.

For such a case the magnitude of u_{neut} and u_{max} decreases as u_o (measure of initial crookedness) decreases. A plot of u_{max} vs. u_o for the case of p = q, critical load, gives a straight line when plotted on log-log paper, figure 40, for the range of u_o between 0.00001 and 0.01. Then as u_o approaches 0 so does the value of both u_{max} and u_{neut}. Also in figure 40 the time required to reach u_{max} and u_{neut} vs. u_o is shown for the range of u_o between 0.00001 and 0.01. The time to reach these values, when plotted on log-log paper, for the case of the load equal to the critical load gives straight lines. The time to reach these values increases as the initial crookedness decreases. The time in this plot is expressed in terms of $1/\sqrt{q}$. As the value of u_o approaches 0 the value of the time

1.3 Diagnostics

approaches ∞ ; showing that for a perfectly straight column with no disturbing moment the column will not deflect under the critical load. The time it takes a column to deflect under the load may be an important factor. For $u_o = 0.01$ the time to reach u_{neut} is $8.7(1/\sqrt{q})$ and time to reach u_{max} is $15.4(1/\sqrt{q})$, $(p = q)$, whereas for $u_o = 0.00001$ the time to u_{neut} is $41(1/\sqrt{q})$ and the time to u_{max} is 63 $(1/\sqrt{q})$. In studying a specific case these times would be compared to the load pulse duration. If the load pulse duration is longer than the time required to reach u_{max} the column would vibrate between u_{max} and u_o with the velocity-displacement relation shown by the phase plane diagram, figure 39.

When the p/q ratio is increased above 1 the values of u_{max} and u_{neut} are increased above the values for the load equal to the critical load. A plot of these, as well as the time to reach these values, is shown in figure 40 for p/q = 1.02. These plots are no longer linear even when plotted on log-log paper. The curves for u_{max} and u_{neut}, as u_o approaches 0, approach a horizontal asymptote of $p/q\ u = \sin^{-1}u$. However, at u_o equal to 0, this value of u_{max} and u_{neut} is meaningless, as some crookedness or eccentricity is required to trigger off the column. For the larger values of u_o, range of 0.001 to 0.01, the time required to reach u_{neut} is greater than for the case of the critical load and the time required to reach maximum deflection is less than for the case of the load equal to the critical load. As u_o decreases the values of the times decreases from those for the case of the critical load, as shown in figure 40; but the plots do slope upward to the left with increasing time for decreasing u_o.

APPENDIX II. INITIALLY STRAIGHT ELASTIC COLUMN GIVEN INITIAL DISPLACEMENT

II.1 Scope and Computation

A study is made here of the case of an initially straight column subjected to an axial load equal to or greater than the critical buckling load. After the load is applied the column is then given an initial displacement, u_1, and released. The effect of the magnitude of the displacement on the maximum displacement and time to reach this maximum displacement is to be investigated. As a specific example the case of $p/q = 1.57$ is taken and the response investigated.

$$\ddot{u} = q\left[p/q\ u - (\sin^{-1}u - \sin^{-1}u_0)\right] \qquad \text{(II.1.1)}$$

But $u_0 = 0$ and therefore: $\ddot{u} = q\left[pu/q - \sin^{-1}u\right]$

For the static equilibrium position: $p/q\ u = \sin^{-1}u$.

For $p/q = 1$, $\sin^{-1}u > u$ for all values of $u > 0$; and u_{neut} for $p/q = 1$ is 0. For all values of $p/q > 1$, u_{neut} is greater than 0. The work done on the mass M in going from u_1 to some other u_2 is:

$$\text{WORK} = Ma^2q\left[pu^2/2q - u\sin^{-1}u - \sqrt{1-u^2}\right]_{u_1}^{u_2} \qquad \text{(II.1.2)}$$

This work goes into changing kinetic energy of the mass. Thus:

$$\sqrt{\dot{u}_2^2 - \dot{u}_1^2} = \sqrt{q}\sqrt{\left[pu^2/2q - u\sin^{-1}u - \sqrt{1-u^2}\right]_{u_1}^{u_2}} \qquad \text{(II.1.3)}$$

For the case being studied $\dot{u}_1$ has been taken as 0. And for any value of $u_2 > u_{max}$ (u_{max} determined by u_1) expression II.1.3 for velocity becomes imaginary.

These phase diagrams have been constructed for u_1 equal to 0.771, 0.64, 0.1, 0.30, 0.53 and 0.30. To obtain the motion of the column a numerical solution of $\ddot{u} = q\left[pu/q - \sin^{-1}u\right]$ was made using the Beta method of reference 11 and beta taken as 0 with a five time interval. Also, the energy of the system can be used to determine the velocity at desired points of displacement. For both methods

extreme accuracy must be used. If more than the velocity at two or three points is desired the numerical method is advantageous over the use of the energy of the system.

II.2 Discussion

The phase plane diagrams computed are shown as figure 41. There the plot is $\dot{u}$ vs. u. A plot of u_{max} vs. u_1 is shown in figure 42. A plot of the time to reach u_{max} and u_{neut} is shown in figure 43.

As shown by both figures 41 and 42 the amount of the initial disturbance, when less than u_1 equal 0.1, has very little effect on the maximum displacement. This is borne out when the small amount of energy removed from the system by the smaller initial displacements is considered.

As u_1 ($u_1 < u_{neut}$) is increased the value of u_{max} will decrease, but will be greater than u_{neut}. u_{neut} is independent of u_1. If u_1 is greater than u_{neut}, but less than u_{max} for $u_1 \rightarrow 0$, the deflection will not increase when released, but will decrease, and the minimum value will be the same as u_1 would have had to be to produce a u_{max} equal in magnitude to this induced u_1.

If u_1 is greater than u_{max} for $u_1 \rightarrow 0$, the mass will have kinetic energy when the column reaches the zero deflection position. The column will then continue on past the equilibrium position and will repeat the loop on the opposite side. A case of this is shown in figure 41 for u_1 equal 0.50 and u_{max} for $u_1 \rightarrow 0$ is 0.469. For $u_1 > u_{max}$ for $u_1 \rightarrow 0$, u_1 is u_{max}.

For the case of p/q equal 1.02 the time required to reach the static equilibrium position and maximum deflection is shown in figure 43. This is a plot of time vs. initial deflection and is given on log-log paper. For p/q = 1.02 the time to reach the maximum deflection plots as a straight line when the initial disturbance is less than the static equilibrium position. If the value of u_1 equal to or greater than the static equilibrium position the time reduces to 0, as u_1 is then u_{max}. The plot of the time to reach the static equilibrium posi-

tion is also shown in figure 11 for $p/q = 1.02$. This does not plot as a straight line on the log-log paper. However, for values of $w_1 < w_{max}$, it does have a constant difference of time from the time required to reach maximum deflection.

In this case that has been worked out to show the influence of the initial disturbance on the maximum deflection and time to displace the amount of the axial load has been taken as only 1.02 of the critical load and the large deflection theory used. Even this small amount of load above the critical load makes a large difference in the amount of the deflection.

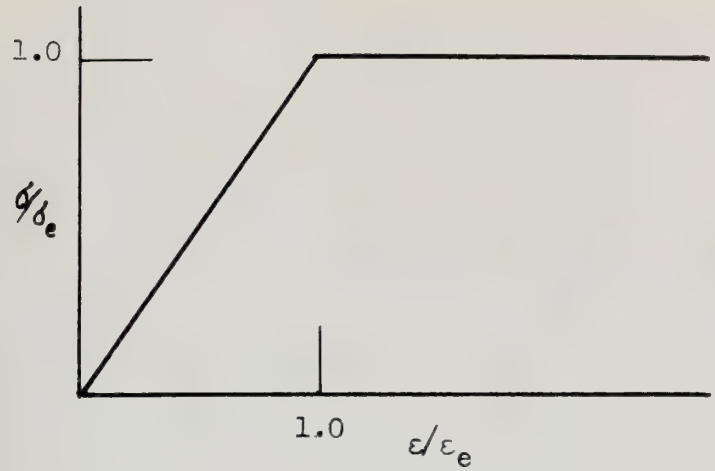

Fig. 1 - Stress - Strain Curve for Ideal Plastic Material

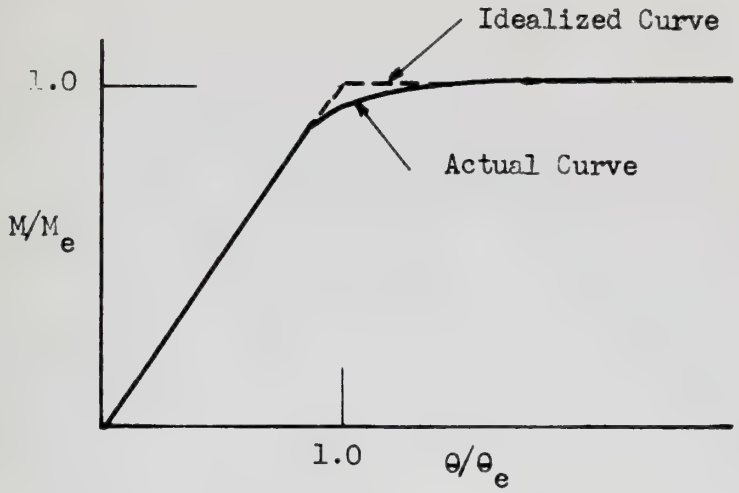

Fig. 2 - M - θ Curve for Ideal Plastic Material and H Type Section

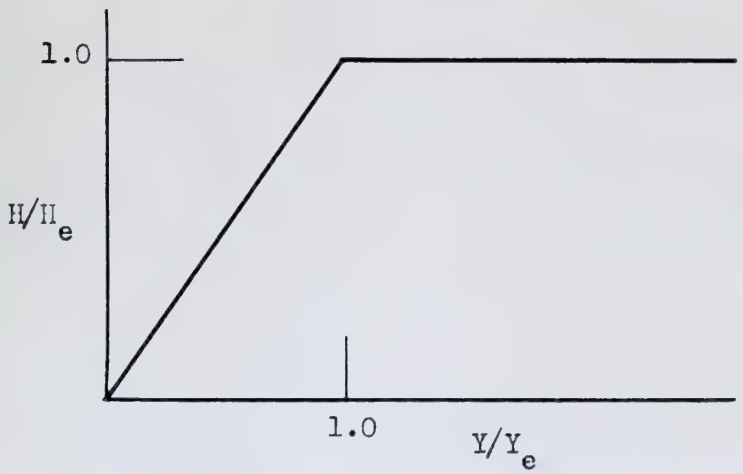

Fig. 3 - H/H_e vs. Y/Y_e for P and a Equal to 0

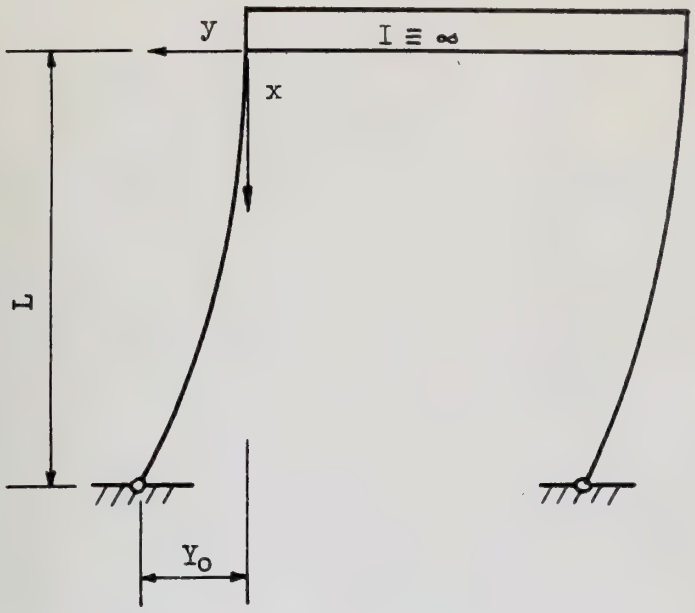

Fig. 4 - Pinned- Base Frame

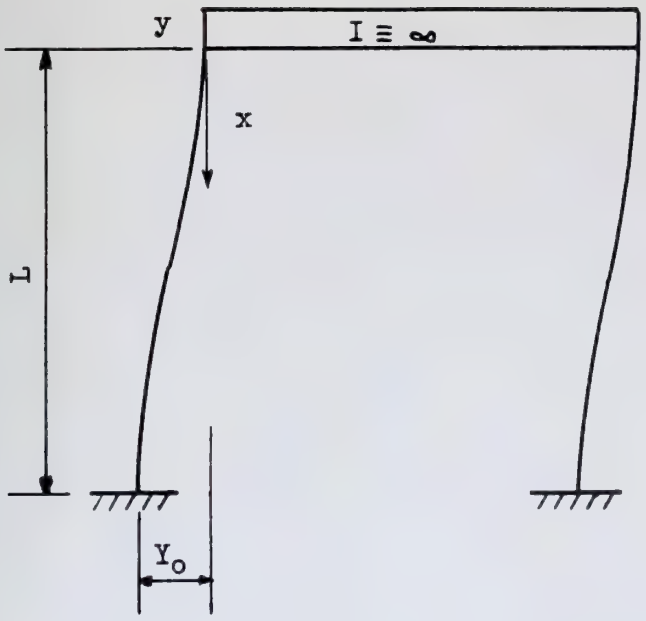

Fig. 5 - Fixed - Base Frame

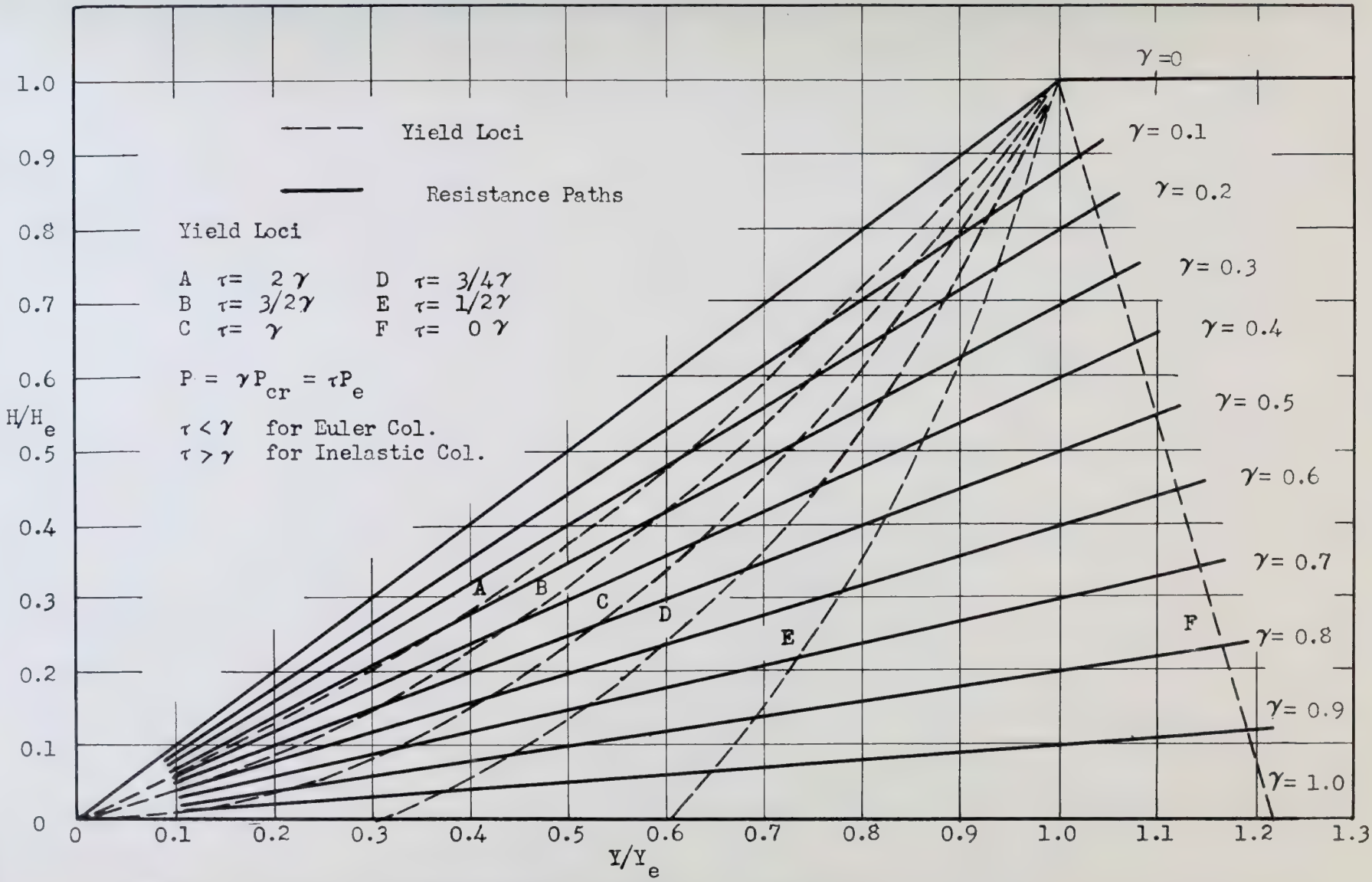

Fig. 6 - Elastic Resistance Paths and Yield Loci for Both Fixed and Pinned - Base Frame Columns and for α = 0

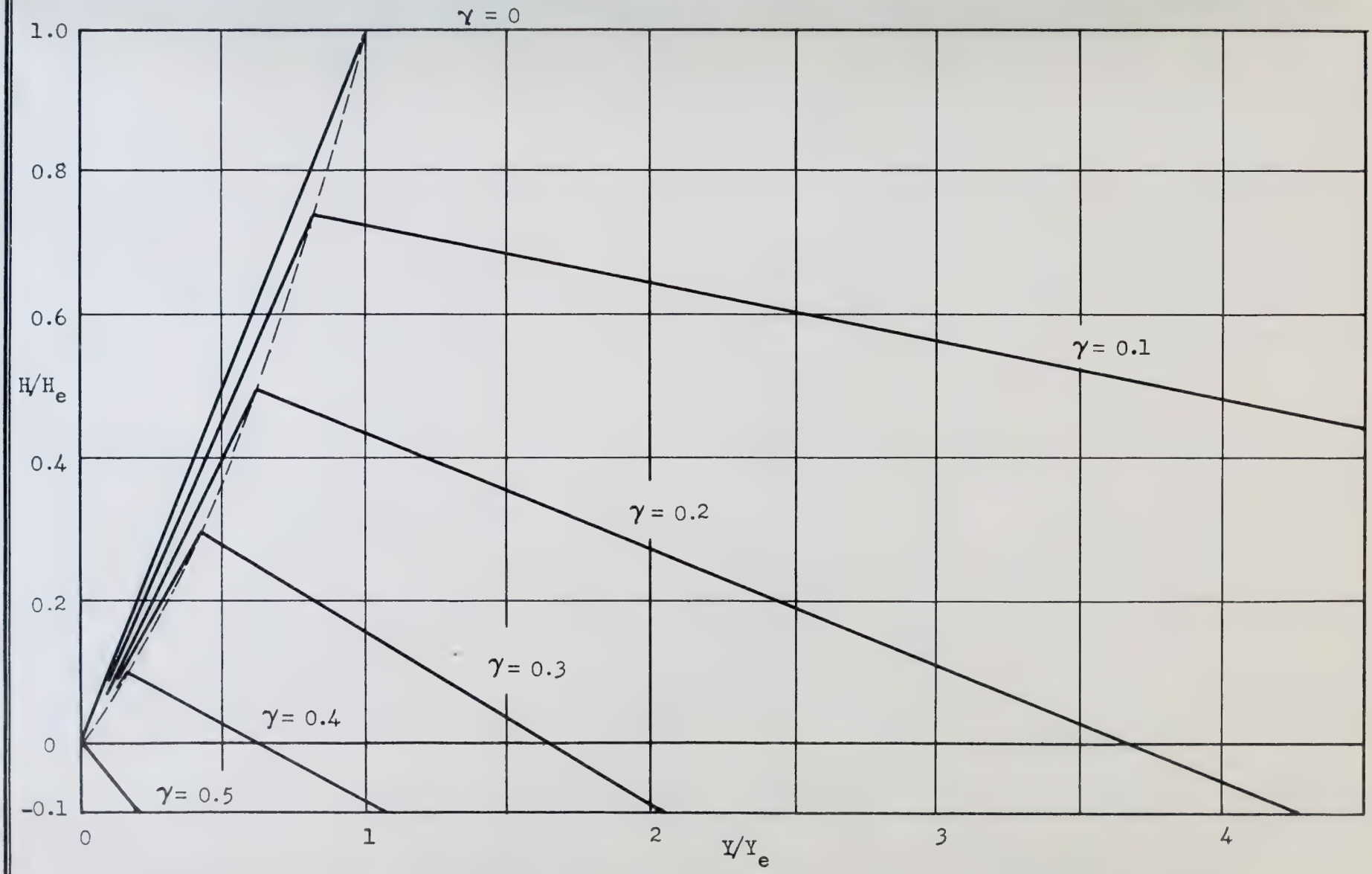

Fig. 7 - Resistance Paths for $\tau = 2\gamma$, for Both Fixed and Pinned - Base Frames

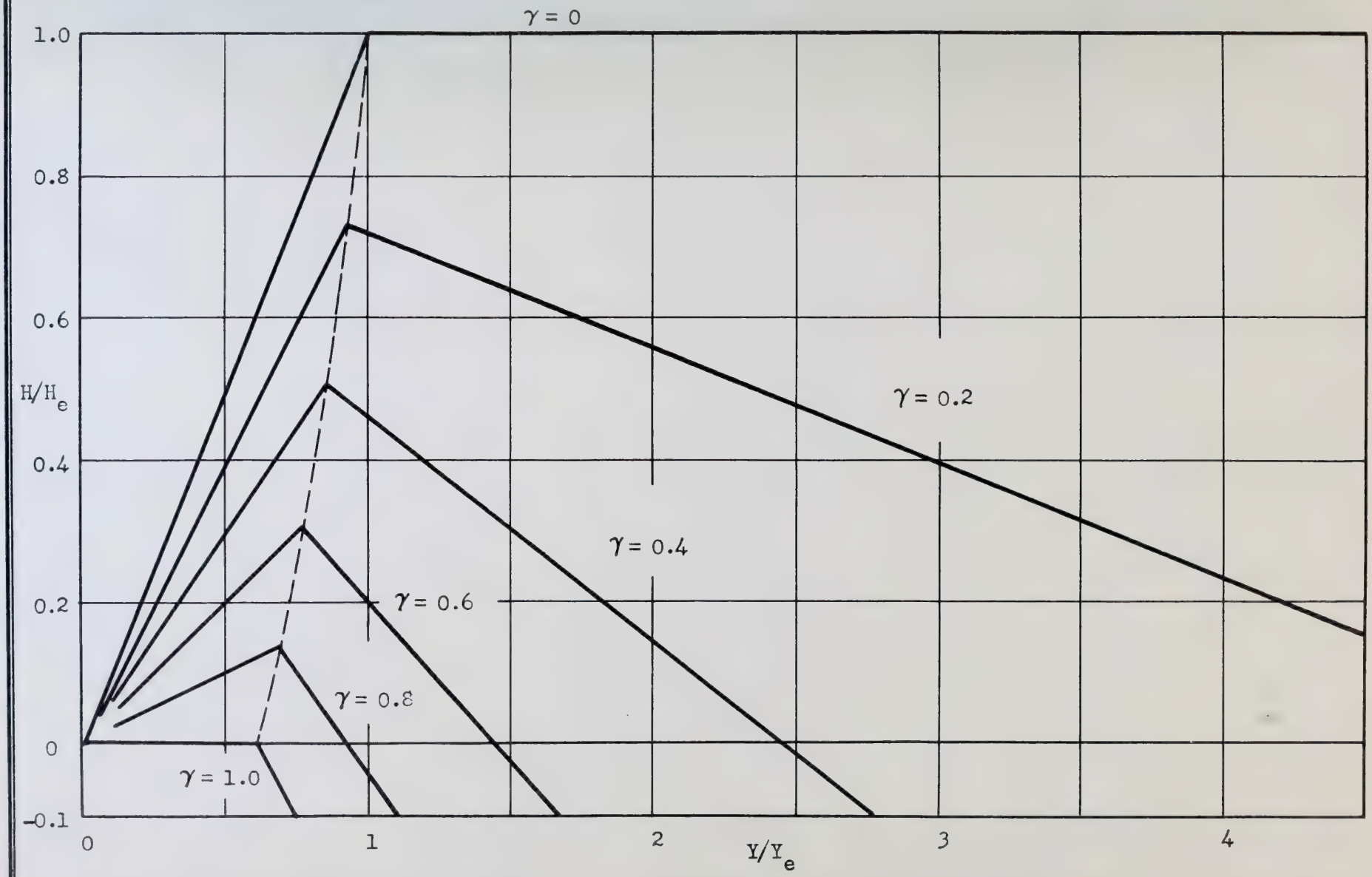

Fig. 8 - Resistance Paths for $\tau = 1/2\gamma$,for Both Fixed and Pinned - Base Frames

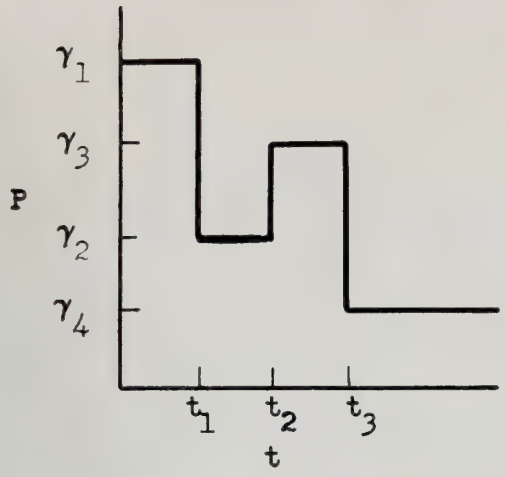

Fig. 9 (a)

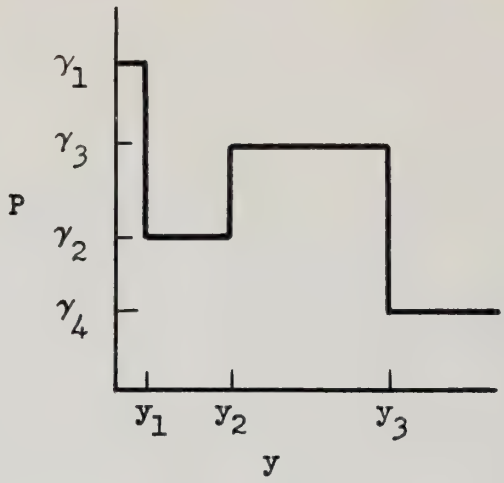

Fig. 9 (b)

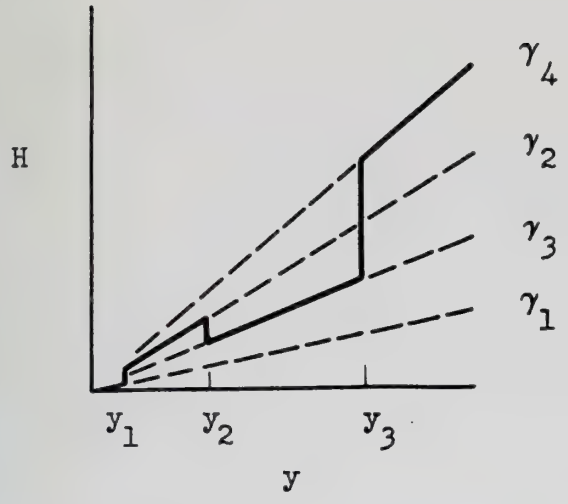

Fig.9 (c)

Fig. 9 - Variation of H with Changes in P in Elastic Range

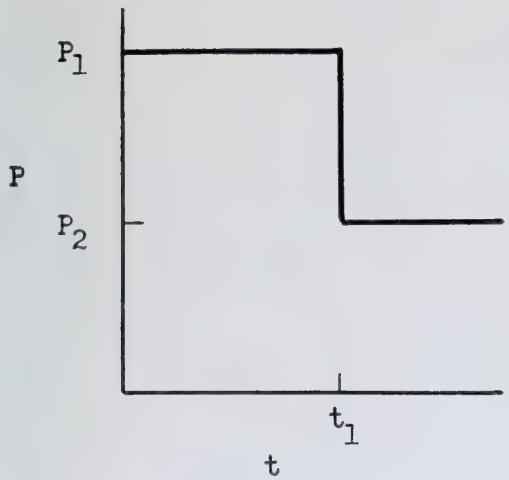

Fig. 10 (a)

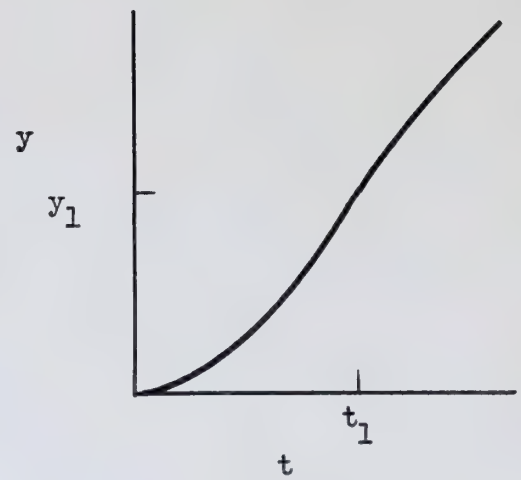

Fig. 10 (b)

Fig. 10 - Step Function Variation of Vertical Load

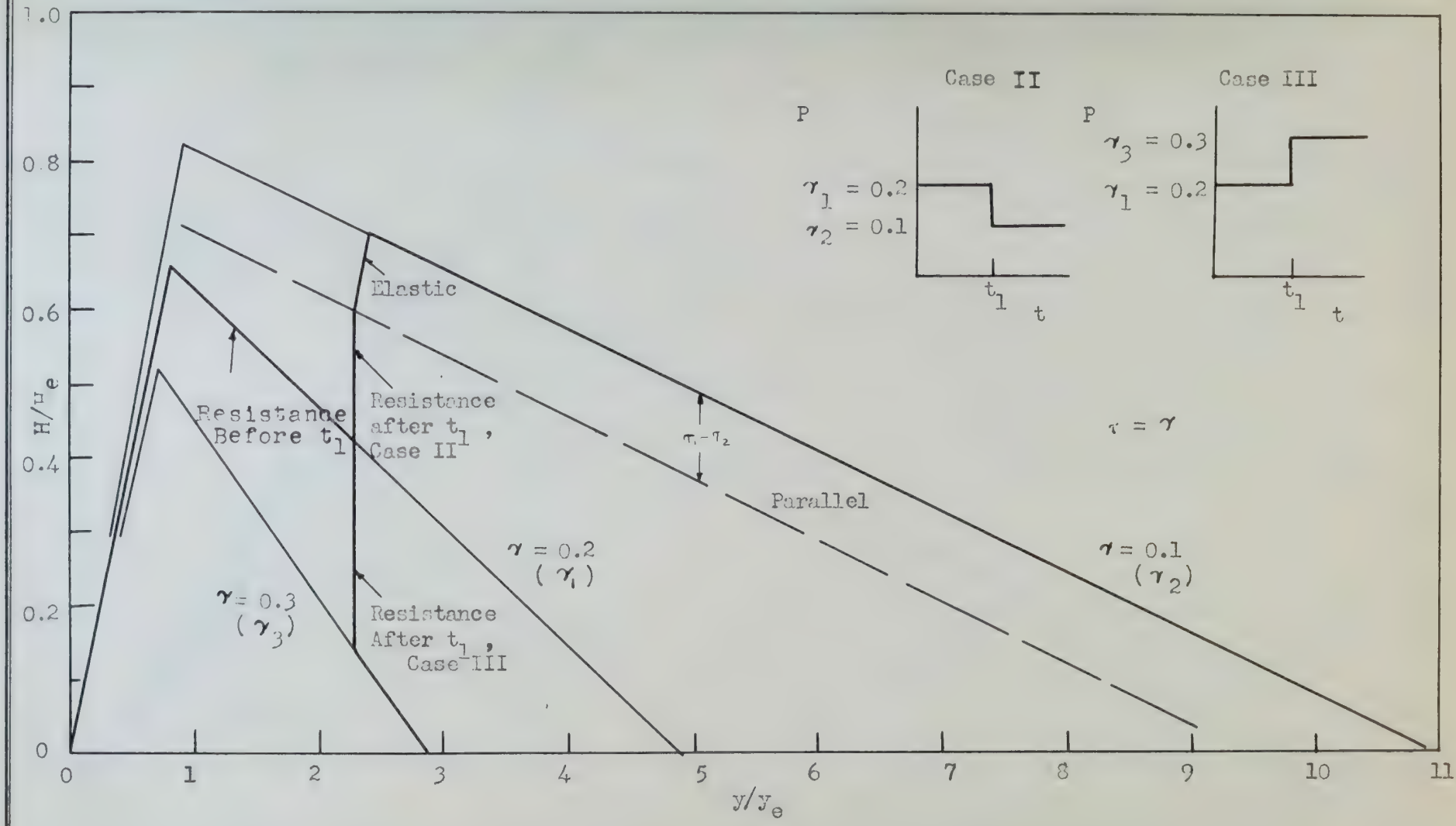

Fig. 11 - Transition Between Resistance Paths for Step Function

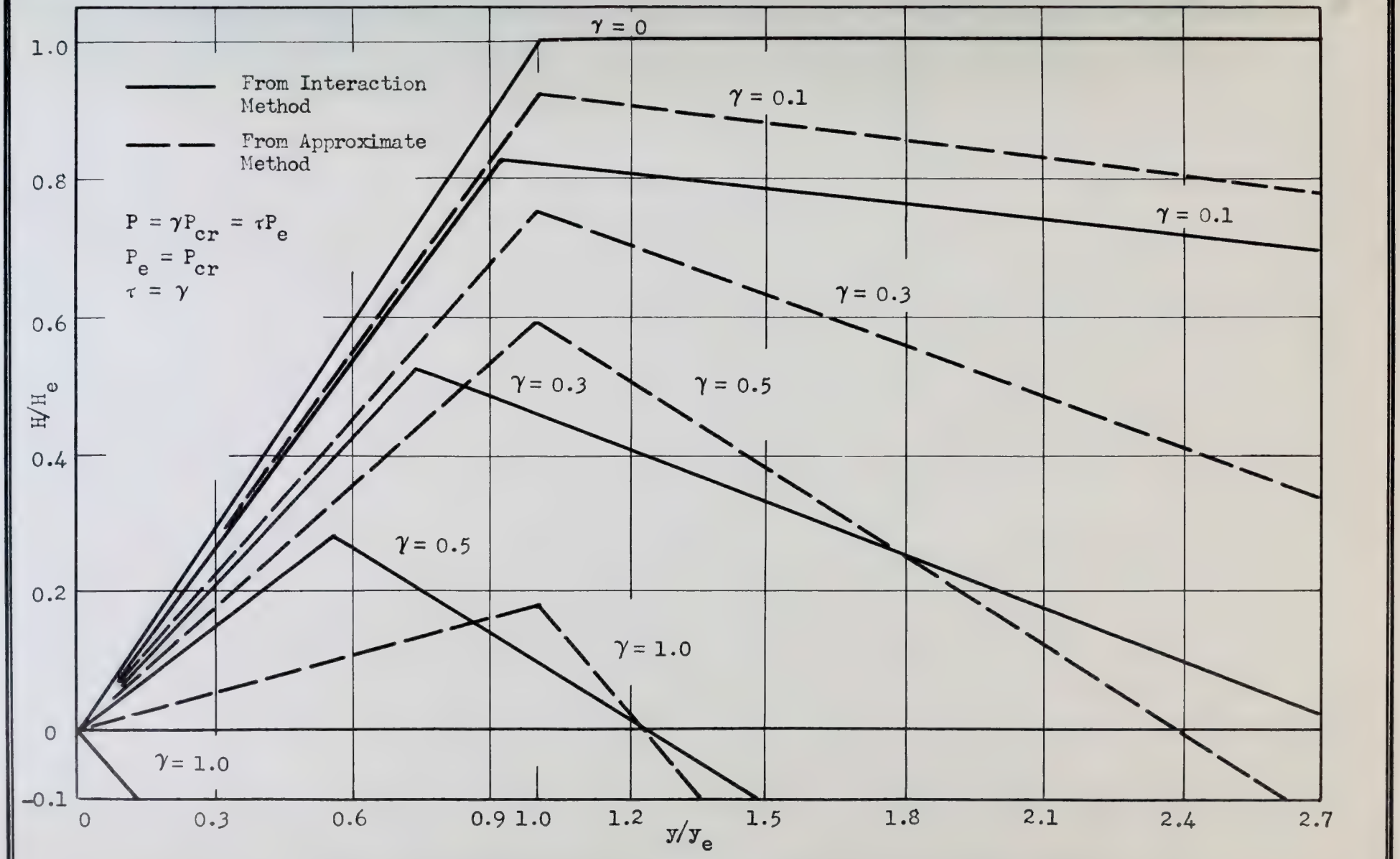

Fig. 12 - Comparison of Interaction Method with Approximate Method for $P_e = P_{cr}$. α of Structure H/H_e vs. y/y_e Equal to 0

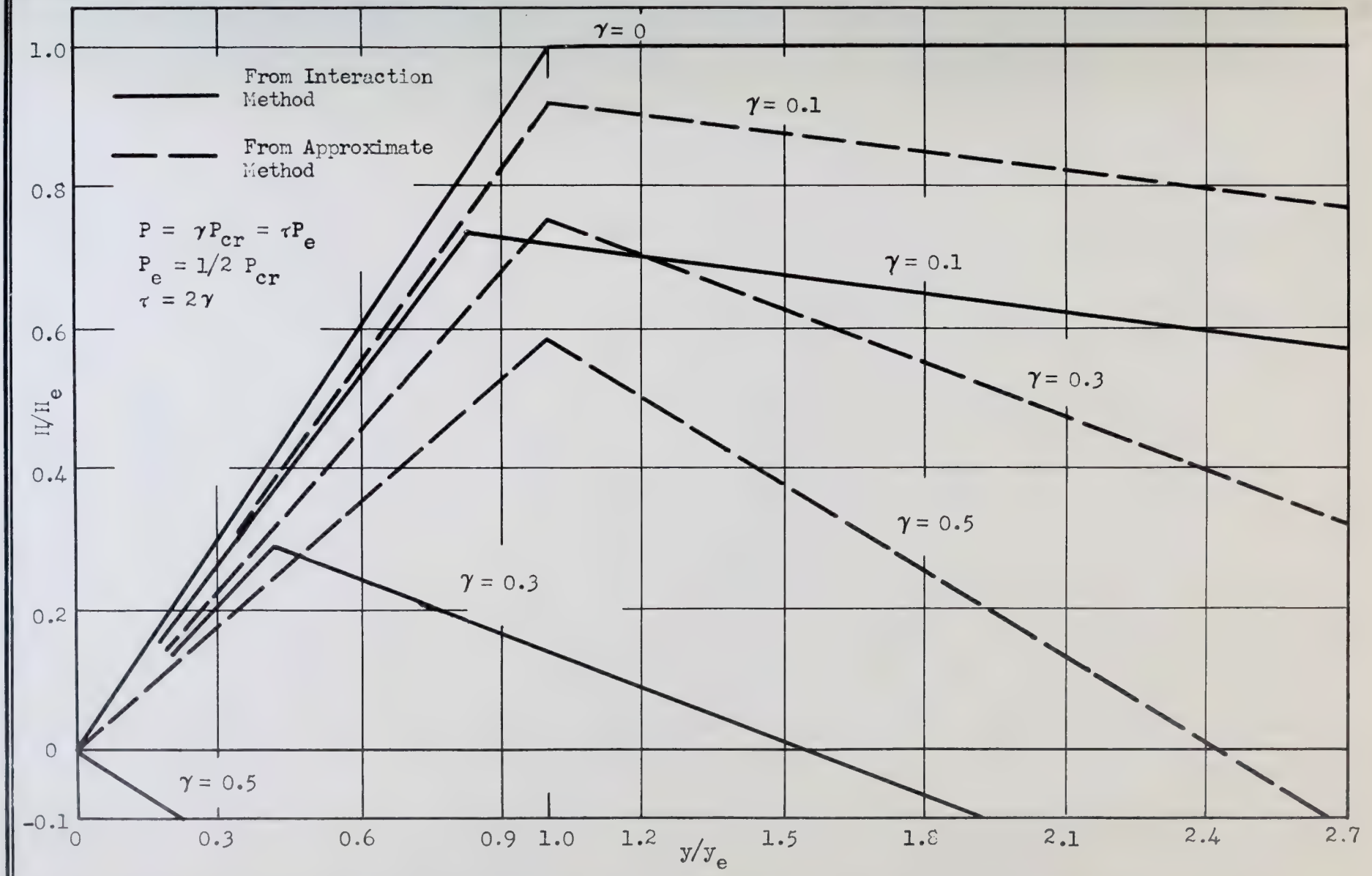

Fig. 13 - Comparison of Interaction Method with Approximate Method for $P_e = 1/2\ P_{cr}$. α of Structure H/H_e vs. y/y_e Equal to 0

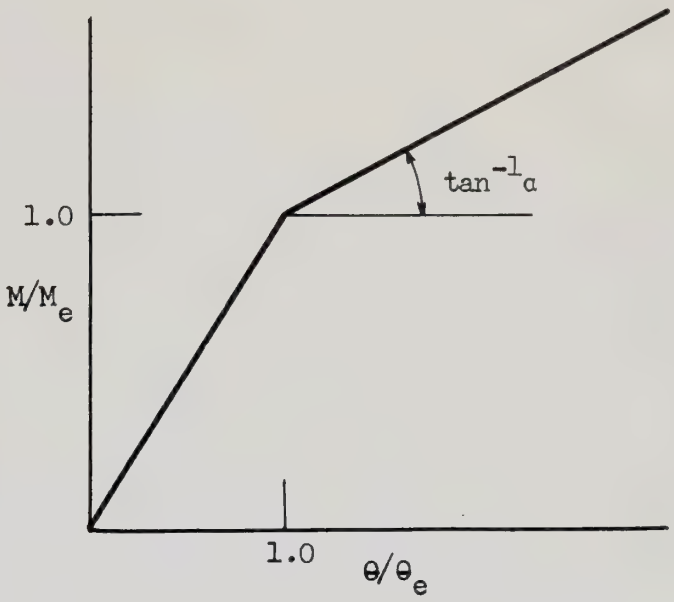

Fig. 14 - Idealized M/M_e vs. θ/θ_e Diagram for Work Hardening Material

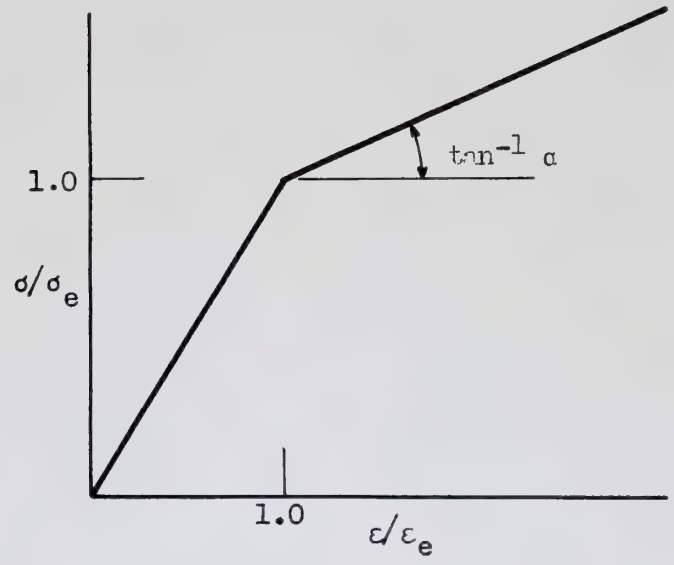

Fig. 15 - Stress - Strain Curve for Work Hardening Material

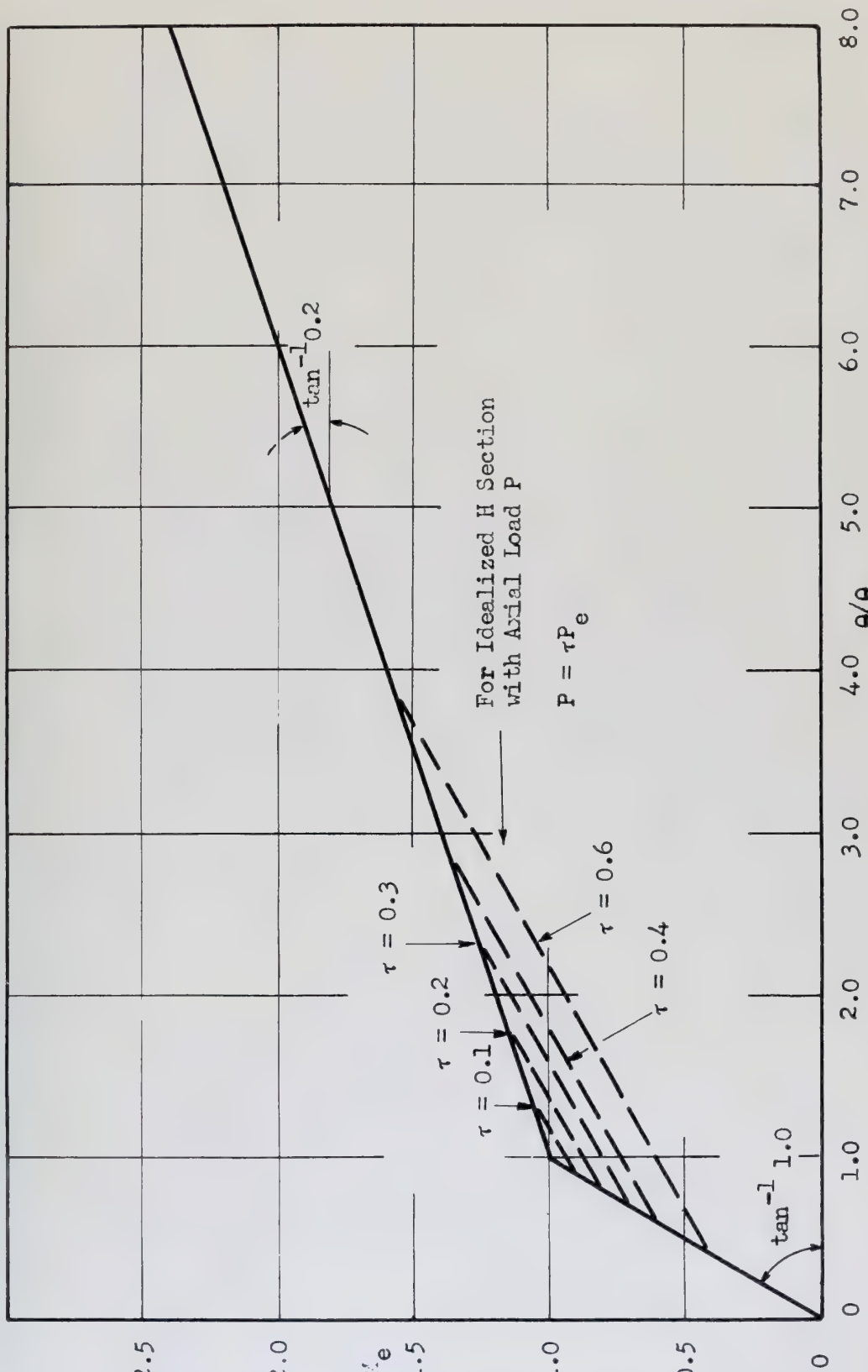

Fig. 16 - M/M_e vs. θ/θ_e Relation for $\alpha = 0.2$:
Showing Effect of Axial Load on Section

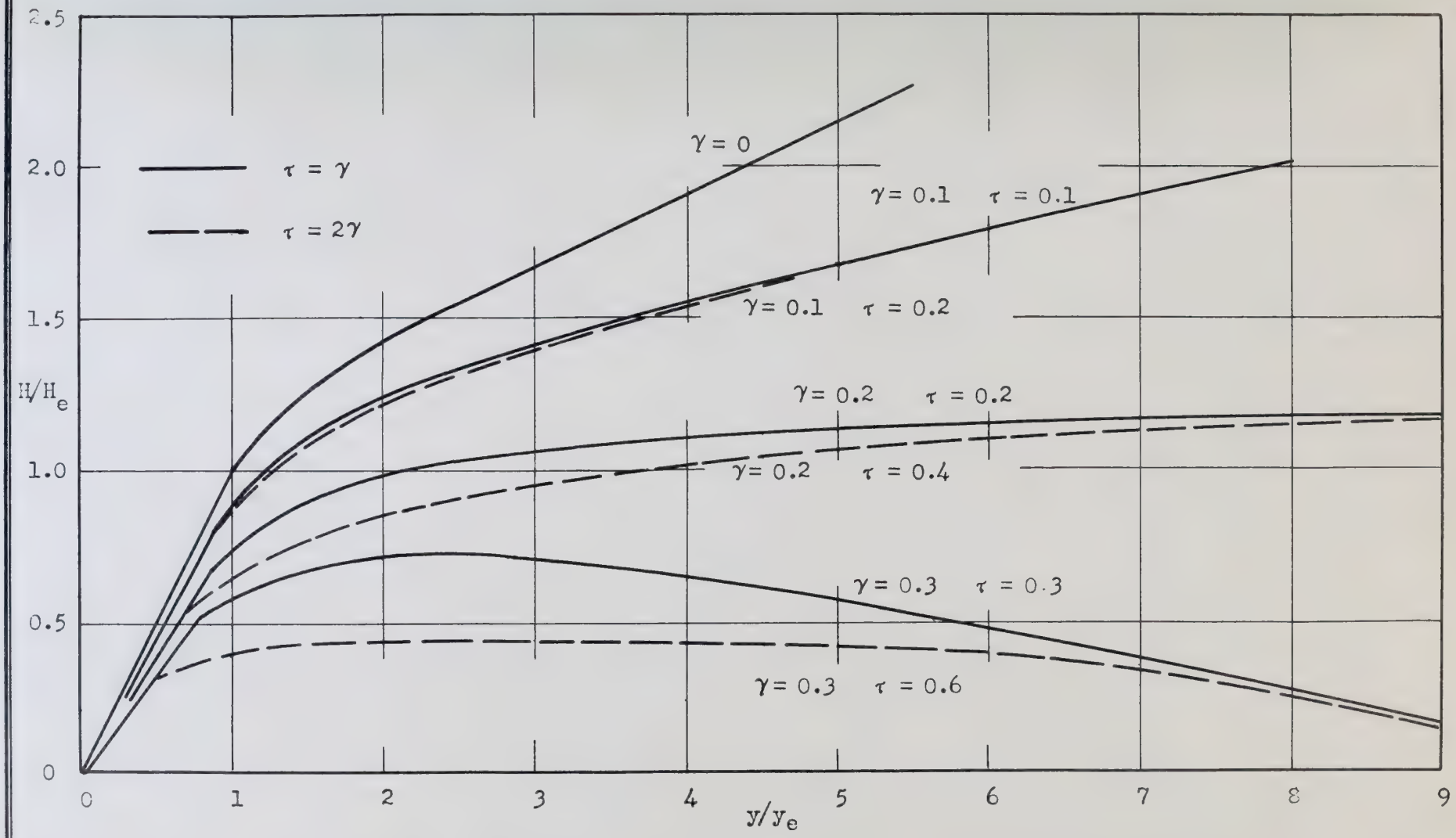

Fig. 17 - H/H_e vs. y/y_e for Idealized H Section and α of M/M_e vs. θ/θ_e Equal to 0.2 . τ/γ = 1.0 and 2.0

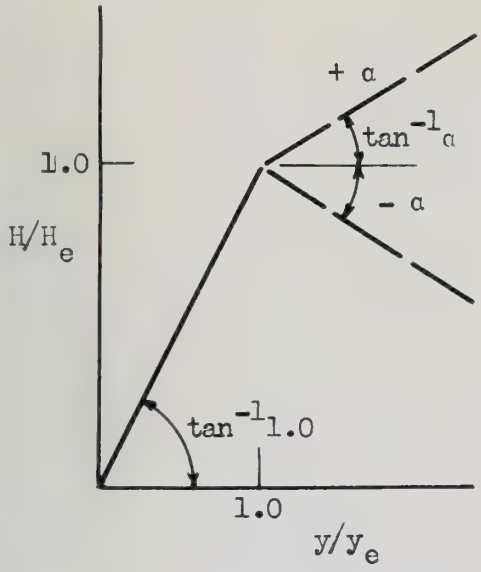

Fig. 18 - α Designation

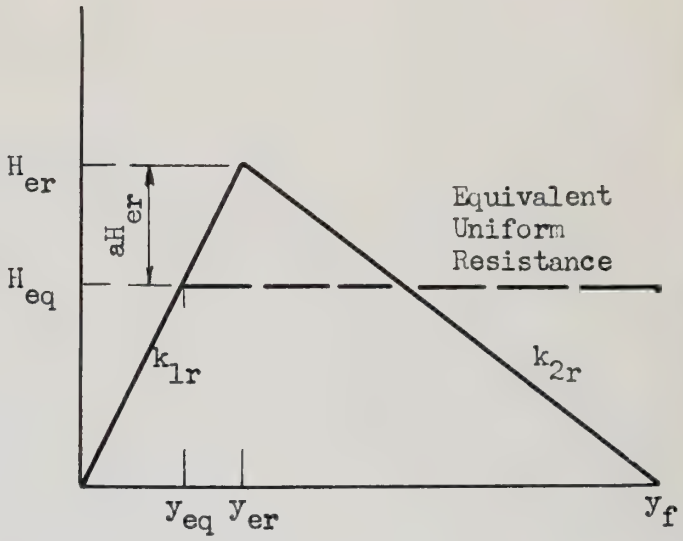

Fig. 20 - Equivalent Uniform Resistance for $y_m = y_f$

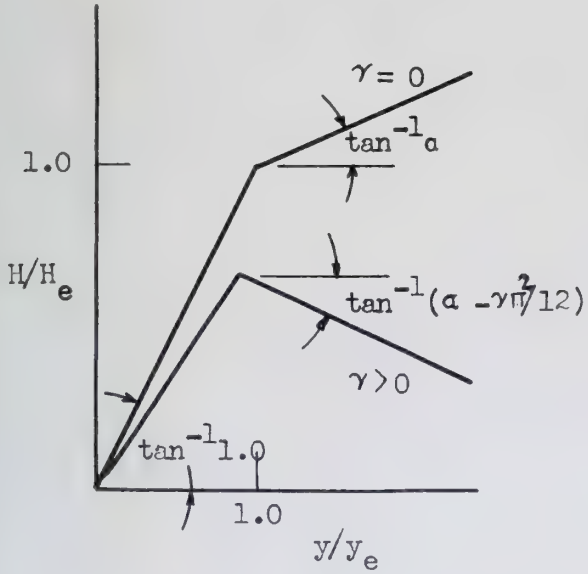

Fig. 19 - Form of Structure Resistance Where $\alpha \neq 0$

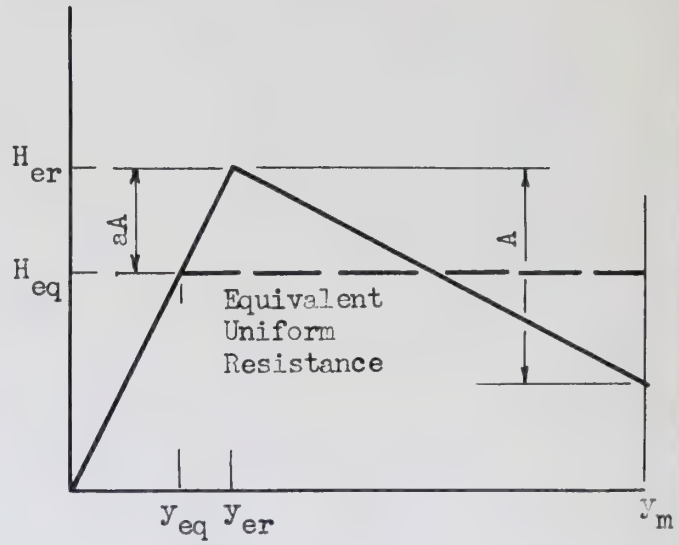

Fig. 21 - Equivalent Uniform Resistance for $y_m < y_f$

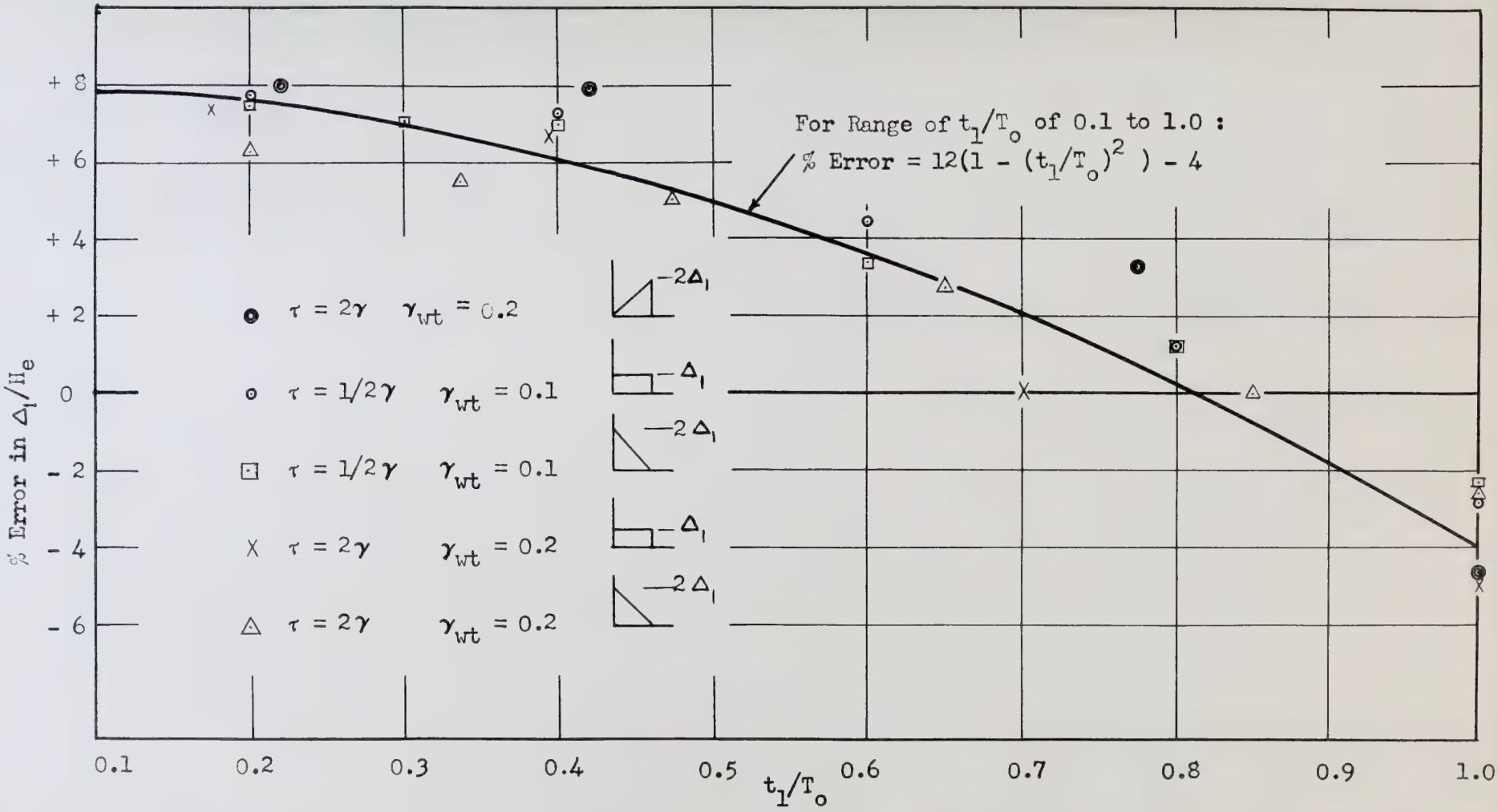

Fig. 22 - Error in Δ_1/H_e From Approximate Equivalent Uniform Resistance Method for $y_m = y_f$

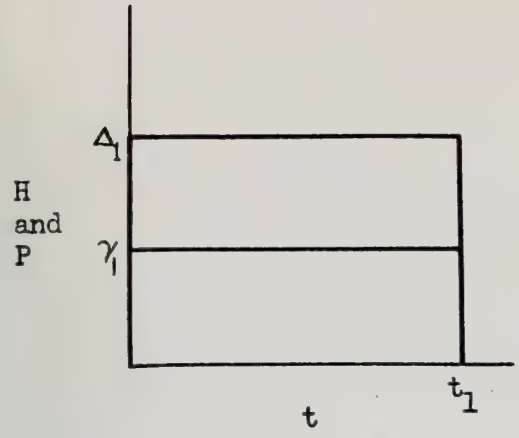

(a) Step Pulse

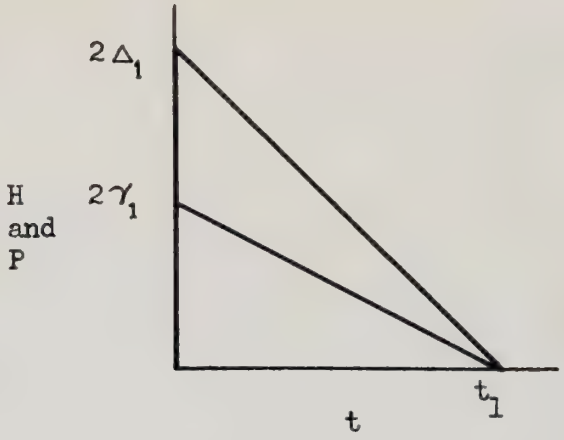

(b) Initial Peak Pulse

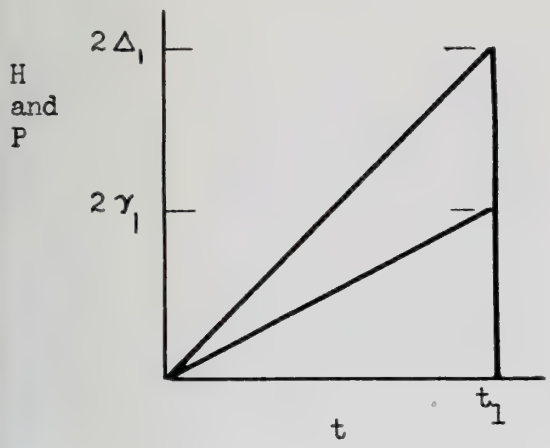

(c) Terminal Peak Pulse

Fig. 23 - Load Pulse Shapes

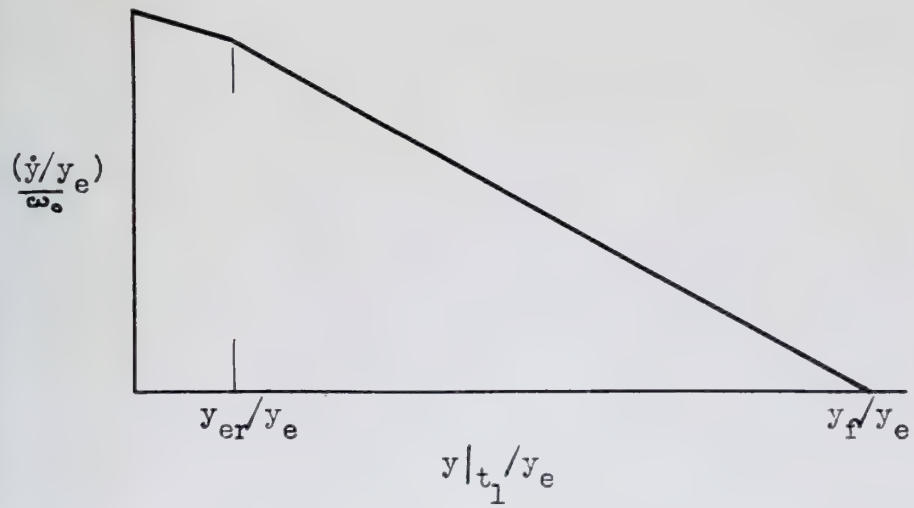

Fig. 24 - Velocity , $\frac{(\dot{y}/y_e)}{\omega_o}$, Required at t_1 and $y|_{t_1}$ for $y_m = y_f$

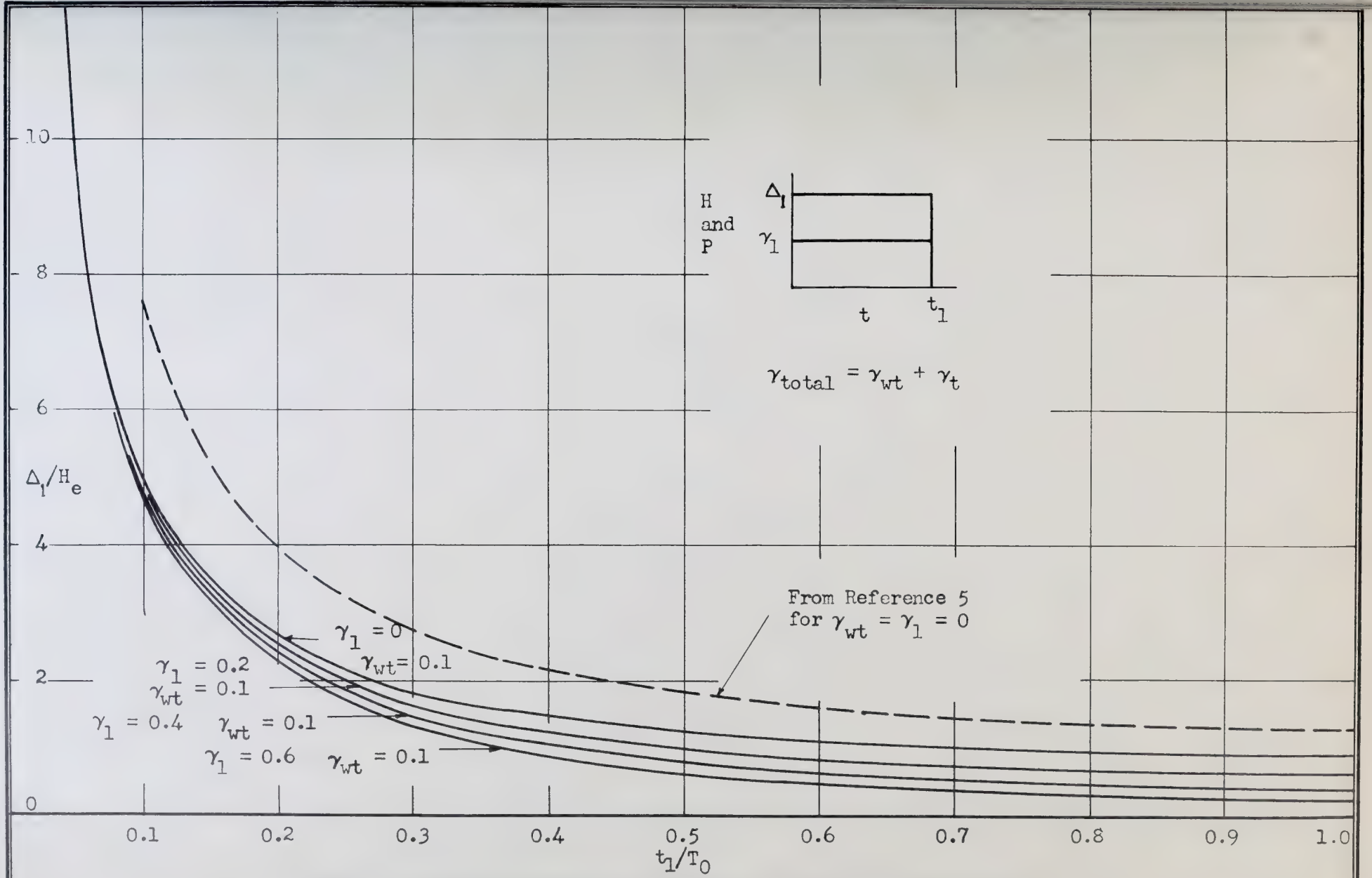

Fig. 25 - Structure Response Curves for Frame A for Step Pulse :
$y_m/y_e = y_f/y_e = 11.55$, $r = 1/2\gamma$, $\gamma_{wt} = 0.1$

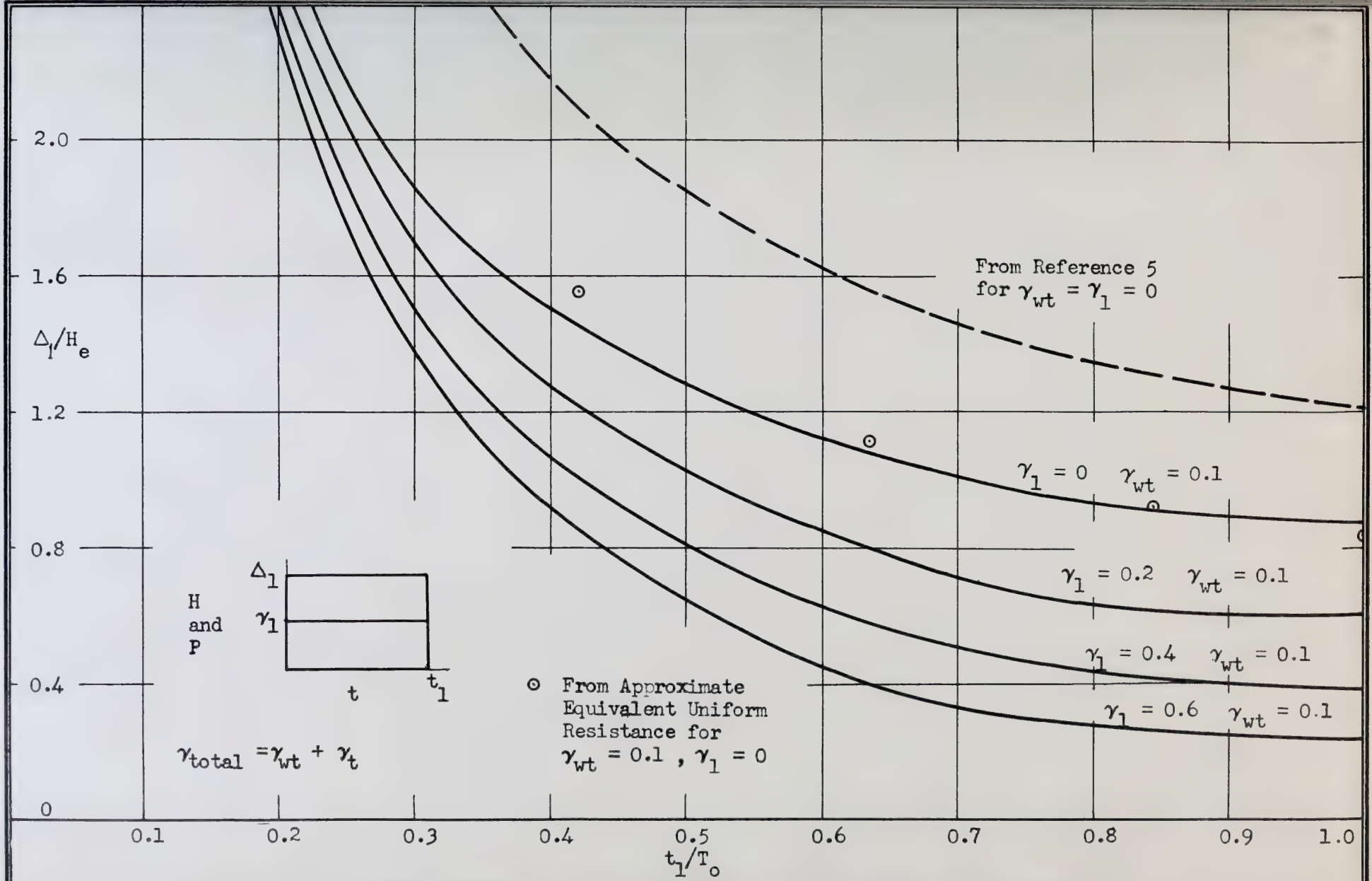

Fig. 26 - Structure Response Curves for Frame A for Step Pulse : (Enlargement of a Portion of Fig. 25) , $y_m/y_e = y_f/y_e = 11.55$, $\tau = 1/2\gamma$, $\gamma_{wt} = 0.1$

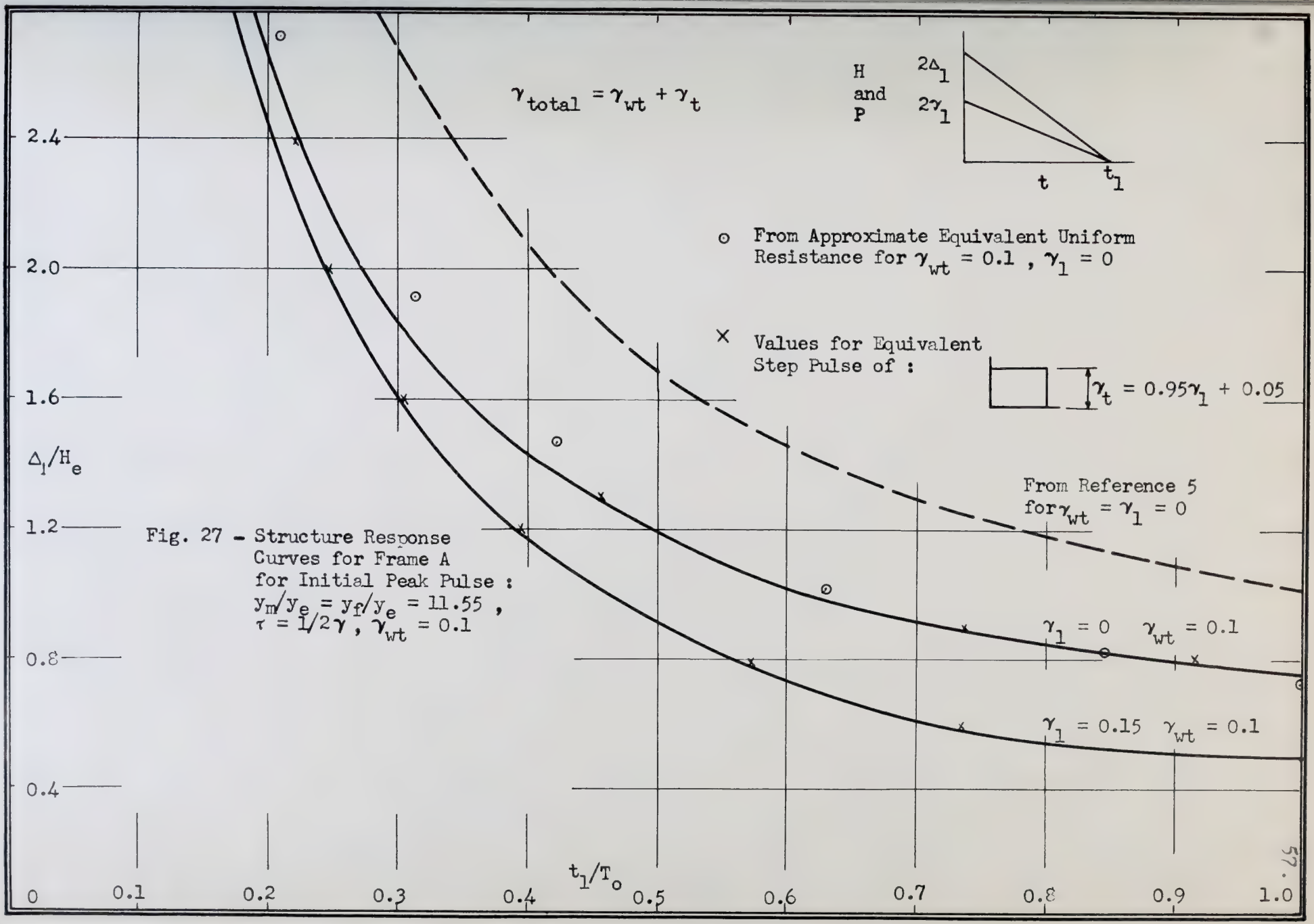

Fig. 27 - Structure Response Curves for Frame A for Initial Peak Pulse : $y_m/y_e = y_f/y_e = 11.55$, $\tau = 1/2\gamma$, $\gamma_{wt} = 0.1$

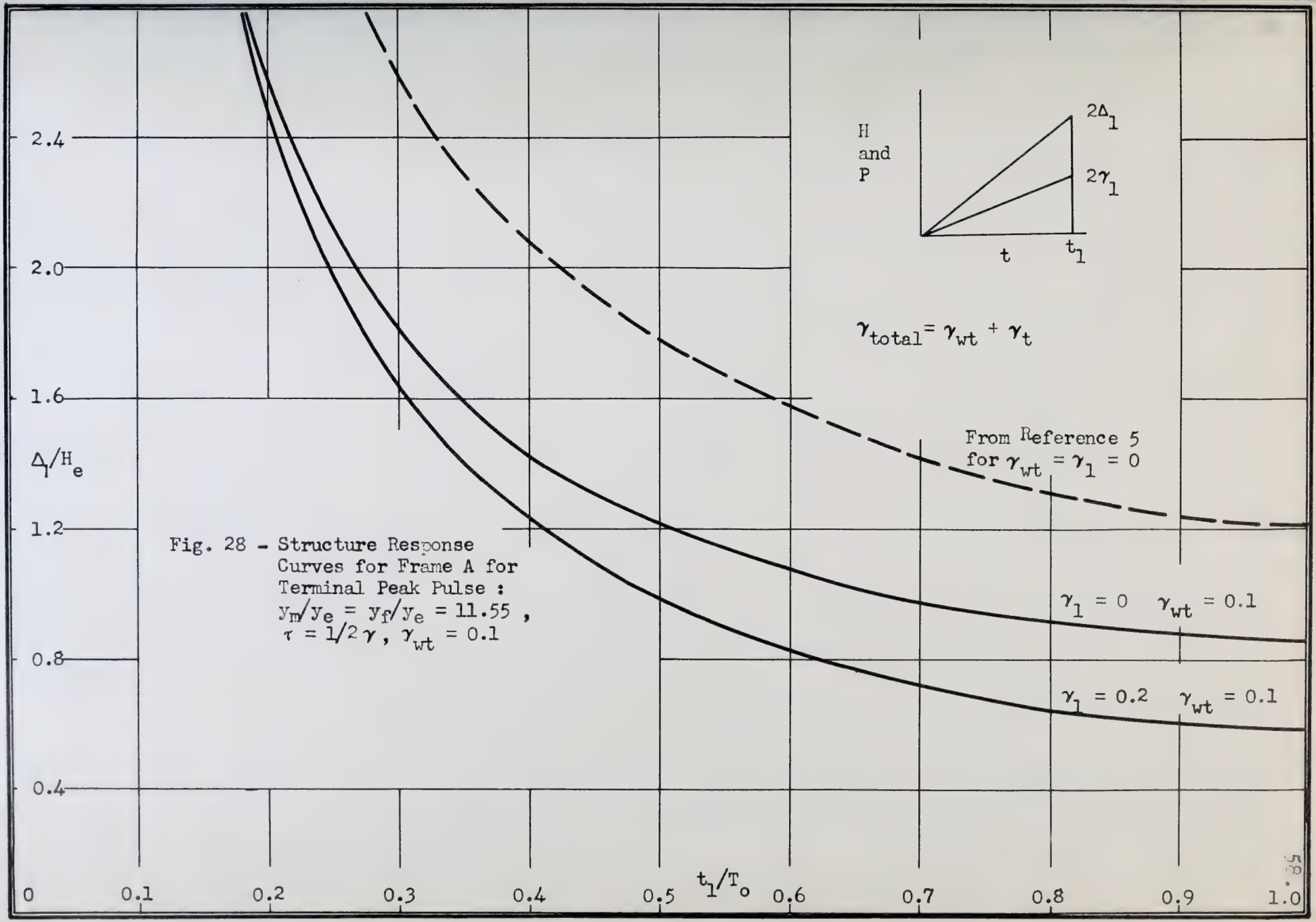

Fig. 28 - Structure Response Curves for Frame A for Terminal Peak Pulse : $y_m/y_e = y_f/y_e = 11.55$, $\tau = 1/2\,\gamma$, $\gamma_{wt} = 0.1$

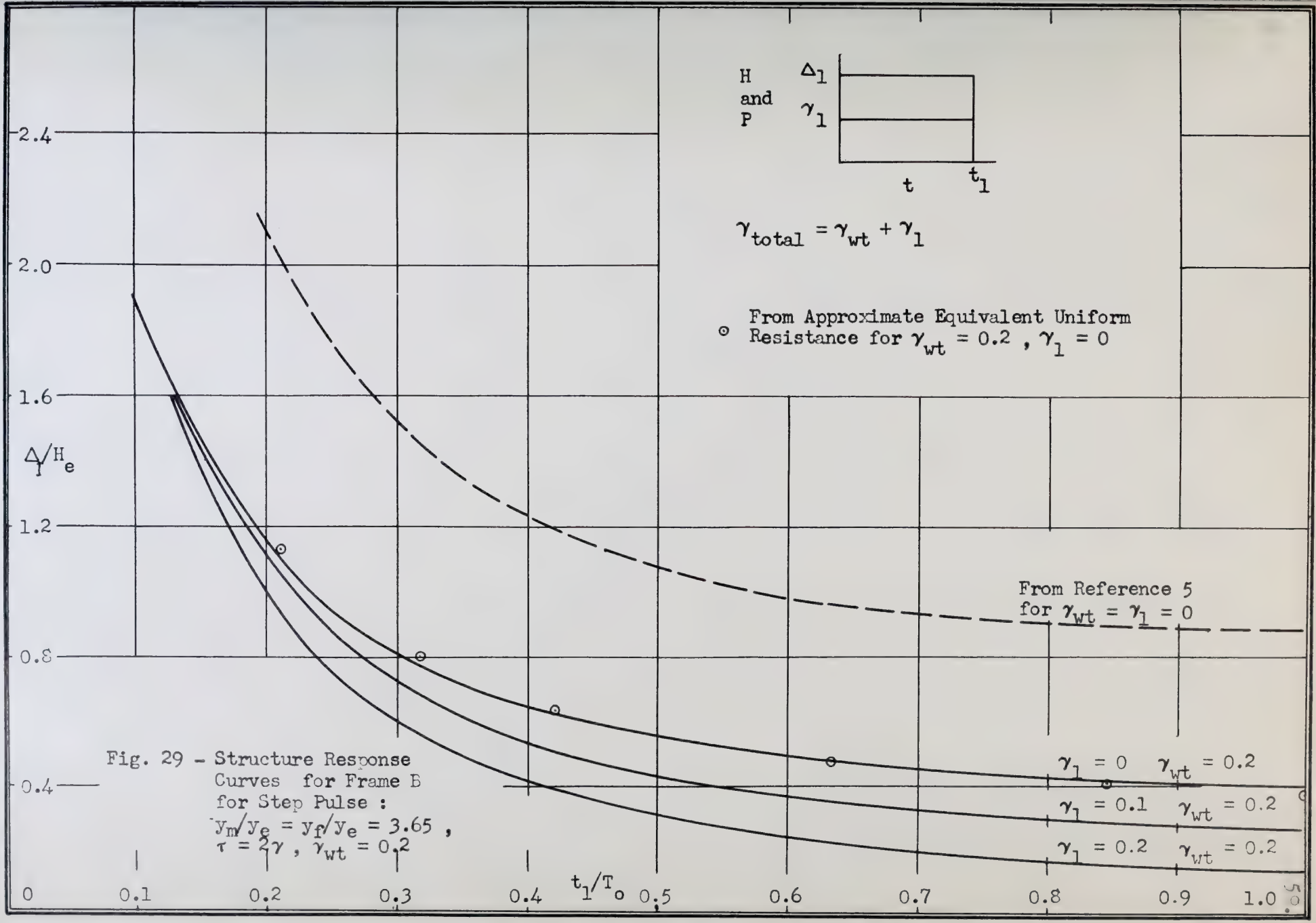

Fig. 29 - Structure Response Curves for Frame B for Step Pulse : $y_m/y_e = y_f/y_e = 3.65$, $\tau = 2\gamma$, $\gamma_{wt} = 0.2$

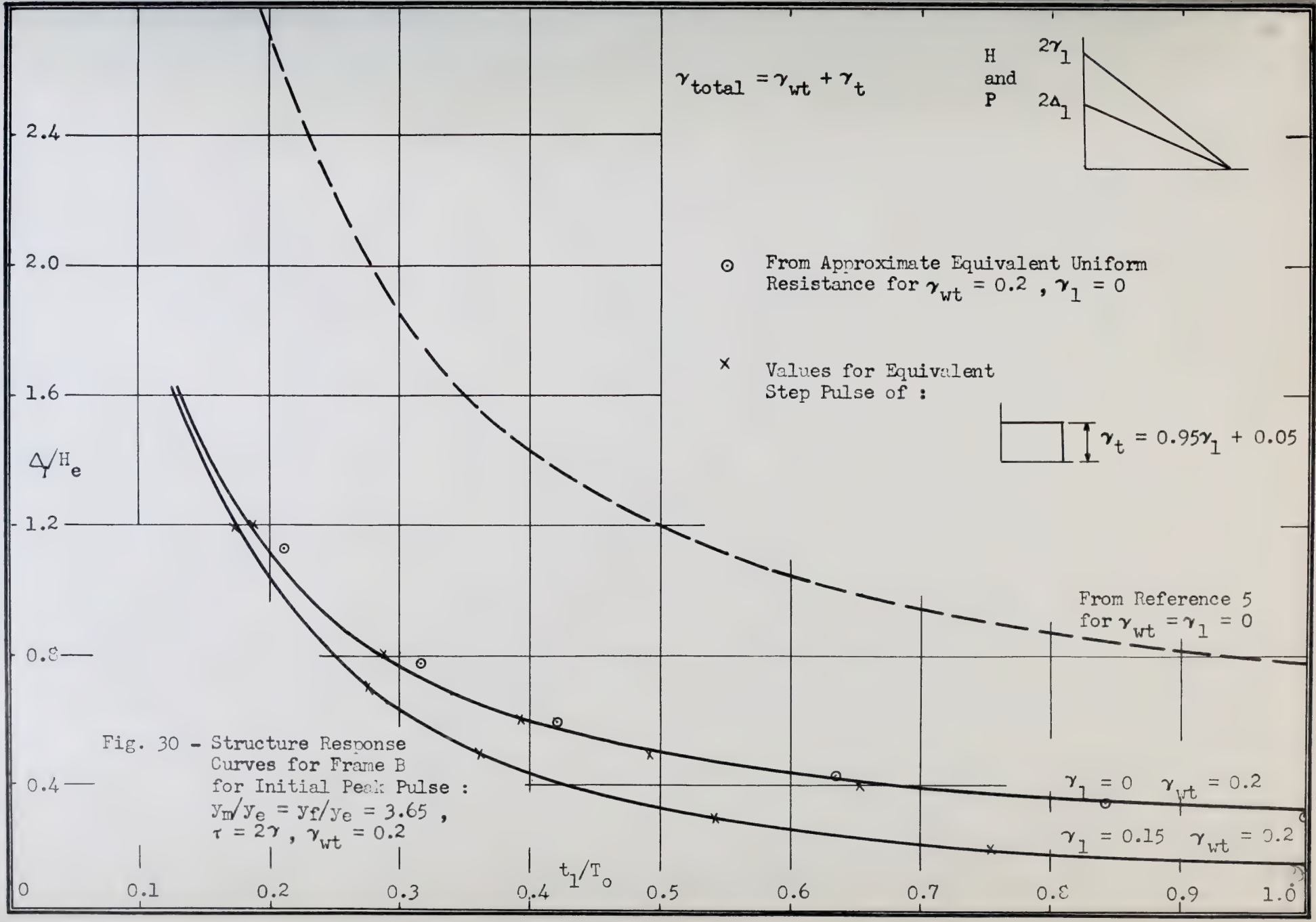

Fig. 30 - Structure Response Curves for Frame B for Initial Peak Pulse : $y_m/y_e = y_f/y_e = 3.65$, $\tau = 2\gamma$, $\gamma_{wt} = 0.2$

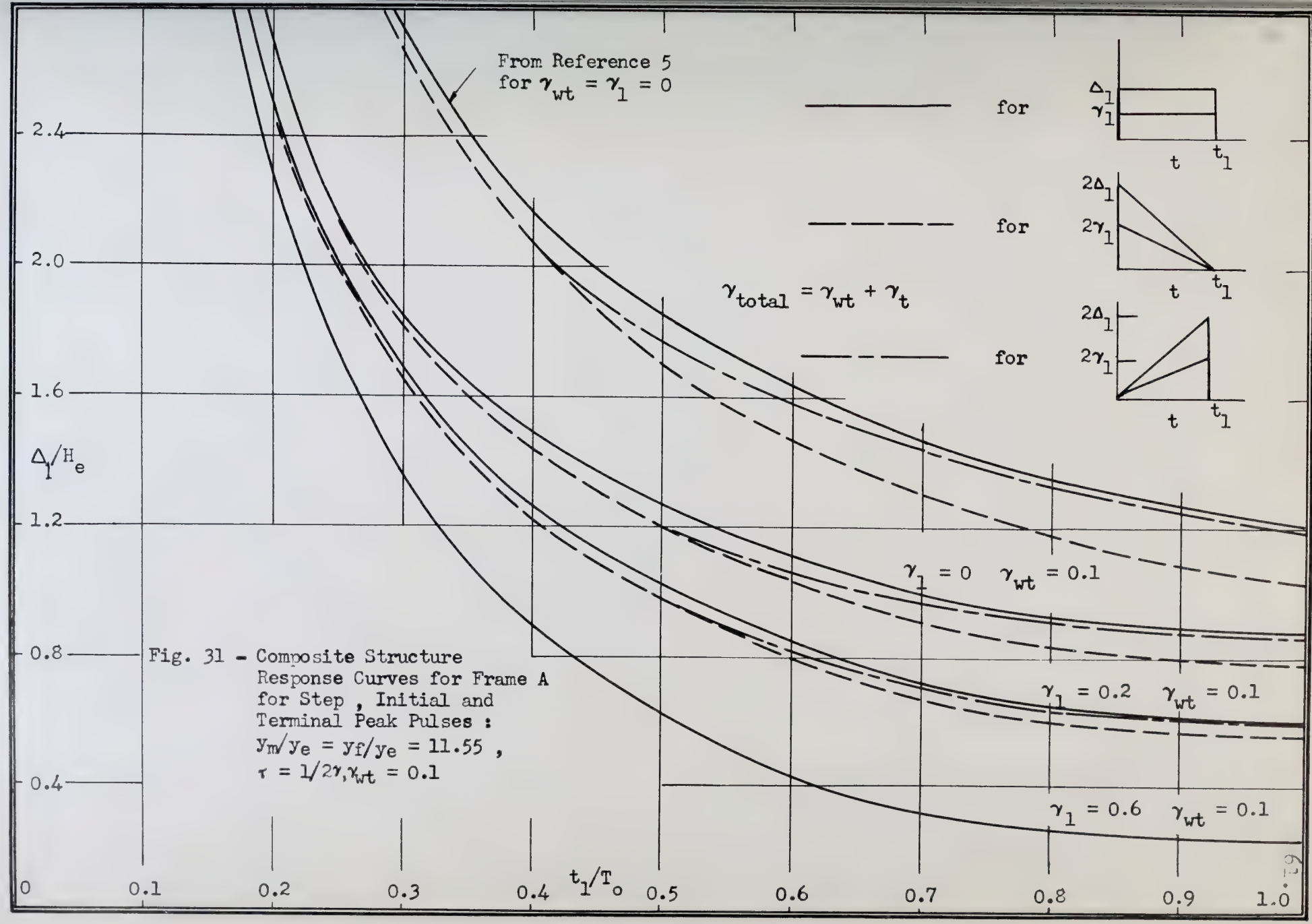

Fig. 31 - Composite Structure Response Curves for Frame A for Step , Initial and Terminal Peak Pulses : $y_m/y_e = y_f/y_e = 11.55$, $\tau = 1/2\gamma, \gamma_{wt} = 0.1$

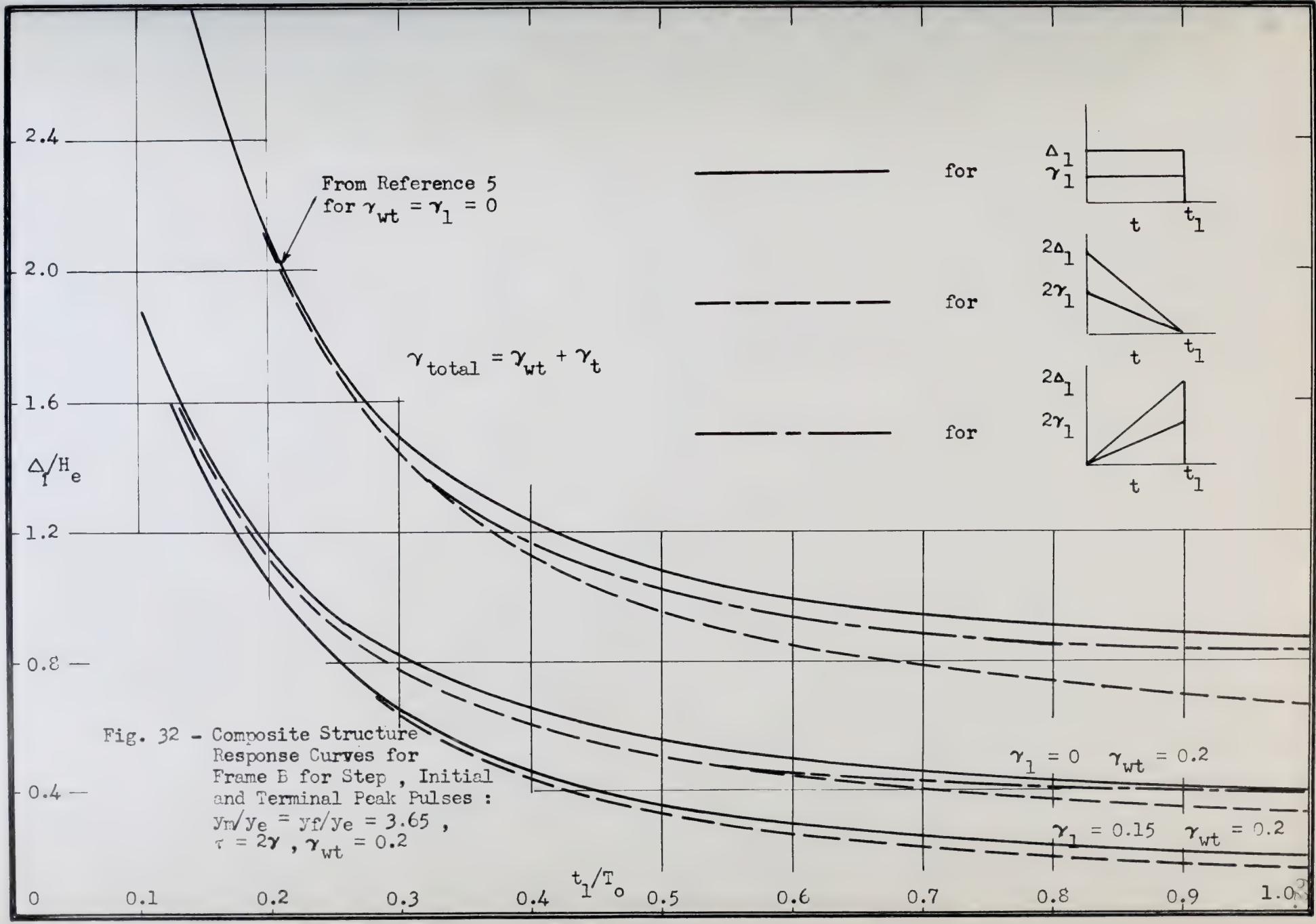

Fig. 32 - Composite Structure Response Curves for Frame B for Step , Initial and Terminal Peak Pulses : $y_m/y_e = y_f/y_e = 3.65$, $\tau = 2\gamma$, $\gamma_{wt} = 0.2$

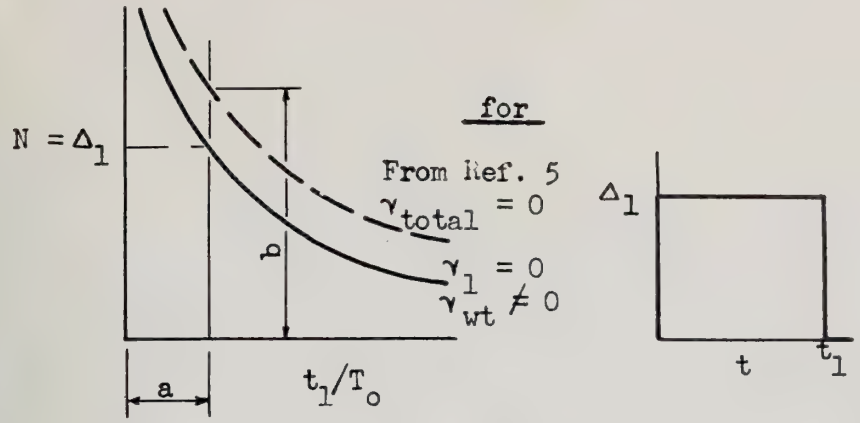

Fig. 33 (a) $d = a(c/b)$

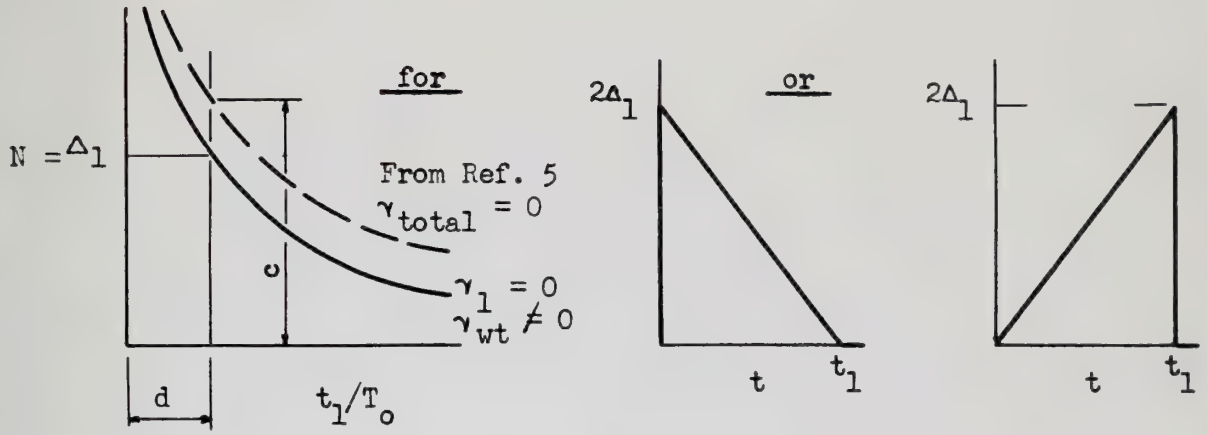

Fig. 33 (b)

Fig. 33 - Proportionality Between Pulse Types for $\gamma_1 = 0$ and $y_m = y_f$. (γ_{wt} and τ/γ same for all types)

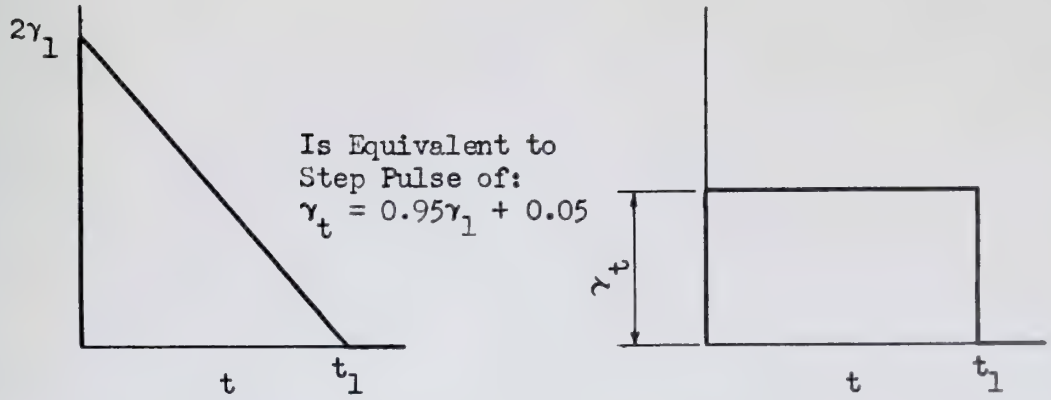

Fig. 34 - Equivalence Between Initial Peak and Step Pulse for $y_m = y_f$. (Δ_1 same for Both Pulses)

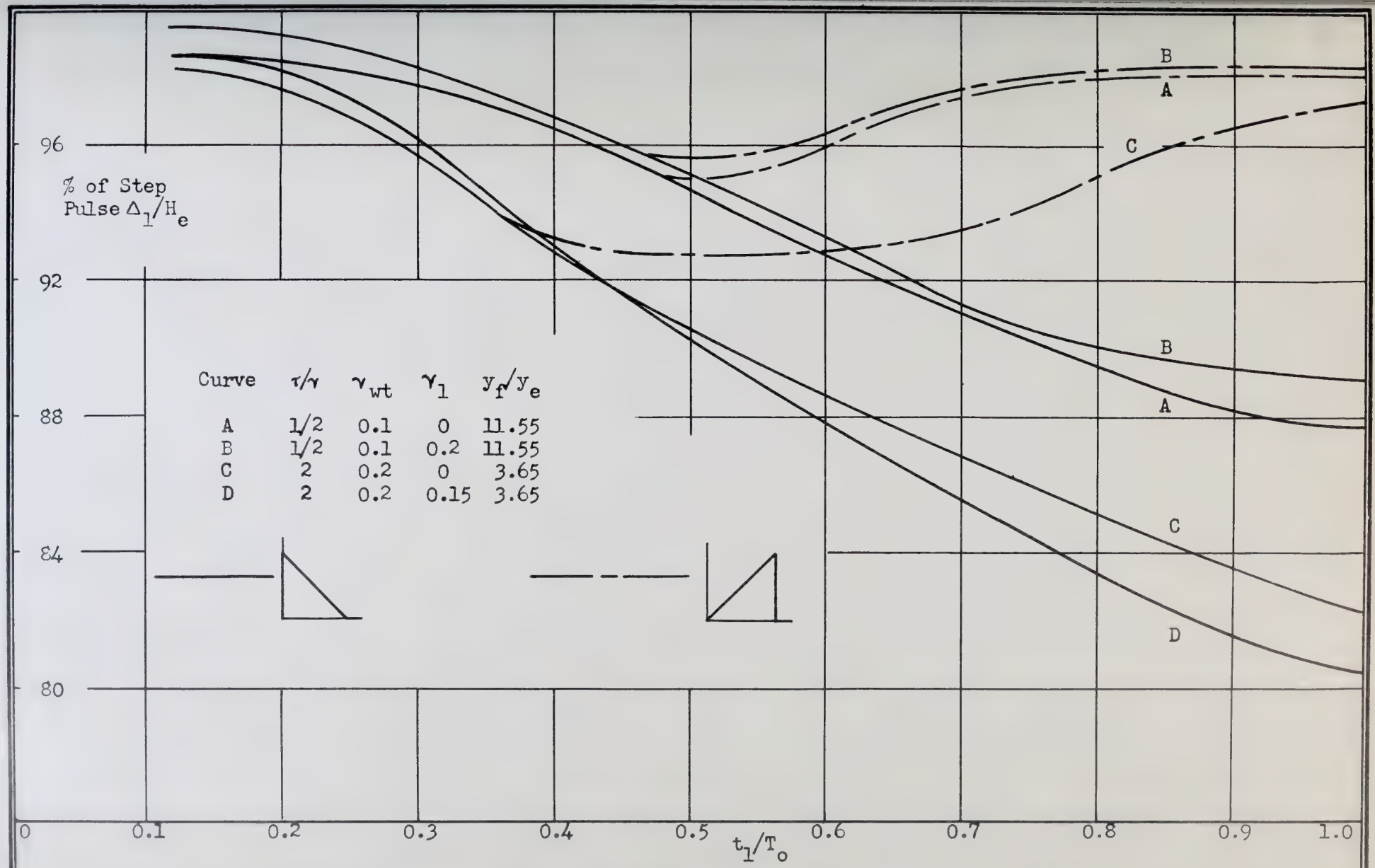

Fig. 35 - Δ_1/H_e for Initial and Terminal Peak Pulses Expressed as % of Δ_1/H_e for Step Pulse and same γ_1 , γ_{wt} and t_1 . $y_m = y_f$

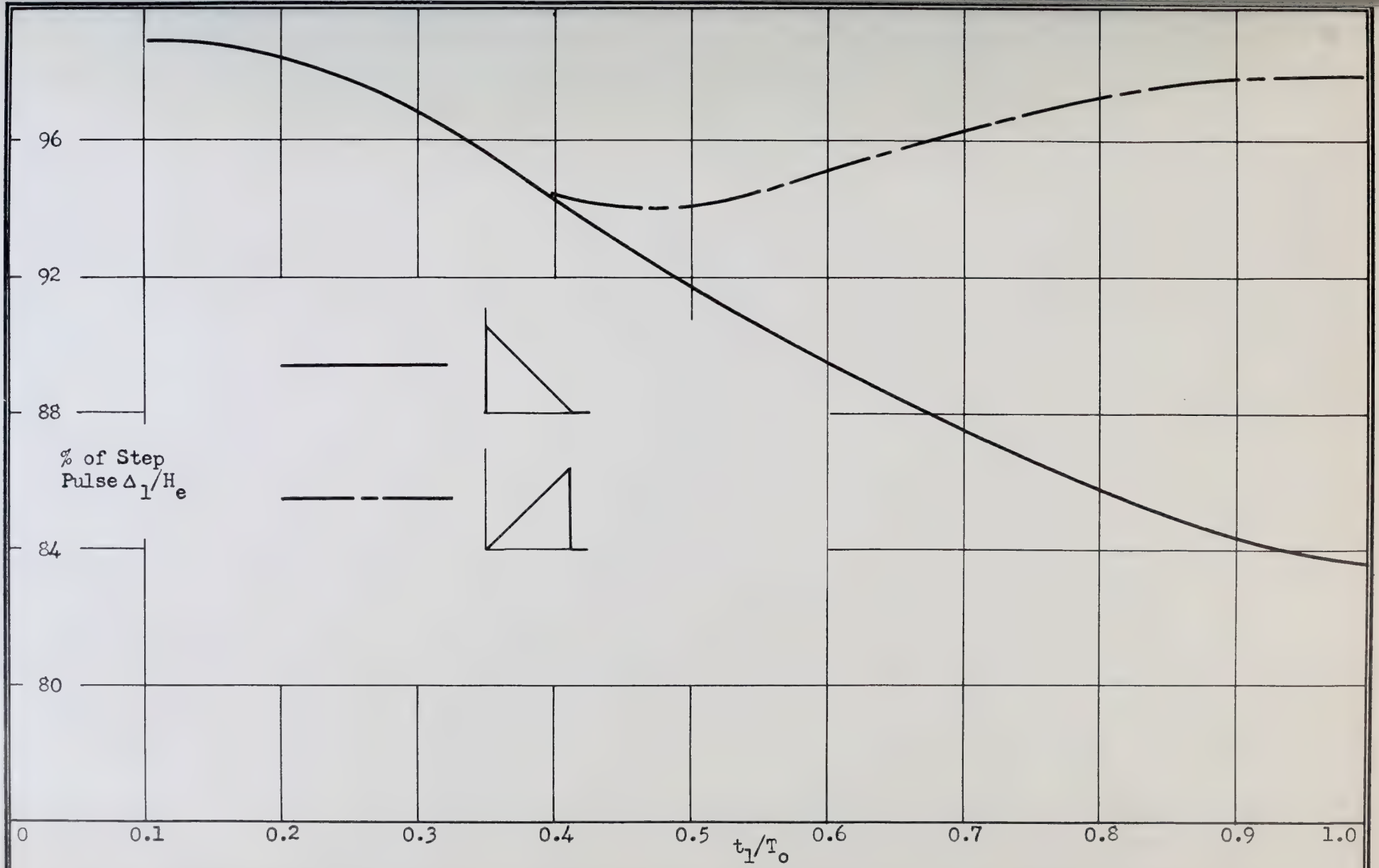

Fig. 36 - Approximate % Conversion Factor to Construct Δ_1/H_e vs. t_1/T_o Curves for Initial and Terminal Peak Pulses for $y_m = y_f$ using Δ_1/H_e vs. t_1/T_o for Step Pulse. (Same τ/ν , ν_{wt} and ν_1)

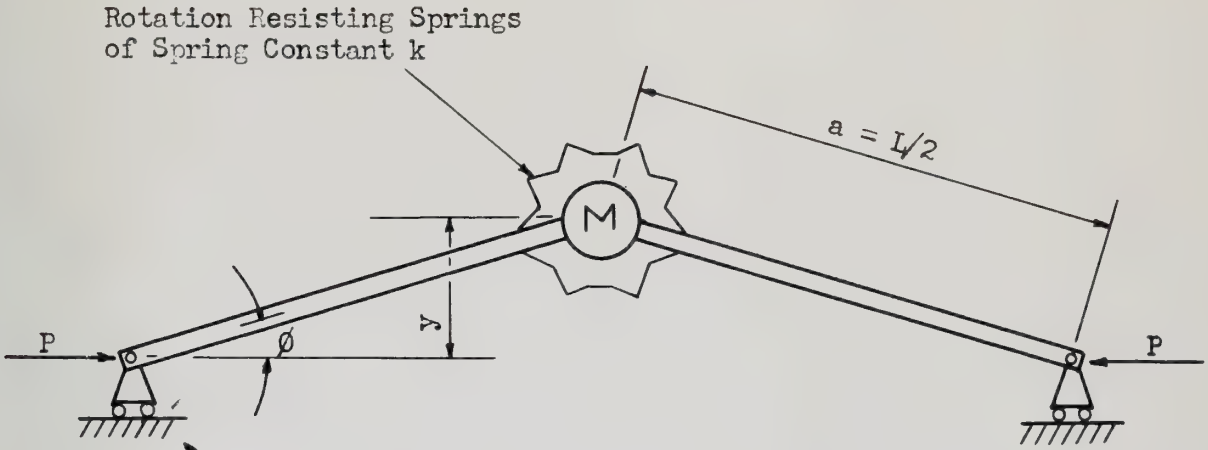

Rollers Both Ends ; Mass , M ,
not to Move Longitudinally

$\emptyset_o$ and y_o are Measures of
Initial Crookedness

$u = y/a$

Fig. 37 - Column Model for Appendixes I and II

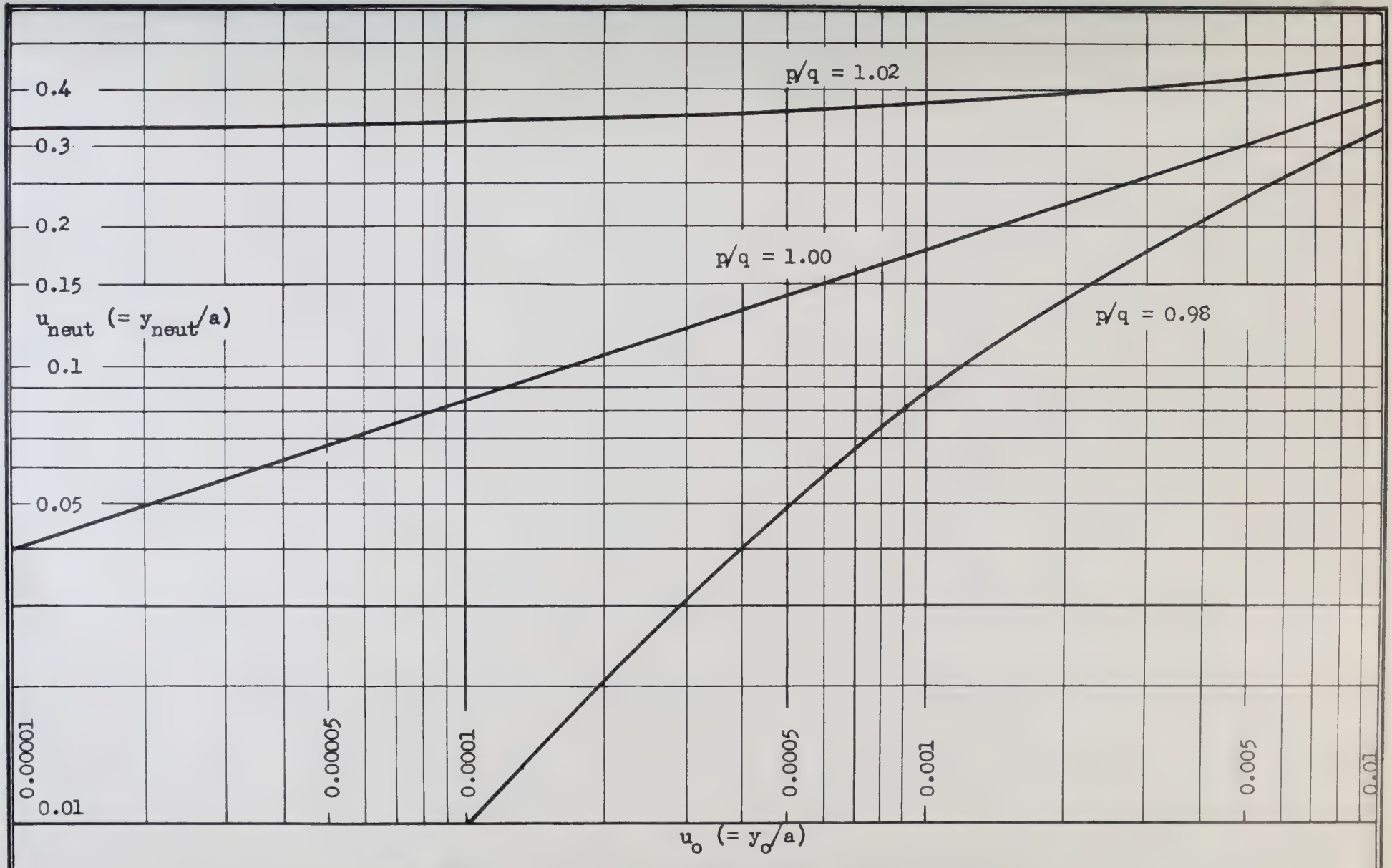

Fig. 38 - u_{neut} vs. u_o for p/q = 1.02 , 1.00 and 0.98

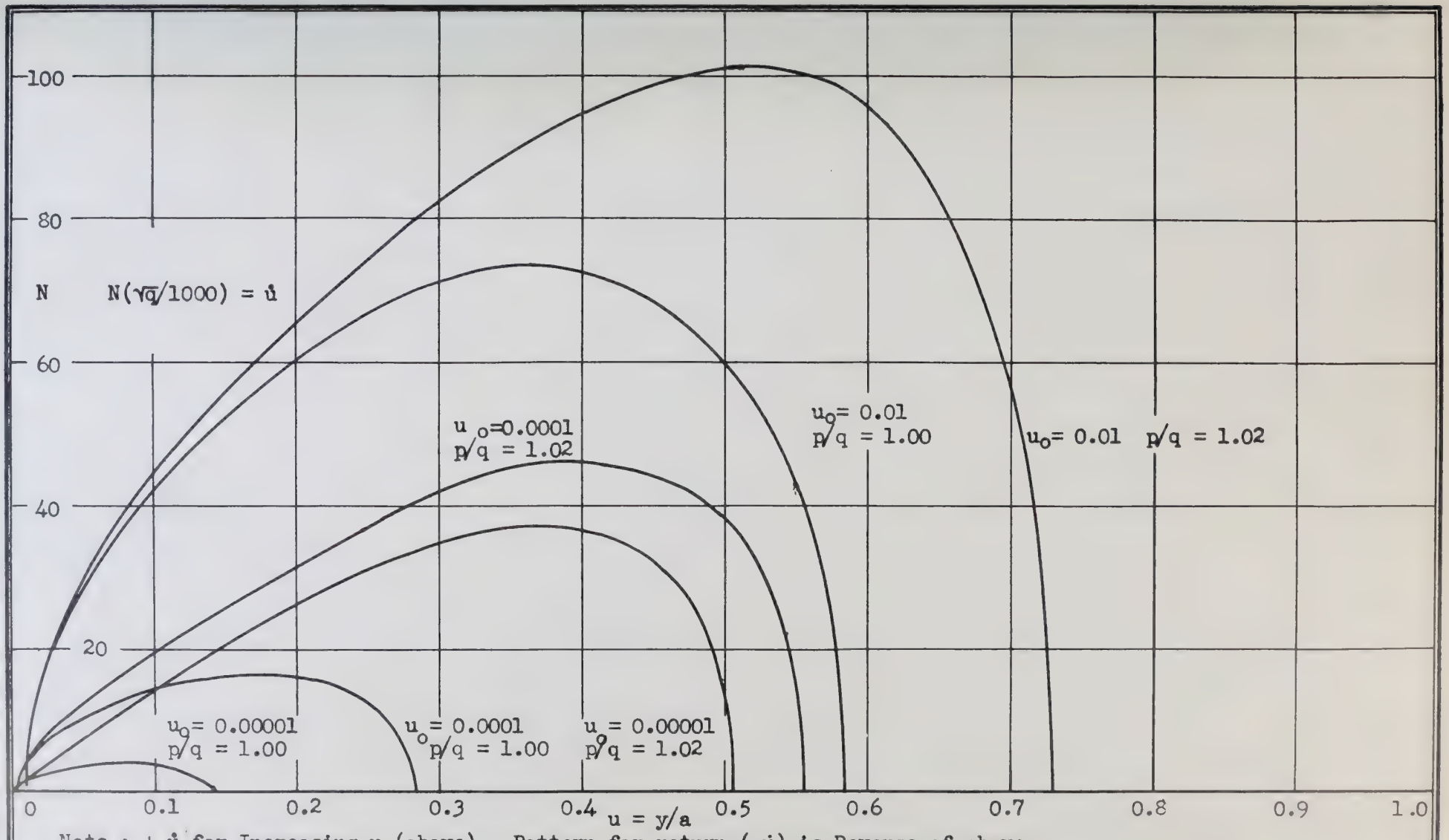

Note : + u̇ for Increasing u (above) . Pattern for return (-u̇) is Reverse of above.

Fig. 39 - Phase Plane Diagrams for Initial Crookedness. p/q = 1.00 and 1.02 and Column Elastic

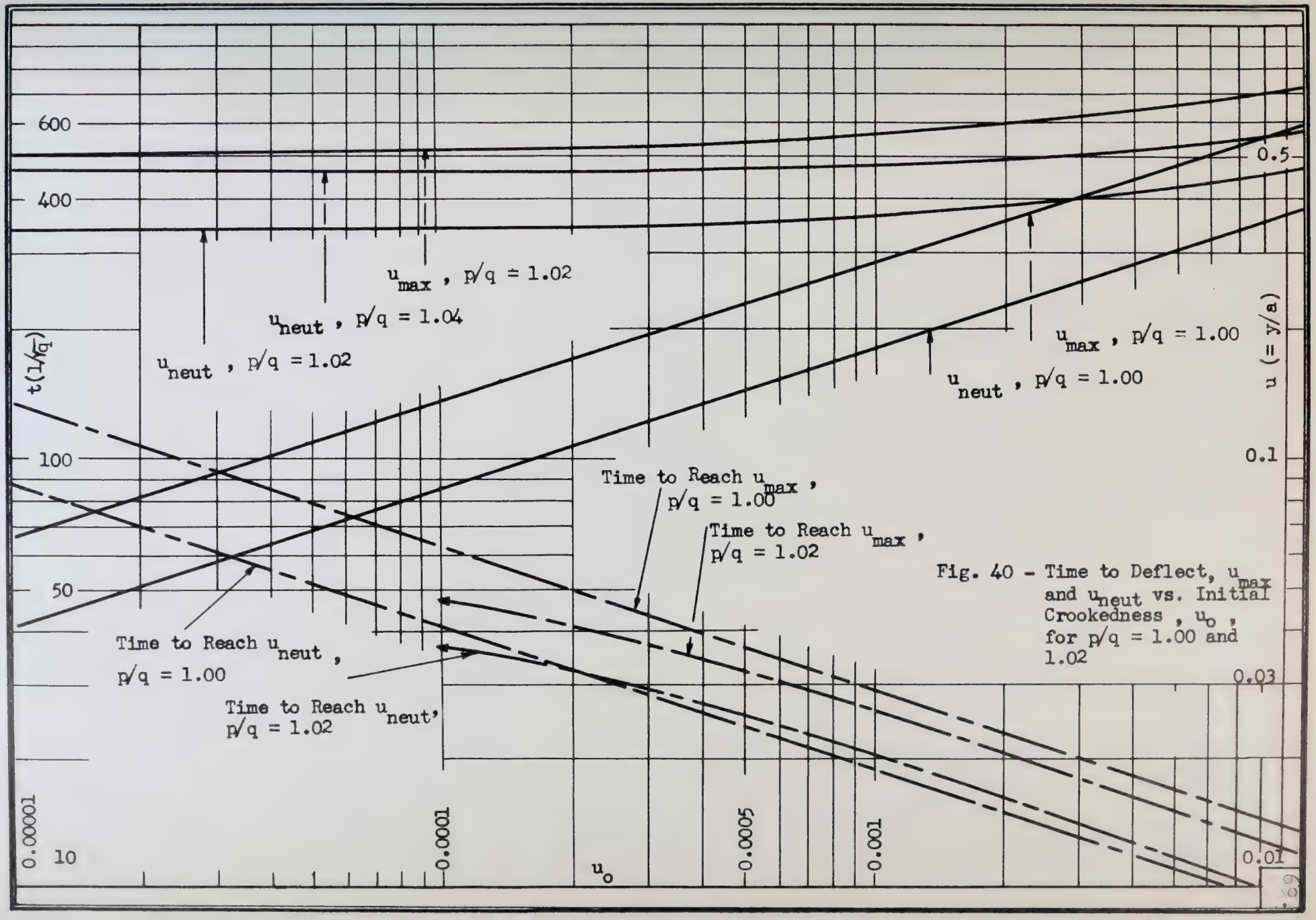

Fig. 40 - Time to Deflect, u_{max} and u_{neut} vs. Initial Crookedness , u_o , for p/q = 1.00 and 1.02

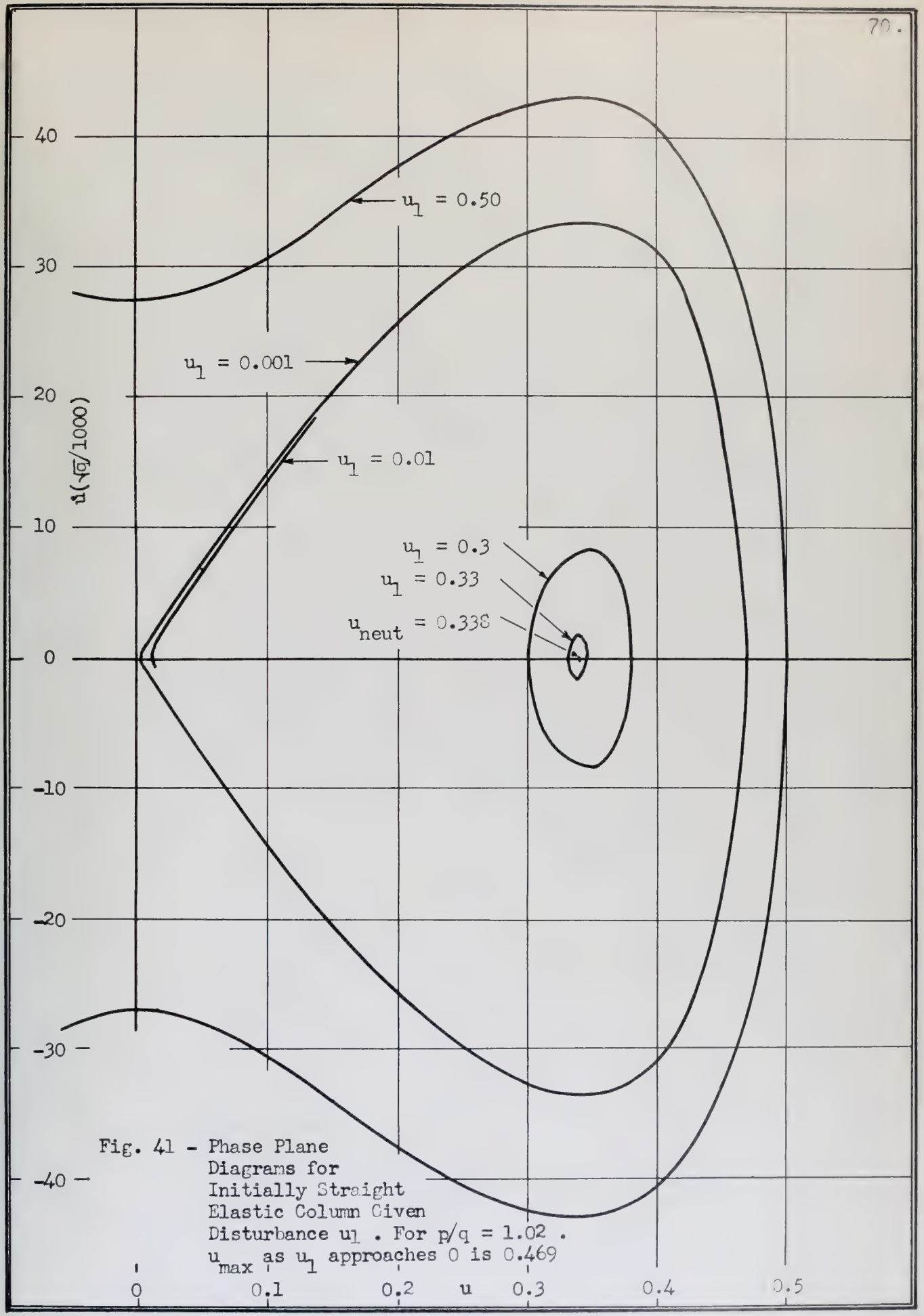

Fig. 41 - Phase Plane Diagrams for Initially Straight Elastic Column Given Disturbance u_1 . For $p/q = 1.02$. u_{max} as u_1 approaches 0 is 0.469

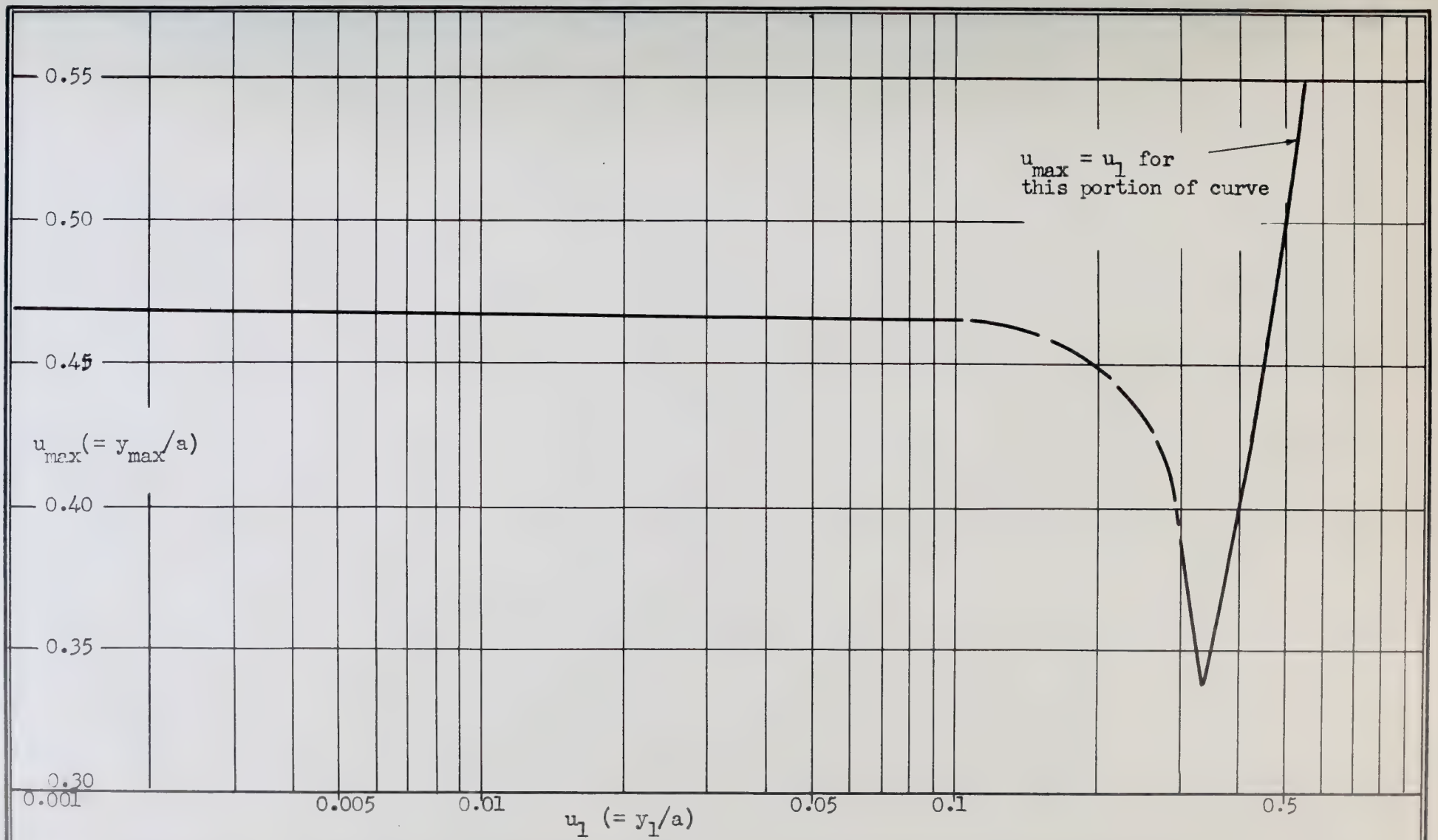

Fig. 42 - u_{max} vs. u_1 for Initially Straight Elastic Column Given Initial Displacement u_1 .
$p/q = 1.02$

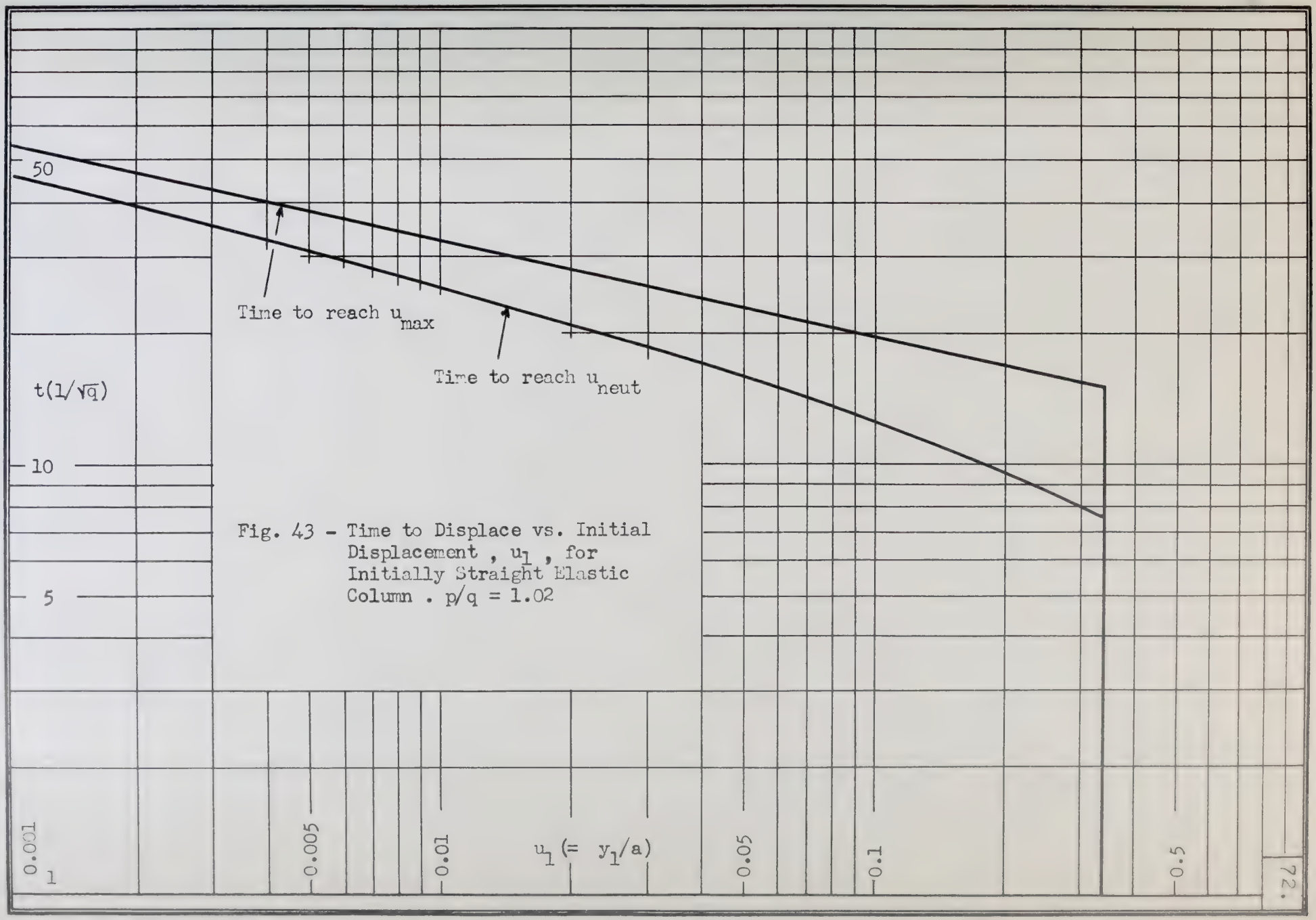

Fig. 43 - Time to Displace vs. Initial Displacement , u_1 , for Initially Straight Elastic Column . $p/q = 1.02$

VITA

Henry Edward Stephens was born on September 13, 1921, in Fairburn, Georgia. He completed his high school education at Campbell High School, Fairburn, Georgia, in 1938 and entered Georgia School of Technology in July of that year, where he studied Mechanical Engineering until June, 1941. In August, 1941, he received an appointment to the U.S. Naval Academy and received the degree of Bachelor of Science, with honors, from that institution in June, 1944. He has served continuously in the U.S. Navy from August, 1941, to the present, and served from July, 1944, to October, 1945, in the Pacific Theater. He entered Rensselaer Polytechnic Institute in January, 1946, as a Navy graduate student and received the degree of Bachelor of Science in Civil Engineering from that institution in September, 1947. In September, 1947, he transferred from the Navy Line to the Navy Civil Engineer Corps and continued his graduate work at Rensselaer Polytechnic Institute where he received the degree of Master of Science in Civil Engineering in June, 1948. From June, 1948, to June, 1952, he served at Key West, Florida, and Yorktown, Virginia. At Key West he had experience in design, construction, maintenance and transportation. He was head of the Public Works Department, Naval Schools, Mine Warfare, Yorktown, Virginia, from January, 1950, to June, 1952. In June, 1952, he entered the University of Illinois as a graduate student in the Structural Dynamics curriculum.

He was elected a member of Tau Beta Pi and Chi Epsilon in September, 1947, and an associate member of Sigma Xi in June, 1948.

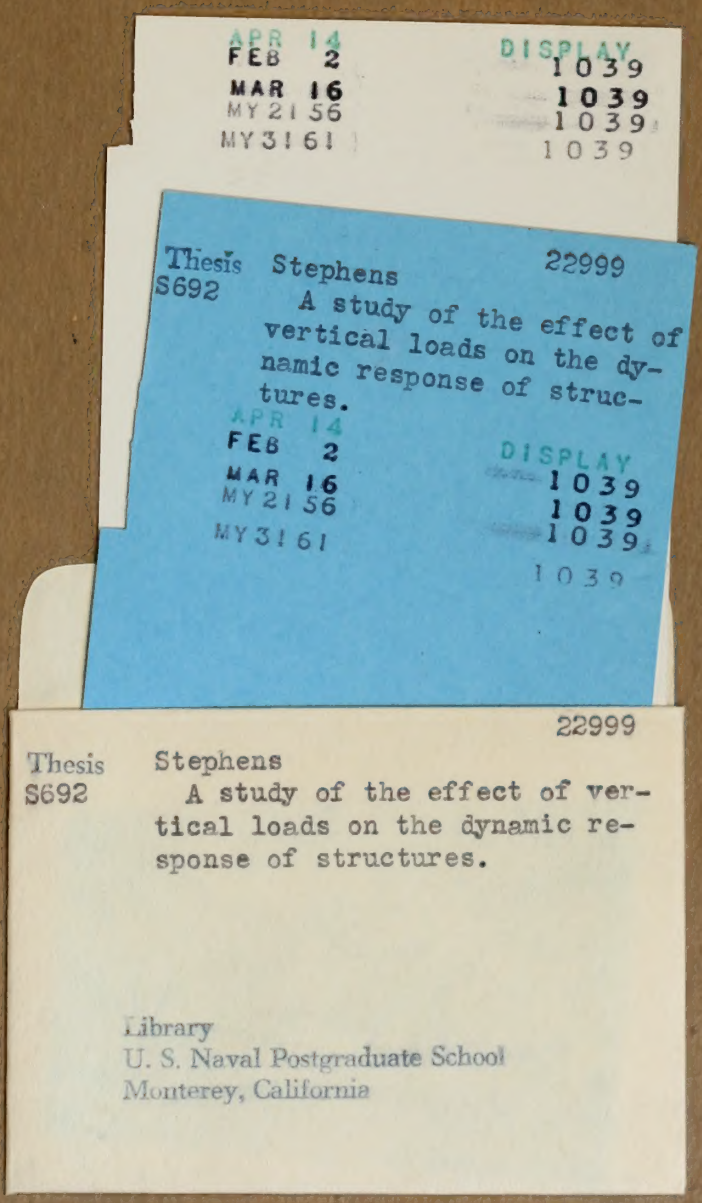
APR 14
FEB 2
MAR 16
MY 21 56
MY 31 61
DISPLAY
1039
1039
1039
1039
Thesis S692 Stephens
22999
A study of the effect of vertical loads on the dynamic response of structures.
APR 14
FEB 2
MAR 16
MY 21 56
MY 31 61
DISPLAY
1039
1039
1039
1039
22999
Thesis S692 Stephens
A study of the effect of vertical loads on the dynamic response of structures.
Library
U. S. Naval Postgraduate School
Monterey, California

thesS692
A study of the effect of vertical loads
3 2768 002 02265 9
DUDLEY KNOX LIBRARY